

ESTIMATION OF NON-STATIONARY HYDROLOGICAL
MODEL PARAMETERS FOR THE POLISH WELNA
CATCHMENT



W.J.M. Knoben
December 10, 2013

UNIVERSITY OF TWENTE.



Title Estimation of non-stationary hydrological model parameters for the Polish Welna catchment

Thesis for the degree of Master of Science in Civil Engineering and Management

Author Wouter Johannes Maria Knoben

Institute University of Twente
Institute of Geophysics, Polish Academy of Sciences

Supervisors Dr. ir. M.J. Booij
University of Twente, Department of Water Engineering and Management

Dr. M.S. Krol
University of Twente, Department of Water Engineering and Management

Advisers Prof. dr. hab. eng. R.J. Romanowicz
Polish Academy of Sciences, Institute of Geophysics, Department of Hydrology and Hydrodynamics

Dr. M. Osuch
Polish Academy of Sciences, Institute of Geophysics, Department of Hydrology and Hydrodynamics

Date December 10, 2013

Title page image Welna river near the village Rożnowice
(source: ©Arkadiusz Kubale, *Welna_river*. 27 Nov 2013, http://pl.wikipedia.org/wiki/Plik:Welna_river.jpg)

Summary

Recent research (e.g. Bastola et al., 2011; Coron et al., 2012; Merz et al., 2011; Vaze et al., 2010) has shown that the performance of calibrated conceptual models (measured as the value of an objective function) can deteriorate when the models are used for periods with different climatic conditions than were present during calibration of the model. This can decrease the confidence in model functioning during climate change impact assessment, where hydrological models might be applied to different climatic conditions than were present during their calibration period. Merz et al. (2011) showed that correlations exist between optimal parameter values and certain climate characteristics. The goal of this study is to use these correlations to establish relationships between optimal model parameters and climate variables, to quantify how well these relationships perform during validation and to assess how these relationships perform during climate change impact assessment, compared to a traditional hydrological approach towards calibrated parameters.

The Hydrologiska Byråns Vattenbalansavdelning (HBV) model is used, with the Polish Wełna catchment as test case. According to the sensitivity analysis, parameters FC , LP , α , K_s , $PERC$ and TT have the most influence on overall model output variance, and these parameters are used in further analyses. The other HBV parameters are fixed at default values.

Parameters FC , α , K_s and $PERC$ show significant linear correlations with various precipitation related climate characteristics. Moreover, these correlations are sensible from a hydrological point of view, and they are thus possibly the result of an actual relationship between parameter values and climatic conditions, rather the result of coincidence. Parameter LP is significantly correlated with a single climate characteristic, which is deemed a coincidence. Parameter TT shows no significant correlations.

Linear regression analysis is used to establish regression equations that estimate time-varying values of FC , α , K_s and $PERC$, depending on climatic conditions that show significant and explainable correlation with the individual parameters. The equations vary in their ability to capture the variance in parameter values. Respective fits of the regression equations are: $R_\alpha^2 = 0.54$, $R_{PERC}^2 = 0.42$, $R_{FC}^2 = 0.40$ and $R_{K_s}^2 = 0.18$. Given the complexity of the problem, the equations for α , $PERC$ and FC estimate their respective parameter values fairly well and these equations are used to establish regression models. The equation for K_s is considered too inaccurate

to be used.

Four regression models are established that estimate the value(s) of (1) α , (2) α and *PERC*, (3) α and *FC* and (4) α , *PERC* and *FC* respectively. Model functioning is compared to that of the base model, which uses only calibrated parameters. Performance during calibration is similar for the base and regression models, but validation performance is significantly better for the base model (see table).

	Base model	Regression models			
		1	2	3	4
Calibration					
Y [-]	0.73	0.73	0.71	0.73	0.71
NS [-]	0.73	0.73	0.71	0.73	0.71
RVE [-]	0.00	0.00	0.00	0.00	0.00
Validation					
Y [-]	0.69	0.52	0.50	0.56	0.56
NS [-]	0.78	0.60	0.65	0.63	0.69
RVE [-]	0.13	0.15	0.27	0.12	0.23

Although the base model performs better during validation, one regression model is selected to explore the effects of using a regression model on climate change impact assessment results. Regression model 1 is selected, because parameter estimates of *FC* and *PERC* are affected by biases in GCM-RCM input and lead to unrealistic model behaviour. With the same input, the selected regression model has a tendency to simulate higher high and low flows, whereas the base model simulates higher medium flows. The base and regression model react similarly to GCM-RCM input, and both models project an increase in future average runoff. Generally the base model projects bigger changes than the regression model, except during summer months where the regression model projects bigger changes.

Concluding, using a regression model rather than a base model affects the outcomes of the climate change impact assessment. Since the base model has better validation performance, it is infeasible to use a regression model in this specific case. However, the methodology used in this study seems promising but is hindered by several data quality issues. Judging from validation performance, regression models might be a viable alternative to using only calibrated parameters in a hydrological model.

However, this study assumes that a relationship exists between parameter values and climatic conditions but this is, as of yet, not certain and this lowers confidence in the applicability of the regression model for future conditions. Therefore several recommendations are made that might assist in further clarifying the potential relationships between parameter values and climatic conditions in future research.

Preface

In this document I present the findings of my Master's thesis, conducted in cooperation with the University of Twente and the Institute of Geophysics, Polish Academy of Sciences. The goal of this work was to improve hydrological model functioning under climate change, which turned out to be a lot more complex than I originally thought. This study provided me with ample opportunity to improve my modelling and analytical skills, and hopefully also my academic writing.

I spent three, rather snowy, months at the Institute of Geophysics in Warsaw where the foundation for this research was created. I'm very grateful for the warm welcome I got from all the people at IGF, and especially from my supervisors Renata and Marzena. I can honestly say that the time in Warsaw was, despite the distinct lack of anything resembling sunshine or spring, one of the best periods in my entire time as a student.

I would also like to thank my UT supervisors Maarten and Martijn, for the thorough feedback on however many pages I delivered, for the critical look at my work and for providing me the motivation to keep going with fresh ideas.

To Mart, Lieke en Marijke, to all my friends, colleagues and fellow students, many thanks for the motivation and the distractions, the feedback and criticism, the discussions and the many good times!

A special place is reserved for my parents, for their unwavering support both mentally and financial and their understanding for the way I spent my time as a student. Papa en mama, dankjewel voor alles.

Wouter Knoben
Enschede, 10-12-2013

Contents

Summary	4
Preface	6
1 Introduction	16
1.1 Problem summary	16
1.1.1 Climate change	16
1.1.2 Hydrological changes	17
1.1.3 Parameter non-stationarity	18
1.1.4 Problem definition	18
1.2 Research goal	19
1.3 Research questions	19
1.4 Research strategy and reading guide	19
2 Study area and data	21
2.1 Study area	21
2.2 Data collection	22
2.2.1 Historical observations	22
2.2.2 Climate change predictions	24
3 Hydrological modelling	26
3.1 Model choice	26
3.2 HBV model description	27
3.2.1 Model structure and equations	27
3.2.2 Model parameters	32
3.3 Sensitivity analysis	33
3.3.1 Objective function	33
3.3.2 Sobol' sensitivity analysis	34
3.3.3 Results	36
3.3.4 Discussion and parameter selection	37
4 Methodology	40
4.1 Calibration procedure	40
4.1.1 Calibration data	41
4.1.2 Calibration algorithm	42
4.2 Correlations	43

4.2.1	Pearson correlation coefficient	44
4.2.2	Climate characteristics	44
4.2.3	Application	45
4.3	Linear regression analysis	46
4.3.1	Single and multiple linear regression	46
4.3.2	Selection of regression equations	49
4.4	Implementation of regression relations	49
4.4.1	Recalibration and validation performance	49
4.4.2	Regression model performance with GCM-RCM input	50
4.4.3	Selection and evaluation of regression model	51
4.5	Influence on climate change impact assessment	52
4.5.1	Projected climate change	52
4.5.2	Climate change impact assessment method	52
4.5.3	Comparison of predicted changes	53
5	Results	54
5.1	Calibration results	54
5.1.1	Base model	54
5.1.2	5-year windows	55
5.2	Correlation results	56
5.2.1	Explanatory correlations	56
5.2.2	Climate and parameter correlation	59
5.3	Regression analysis	62
5.3.1	Single linear regression	62
5.3.2	Multiple linear regression	63
5.4	Establishment of regression model	65
5.4.1	Recalibration and validation performance	65
5.4.2	Regression model performance with GCM-RCM input	67
5.4.3	Regression model selection and evaluation	68
5.5	Climate change impact assessment	68
5.5.1	Projected climate change	68
5.5.2	Climate change impact assessment	69
5.5.3	Comparison of projected runoff changes	75
6	Discussion	77
6.1	Place in recent developments	77
6.2	Data	77
6.3	Sensitivity analysis	78
6.4	Methodology	79
6.4.1	Research background	79
6.4.2	Calibration procedure	80
6.4.3	Suitability of objective function	81
6.4.4	Correlation procedure	82
6.4.5	Regression analysis	82

Contents

6.4.6	Implementation of regression equations	82
6.4.7	Climate change impact assessment	83
6.5	Results	84
7	Conclusions and recommendations	85
7.1	Conclusions	85
7.2	Recommendations	88
	Bibliography	91
	Appendices	96
A	Sensitivity analysis	96
A.1	Interaction between parameters	96
A.2	Influence of K_f and K_s on calibration	96
B	Calibration process	100
C	Regression analysis	103
C.1	Single linear regression plots	103
C.2	Multiple regression results	104
C.2.1	Regression equations	104
C.3	Parameter estimates with GCM-RCM input	112
D	Climate change impact assessment	117
D.1	Projected climate change	117
D.2	Influence of hydrological models	117
D.3	Influence of GCM-RCM input	119
D.4	Expected impact of climate change	119

List of Figures

2.1	Catchment location and overview	22
2.2	Land use Wełna catchment	23
2.3	Measuring stations in Wełna catchment	24
3.1	HBV model structure	28
3.2	Rain-snow interval used in HBV model	29
3.3	Variance decomposition from sensitivity analysis	37
4.1	Overview of calibration periods	43
4.2	Calibration and validation periods after regression	51
5.1	Calibration results of 5-year windows	56
5.2	Calibration results	57
5.3	FDC of observed and simulated Q (observed input)	70
5.4	FDC of simulated Q (observed and GCM-RCM input)	72
5.5	FDC of simulated Q (present and future GCM-RCM input)	73
A.1	Interaction of β with other parameters	97
A.2	Interaction of K_f with other parameters	98
A.3	Calibration of K_f and K_s	99
B.1	Calibration results of 5 year periods	100
B.2	Correctly and incorrectly modelled fast and slow runoff	102
C.1	Single linear regression of significant correlations FC	104
C.2	Single linear regression of significant correlations α	105
C.3	Single linear regression of significant correlations K_s	105
C.4	Single linear regression of significant correlations $PERC$	106
C.5	Estimates of FC values based on GCM-RCM input	112
C.6	Estimates of α values based on GCM-RCM input	113
C.7	Estimates of $PERC$ values based on GCM-RCM input	114
C.8	Climate characteristics from GCM-RCM projected present P	115
C.9	Climate characteristics from GCM-RCM projected future P	116

List of Tables

2.1	Global and Regional Climate Models	25
3.1	HBV parameter ranges	32
3.2	Variance decomposition from sensitivity analysis	38
3.3	Default values for HBV parameters	39
4.1	Calibration and validation periods	42
4.2	SCEM-UA settings	43
4.3	F-values for regression significance	49
5.1	Calibration and validation of base model	54
5.2	Interrelation of climate variables and correlation with runoff .	58
5.3	Correlation coefficients for climate characteristics	59
5.4	Single linear regression results	62
5.5	Multiple linear regression results FC	63
5.6	Multiple linear regression results α	64
5.7	Multiple linear regression results K_s	64
5.8	Multiple linear regression results $PERC$	65
5.9	Regression equation fit and implementation in HBV	66
5.10	Calibration and validation of regression models	66
5.11	Statistics of observed and simulated Q (observations as input)	70
5.12	Statistics of simulated Q (observed and GCM-RCM input) . .	72
5.13	Statistics of simulated Q (present and future GCM-RCM input)	74
5.14	Differences in changes projected by base and regression model	75
6.1	Observed and estimated frequency of wet days ($P>0.1\text{ mm}$) .	84
7.1	Results of calibrated regression coefficients	90
B.1	Restricted parameters ranges for calibration	102
C.1	Full multiple linear regression results FC	107
C.2	Indices of multiple linear regression FC	107
C.3	Full multiple linear regression results α	108
C.4	Indices of multiple linear regression α	109
C.5	Full multiple linear regression results K_s	110
C.6	Indices of multiple linear regression K_s	110

List of Tables

C.7 Full multiple linear regression results *PERC* 111
 C.8 Indices of multiple linear regression *PERC* 111

D.1 Comparison of observed and GCM-RCM projected P 117
 D.2 Comparison of observed and GCM-RCM projected T 118
 D.3 Comparison of observed and GCM-RCM projected PET 118
 D.4 Observed and simulated Q (observations as input) 118
 D.5 Simulated Q (observed and GCM-RCM input) 119
 D.6 Simulated Q (present and future GCM-RCM input) 120

List of Symbols

α	Non-linearity parameter, HBV parameter
β	Non-linearity parameter, HBV parameter
ar_{μ}	5-year average aridity index
$c_{1,2,\dots}$	Regression coefficients
$c_{n,scem}$	Jump rate, SCEM-UA parameter
cov_{x_i,y_i}	Covariance between series x_i and y_i
<i>CFLUX</i>	Rate of capillary rise, HBV parameter
<i>CFMAX</i>	Degree-day factor, HBV parameter
<i>CFR</i>	Refreezing factor, HBV parameter
et_a	Actual evapotranspiration
<i>FC</i>	Field capacity or maximum soil moisture storage, HBV parameter
<i>FOCFMAX</i>	Degree-day factor corrected for forests, HBV parameter
K_f	Fast run-off parameter, HBV parameter
K_s	Slow run-off parameter, HBV parameter
<i>LP</i>	Factor limiting actual evapotranspiration, HBV parameter
m	Degrees of freedom in the regression equation
MS_E	Mean squares due to errors
MS_R	Mean squares due to regression
n_{scem}	Number of parameters, SCEM-UA parameter
<i>NS</i>	Nash-Sutcliffe coefficient
p	Significance level
p_z	Coefficient of regression polynomial
$P_{\mu,s}$	5-year average of daily P observations during summer (June, July, August)
$P_{\mu,w}$	5-year average of daily P observations during winter (December, January, February)
P_{μ}	5-year average of daily P observations

List of Tables

P_{max}	5-year average of annual maximum P observations
$P_{wet,\mu,s}$	5-year average of daily P_{wet} observations during summer (June, July, August)
$P_{wet,\mu,w}$	5-year average of daily P_{wet} observations during winter (December, January, February)
$P_{wet,\mu}$	5-year average of daily P_{wet} observations
P_{wet}	Precipitation intensity on days with $P > 0.1mm$
P_r	Precipitation as rain
P_s	Precipitation as snow
P	Precipitation
$PERC$	Percolation rate, HBV parameter
$PET_{\mu,s}$	5-year average of daily PET observations during summer (June, July, August)
$PET_{\mu,w}$	5-year average of daily PET observations during winter (December, January, February)
PET_{μ}	5-year average of daily PET observations
PET_{max}	5-year average of annual maximum PET observations
PET	Potential evapotranspiration
q_{in}	Infiltration flux, HBV variable
q_{scem}	Number of complexes, SCEM-UA parameter
q_{seep}	Seepage flux, HBV variable
q_c	Capillary rise flux, HBV variable
q_d	Direct run-off flux, HBV variable
q_f	Fast run-off flux, HBV variable
q_m	Snow melt flux, HBV variable
q_r	Refreezing flux, HBV variable
q_s	Slow run-off flux, HBV variable
q_t	Total run-off flux, HBV variable
Q_{obs}	Observed discharge
Q_{sim}	Simulated discharge
r	Pearson's linear correlation coefficient
R^2	Goodness of fit of regression equation
RVE	Relative volume error
σ_{x_i}	Standard deviation of series x_i
σ_{y_i}	Standard deviation of series y_i
S_{fr}	Fast run-off reservoir storage, HBV variable
$S_{interactions}$	Normalized Sobol' interaction effect of parameter i
S_{mw}	Liquid (melted) water storage, HBV variable
s_{scem}	Population size, SCEM-UA parameter
S_{sm}	Soil moisture storage, HBV variable
S_{sp}	Snow pack storage, HBV variable
S_{sr}	Slow run-off reservoir storage, HBV variable
S_{Ti}	Normalized Sobol' total effect of parameter i

List of Tables

S_i	Normalized Sobol' main effect of parameter i
SS_E	Error sum of squares
SS_R	Sum of squares due to regression
SS_T	Total sum of squares
$T_{\mu,s}$	5-year average of daily T observations during summer (June, July, August)
$T_{\mu,w}$	5-year average of daily T observations during winter (December, January, February)
T_μ	5-year average of daily T observations
T_{max}	5-year average of annual maximum T observations
T_{scem}	Likelihood ratio, , SCEM-UA parameter
T	Temperature
TT	Temperature threshold, HBV parameter
TTI	Temperature threshold interval length, HBV parameter
$V(Y)$	Variance in model output
V_{Ti}	Sobol' total effect of parameter i
V_i	Sobol' main effect of parameter i
WHC	Water holding capacity of snow, HBV parameter
x	Example series for Pearson's linear correlation coefficient
X_{-i}	Annotation of all parameters apart from parameter i in Sobol' method
X_i	Annotation of i parameters in Sobol' method
y	Example series for Pearson's linear correlation coefficient
$y_{r,i}$	Observed value used to determine the regression equation
$\bar{y}_{r,i}$	Mean of $y_{r,i}$
$\hat{y}_{r,i}$	Estimate of $y_{r,i}$ by the regression equation
$y_r(x)$	Fitted regression equation
Y	Objective function used to quantify model performance
z	Degree of regression polynomial

Chapter 1

Introduction

This chapter introduces the topic of parameter non-stationarity and gives an overview of this study. Section 1.1 presents a summary of recent research on climate change and explains the issue of parameter non-stationarity that can occur when a hydrological model is used for climate change impact assessment. Section 1.2 defines the research goal, which is broken down into several research questions in section 1.3. Section 1.4 gives an overview of the research strategy and a reading guide for this document.

1.1 Problem summary

1.1.1 Climate change

Observations show that recent years (2001-2011) are amongst the warmest in recorded history (National Climatic Data Centre, 2011). Changes in atmospheric concentrations of greenhouse gasses and aerosols (suspended fine soil or liquid in a gas, e.g. clouds and smog) and changes in land cover and solar radiation alter the energy balance of the climate system. It is very likely that recent changes resulting from human activities have lead to the net observed warming effect (International Panel on Climate Change [IPCC]; 2007).

Projections of future climate change start with greenhouse gas emission scenarios. These give possible scenarios of the development of human emissions and are used as input for carbon cycle models (IPCC, 2001a). Projections of future radiative forcing from carbon cycle models are then used as input for Global Climate Models [GCMs] (Coron et al., 2012), resulting in projections of future climate variables (e.g. precipitation and temperature) (IPCC, 2011).

Projections of global averaged surface warming for the year 2100 vary per emission scenario and GCM, within the likely range of +1.1 to +6.4°C, relative to the period 1980-1999 (IPCC, 2007). Temperature increase leads to higher evapotranspiration and an increase of water vapour input into the atmosphere (Nakicenovic et al., 2000), which in turn affects precipitation patterns around the globe. Precipitation changes include changes in the total amount of rainfall, the intensity of rainfall events, or both. Expected changes in average precipitation for the period 2090-2099 vary per

region, up to possible increases and decreases of 20% compared to 1980-1999 (based on averaged results of multiple GCMs). The amount of precipitation is expected to change for many regions in this time frame, leading to more extreme events in both the high and low extremes (i.e. potential for floods and draughts) (IPCC, 2007).

1.1.2 Hydrological changes

Changes in precipitation patterns and average temperature both have impacts on the hydrological cycle: examples include observations of increased runoff and earlier spring peak discharges (IPCC, 2007). Future effects of climate change on runoff are simulated with hydrological models (Andersson et al., 2006). GCM output is however not directly usable as input for hydrological models, due to differences in their respective spatial scales (i.e. global and catchment scale) (Bergström et al., 2001). Various downscaling techniques exist to make GCM output usable as hydrological model input (e.g. Jiang et al. (2007)).

It is a common assumption that a conceptual hydrological model, with parameter values calibrated on historical data, is able to predict future runoff from down-scaled GCM input (i.e. that the optimal parameter set for future climatic conditions is not different from the optimal parameter set derived from calibration). However, it is uncertain whether hydrological models are able to perform well under climatic conditions that are different from the climate conditions during their calibration period. Multiple studies have been undertaken to evaluate model performances under contrasted climate conditions (e.g. Bastola et al., 2011; Chiew et al., 2009; Coron et al., 2012; Merz et al., 2011; Refsgaard and Knudsen, 1996; Seibert, 2003; Vaze et al., 2010; Wilby, 2005; Xu, 1999). As a general conclusion, models perform adequately when changes in average precipitation are small. However, the exact definition of “small changes” varies per study. Merz et al. (2011) present the widest range of precipitation changes for which the hydrological model still performs adequately: -15% to +20%. Models generally show a lower decline in performance when applied to drier conditions than present during calibration, than when applied to conditions wetter than calibration conditions.

Optimal model parameters can be different from calibrated parameters when a hydrological model is used for a period different from its calibration period, for two possible reasons. First, calibrated parameter sets tend to compensate for problems in model structure and data sets. The optimal parameter sets might therefore change when different calibration periods are used, because they compensate for different errors. Second, some parameters might indeed be subject to changes in time, as a result of direct (e.g. changes in land-use or river networks) and indirect (e.g. changes in climatic conditions, such as air temperature and precipitation patterns) human-induced

1.1. Problem summary

changes (Merz et al., 2011), that influence the hydrological processes that the parameters represent. The effect of calibrated parameters changing due to climate fluctuations is currently not well understood (Wagener et al., 2010).

1.1.3 Parameter non-stationarity

Merz et al. (2011) presents strong evidence that a correlation exists between calibrated parameter values and certain climate variables. Because climate variables have changing values over time, and assuming that the observed correlation is the result of an actual relationship between parameter values and climate variables, the common assumption that optimal values of calibrated parameters do not change over time is therefore not always true. These changes in optimal parameter values are here referred to as parameter non-stationarity. That parameter non-stationarity exists lowers confidence in model results when the model is used for predictions with climate variables that are different from those during calibration of the parameters.

Merz et al. (2011) suggest two different approaches: the first option would be expanding the model structure to account for more catchment processes (e.g. including the length of the growing season for plants in the model, since an increase in temperature would lengthen the season and thus increase the amount of evapotranspiration which influences runoff).

The second option would be to explicitly account for non-stationary model parameters. Determined correlations between optimal parameter values and climate variables can be used to predict parameter values for various climate conditions. This approach requires less to no changes in model structure, but might be complicated due to complex correlations.

1.1.4 Problem definition

Performance of conceptual hydrological models is shown to decline when the models are used for predictions under climate conditions that are very different from calibration conditions. This effect seems more notable when the change concerns a shift towards more wet conditions compared to calibration conditions. Long-term climate projections show an expected increase in volume and intensity of precipitation towards the year 2100. This means hydrological models will increasingly be used for projections under wetter conditions than they were calibrated on, potentially leading to a decrease in the accuracy of these projections. This has consequences in the field of water management; long term planning (e.g. construction of new dams, policies related to water use, flood prevention) will become more difficult. It is therefore desirable to improve the long term accuracy of hydrological models.

The decrease in hydrological model performance stems from parameter

1.2. Research goal

non-stationarity; the traditional assumption that calibrated parameters can accurately predict future runoff is not in all cases valid. It has been shown that certain calibrated parameters are correlated with climatic variables, and that optimal parameter values change when changes in climatic variables occur. This study attempts to account for parameter non-stationarity in hydrological models, to increase confidence in future runoff predictions.

It is however difficult to determine when a long-term runoff projection is more accurate than before. While calibration and validation procedures are done based on historical observations, the future can only be predicted and not known for certain. The added value of any approach concerning parameter non-stationarity is therefore difficult to verify.

1.2 Research goal

The research goal is to establish relationships between optimal model parameters and climate variables, to quantify how well these relationships perform during validation and to assess how these relationships perform during climate change impact assessment, compared to a traditional hydrological approach towards calibrated parameters. The Polish Wena catchment is used as a test case.

1.3 Research questions

The research goal is broken down into three research questions:

1. Which significant correlations are present between parameter values and climate variables and can these significant correlations be explained from a hydrological point of view?
2. For which parameters can these significant correlations be used to establish a significant regression equation, and what do these regression equations look like?
3. What is the influence of estimating certain parameter values from their relationship with climate variables on the changes predicted during climate change impact assessment, when compared with a traditional hydrological approach to climate change impact assessment?

1.4 Research strategy and reading guide

A test case with data, a hydrological model and a research set-up are required to fulfil the research goal. Chapter 2 describes the catchment and model input data used in this research. Chapter 3 explains the choice for the HBV model and gives a description of this model. Chapter 3 also includes a sensitivity analysis that is used to prepare the HBV model for this study, by reducing the number of calibration parameters. Chapter 4 explains the methodology followed in this study.

In short, the methodology leads to the establishing of a regression model, which uses estimated, rather than calibrated, parameter values. First, the HBV model is calibrated in two different ways, which leads to a base model (calibrated on 20 years of data) and optimal parameter sets for multiple 5-year windows. Second, correlations between the optimal 5-year parameter values and certain climate characteristics during these 5-year periods are determined. Significant correlation between two variables does not automatically imply a meaningful relation between these variables. Any significant correlations are therefore also evaluated from a hydrological point of view, to determine if a mathematical relationship based on this correlation might reflect a physically meaningful relation between a parameter value and climate. Third, single and multiple linear regression analysis are used to establish a mathematical equation for parameter values, based on meaningful correlations with climate characteristics. A trade-off is made between goodness-of-fit of the regression equation and the number of climate characteristics it includes, to reduce the chance of over-fitting the regression. Fourth, the regression equations are implemented in the HBV model and any parameters for which no regression equation can be established are recalibrated. Recalibration is used as a way to partly account for interaction between the model parameters estimated with regression equations and fixed parameters. Performance of the recalibrated regression models is quantified during validation and compared to validation of the base model. Last, a climate change impact assessment is performed with both the base and regression model. Results are compared to determine the effect of using a regression model on impact assessment outcome.

Chapter 5 present the results from the methodology described above, with a similar structure of its sections. Discussion of results, research methodology and general applicability is given in chapter 6. Conclusions and recommendations can be found in chapter 7.

Chapter 2

Study area and data

This chapter contains a description of the study area (section 2.1) and summary of the collected data (section 2.2).

2.1 Study area

The relatively small and flat Wełna catchment is used as a test case in this study. This catchment is used because of the strong preference for a Polish catchment. Earlier modelling experience showed that, from the available Polish catchments, Wełna generally provides the best modelling results (personal communication with experts at IGF). The river Wełna and its tributaries are part of the natural Polish river network of the Wielkopolska Lowland. The river network with its large valleys and narrow lakes was formed in the late Pleistocene and Holocene due to the retracting and melting of glaciers (Siniecki, 2009).

The river Wełna originates in lake Wierzbiczańskie, 8 km east of the city Gniezno. Its main tributaries are Mała Wełna, Flinta, Struga Gołaniecka, Struga Potulicka and Nielba. The Wełna joins the river Warta at the city Oborniki, having a total length of 117.8 km (figure 2.1). Warta itself is a tributary from the river Oder, which empties into the Baltic Sea. Including the various sub-catchments of its tributaries, the total catchment area of the Wełna river upstream from the flow measuring station is 2611 km^2 . 23% of the area is covered by forests. The remaining space is mostly used for agriculture, with a few scattered urban areas (figure 2.2, European Environment Agency [EEA], 2011).

Flow measurements are done at Kowanówko, 5.6 km away from the mouth of the Wełna. With the source of the Wełna located at +97 m.a.s.l., and the flow measuring station at +51 m.a.s.l., the average slope is 0.0004. Annual average flow is approximately 10 m^3/s (Wira, 2011).

Ten lakes with controlled discharges are located in the catchment, covering approximately 0.4% of the total catchment area. The catchment also includes 64 fish ponds and water storage systems. Located along the various rivers are 127 water control structures. Operation regimes and total catchment area upstream of the control structures are unknown. The catchment has a storage capacity of approximately 17.5 million m^3 (approximately 5.5%

2.2. Data collection

of the average total annual runoff), divided over dammed lakes (5.9 million m^3), weirs and control structures (4.0 million m^3) and fish ponds and water storage (7.6 million m^3) (Siniecki, 2009).

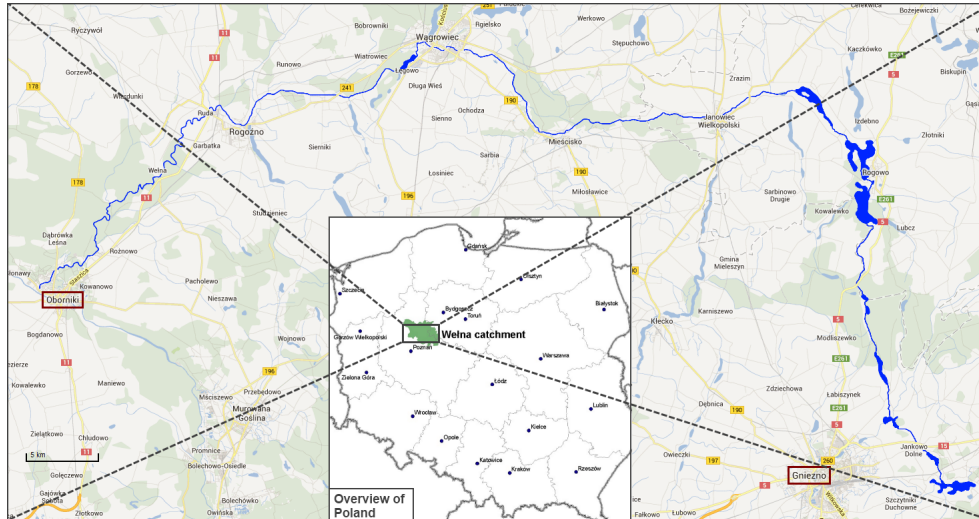


Figure 2.1: Location of the Wełna catchment in Poland (small figure) and overview of the catchment (large figure). The river Wełna (dark blue) originates east of Gniezno (lower right) and joins the river Warta at Oborniki (middle left) (image adjusted from various sources: maps.google.com, http://www.geo.norwid24.waw.pl/index.php?strona=120_mapa_polski and the Polish Academy of Sciences, Institute of Geophysics)

2.2 Data collection

This section describes the data series used in this research. Both historical observations and predictions of the future climate were provided by the Polish Academy of Sciences, Institute of Geophysics (IGF). Historical observations and projections of the future climate are given as daily values for temperature, potential evapotranspiration and precipitation. Daily observations of runoff are also available.

2.2.1 Historical observations

Historical observations of precipitation (P), temperature (T) and runoff (Q_{obs}) are available for the period 01-01-1971 to 31-12-2000.

Precipitation values are measured at 22 stations in and near the catchment. Thiessen polygons are used to generate a time series of catchment averaged precipitation that can be used as model input (figure 2.3). Because the catchment is relatively small and flat, variation in precipitation caused by characteristics in the landscape (e.g. mountains) is minimal. The data reflect this, showing only small differences between the measured pre-

2.2. Data collection

precipitation at the various stations. Temperature values are measured outside the catchment, at the town Szamotuly (figure 2.3, orange dot). This is accepted because of the small catchment size and flat landscape, but it does cast some doubt on the reliability of the data. Because a flat catchment is used, no corrections for differences in altitude are required. Potential evapotranspiration (*PET*) is derived from temperature with the Hamon method (Hamon, 1961). Runoff is measured at Kowanówko (figure 2.3, yellow dot).

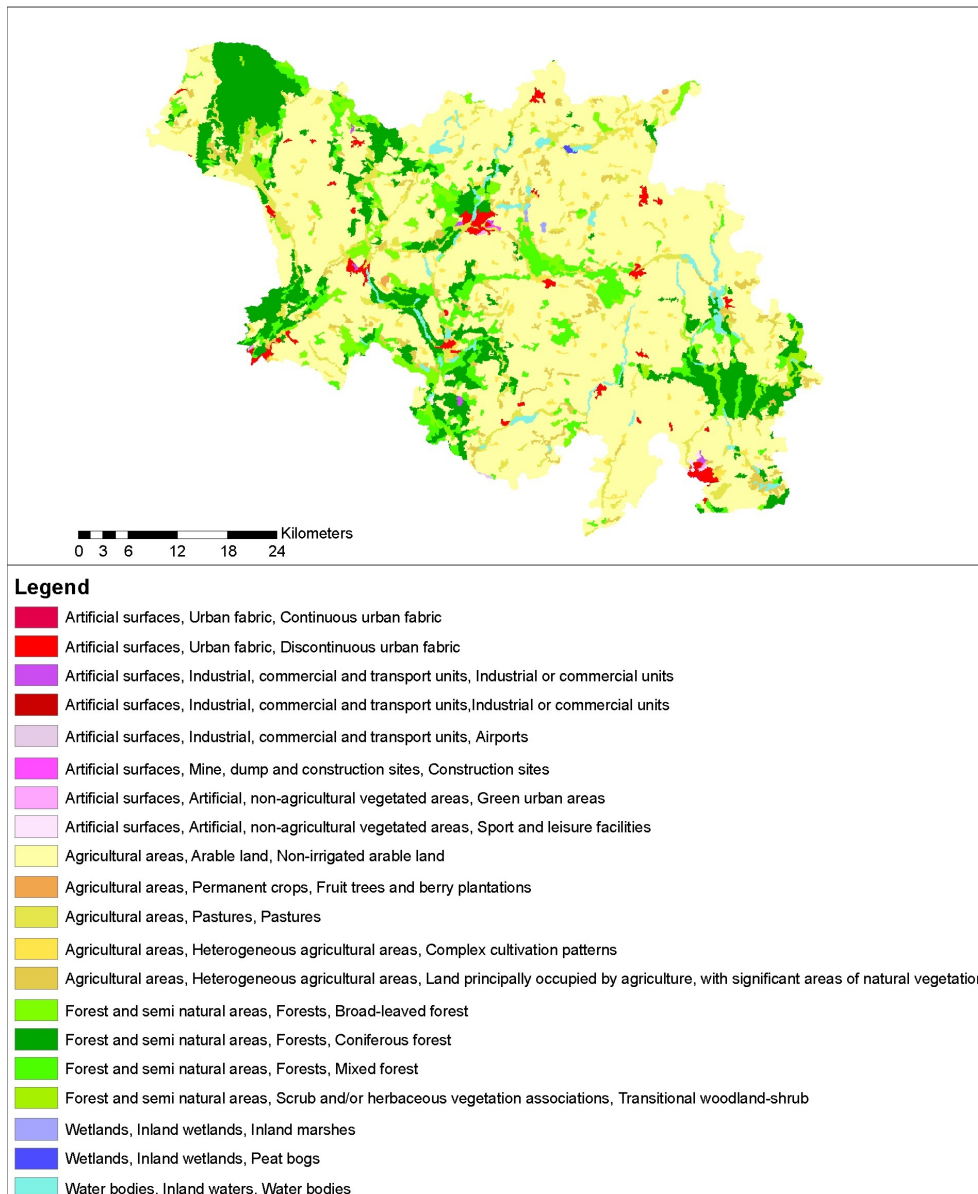


Figure 2.2: Land use in the Wezna catchment (EEA, 2011)

2.2. Data collection



Figure 2.3: Overview of the Wełna catchment (light green area) with Thiessen polygons around precipitation measuring stations. Stations are used for averaging of precipitation relative to the area of the catchment the polygon covers. Used stations are presented with green dots (part of the catchment falls inside the polygon), unused stations in red (no part of the catchment inside the polygon), flow measurement point in yellow and temperature measurement point in orange

P , T and PET are used as model input, while runoff data are used to calibrate and validate the model.

2.2.2 Climate change predictions

Predictions of future changes for precipitation and temperature in the Wełna catchment are available, based on results of five different combinations of Global and Regional Climate Models (GCM and RCM respectively, table 2.1) from the ENSEMBLES experiment (van der Linden and Mitchell, 2009). Five different combinations are used to capture the variability and uncertainty associated with application of different GCMs and RCMs for climate change projections (Déqué et al., 2007). Changes in potential evapotranspiration are estimated from changes in temperature, wind-speed, radiation and humidity by use of standard methods, such as the Penman-Monteith equation (Romanowicz and Osuch, s.d.).

Estimates of the five GCM-RCM combinations are based on the A1B scenario for future greenhouse gas concentrations, which has a time horizon of 2100. The A1 scenarios describe a future with rapid economic growth and introduction of new technologies, with a global population that peaks mid-century (2050) and declines again afterwards. This specific scenario focusses on a balanced (B) usage of fossil and non-fossil energy sources (Nakicenovic

2.2. Data collection

Table 2.1: Combinations of Global Climate Models (GCM) and Regional Climate Models (RCMs) used in this study

GCM	RCM	Source GCM, RCM
ARPEGE	DMLHIRHAM5	Déqué et al. (1994), Christensen et al. (2007)
ARPEGE	RM5.1	Déqué et al. (1994), Radu et al. (2008)
ECHAM5	MPLM_REMO	Roeckner et al. (2003), Jacob (2001)
ECHAM5	KNMI_RACMO_2	Roeckner et al. (2003), van Meijgaard et al. (2008)
BCM	SMHIRCA	Furevik et al. (2003), Kjellström et al. (2005)

et al., 2000).

Output of the GCM-RCM combinations is biased, and not directly usable as input for the hydrological model. Therefore bias-correction of the GCM-RCM estimates is performed with a quantile mapping method. In this method cumulative distribution functions of observed and simulated climate variables are compared and used to determine a transformation function for the simulated climate, such that its transformed distribution resembles the observed distribution (Gudmundsson et al., 2012). Adjustments are based on a re-analysis of climate data. This is a different data set from observed climate data, which leads to differences between average observed and average GCM-RCM projected precipitation, temperature and potential evapotranspiration. GCM-RCM projected P is on average 11% lower than observed, projected T is on average 0.2% lower than observed and projected PET is on average 1.5% higher than observed (appendix D, tables D.1, D.2 and D.3).

Chapter 3

Hydrological modelling

This chapter presents the considerations for using the Hydrologiska Byråns Vattenbalansavdelning (HBV) model (section 3.1). Section 3.2 describes model structure, equations and parameters (section). A sensitivity analysis is used to reduce the number of parameters for calibration from 14 to 6 (section 3.3) and thus prepare the model for use in this study.

3.1 Model choice

A hydrological model aims to simulate certain hydrological processes that occur in a catchment and give an estimate of the total runoff out of the catchment. A wide variety of models exists, each with its own strengths and weaknesses (e.g. physically-based models, conceptual models, empirical models, Romanowicz et al., s.d.). A conceptual model represents those hydrological processes that are considered to be important in determining the relationship between input (temperature, potential evapotranspiration and precipitation) and output (runoff). With conceptual models, not all parameters have a direct physical interpretation but need to be calibrated against observed data (Pechlivanidis et al., 2011).

Recent research based on conceptual rainfall-runoff models, shows that calibrated parameter values are difficult to transpose to periods with different climatic conditions than conditions present during the calibration period (e.g. Bastola et al. (2011); Chiew et al. (2009); Coron et al. (2012); Merz et al. (2011); Seibert (2003); Vaze et al. (2010); Wilby (2005); Xu (1999)). Because the issue of transposing parameters to different climatic conditions is addressed in this study, a conceptual model is used here as well.

The Hydrologiska Byråns Vattenbalansavdelning (HBV) model (Lindström et al., 1997) used in this study is a conceptual rainfall-runoff model. The HBV model is chosen for several reasons. First, it is a proven model and has been in use for a long time, with the first application dating from early 1970. Since then, multiple revisions and adjustments have been made resulting in the HBV-96 model (Lindström et al., 1997). After that, the model has continuously been adapted to specific needs for different studies, catchments, etc.

Second, the model output depends on the climate, since it uses climatic

3.2. HBV model description

variables such as temperature, precipitation and evapotranspiration as input, in order to estimate catchment runoff. This makes it suitable for this study, which aims to clarify the potential relation between climatic variables and model parameter values.

Third, the HBV model has been applied at both the University of Twente and the Institute of Geophysics before. Experience with the model is thus available at both institutes.

3.2 HBV model description

The HBV version used in this research is an adjusted version from the model applied by Tillaart (2010), which is a Matlab implementation of the HBV-15 model developed in Fortran by Booij (2002). The HBV-15 model links 15 sub basins of the Meuse river. Individual sub basins are modelled with the HBV-96 model (Booij, 2005). In this study a single basin is considered.

The adjustments to the model for this study are the inclusion of limits to equations for several fluxes and storages, to stay within physical bounds. Under certain conditions, some storages could reach negative values, leading to complications in the calculations for later time steps. This has been corrected.

3.2.1 Model structure and equations

Figure 3.1 shows the HBV model structure as implemented in Matlab. Model parameters are given on the left side of the figure.

The model consists of four active routines, concerning the accounting of precipitation, soil moisture balance, quick runoff and slow runoff. Delays in flood routing and flood wave attenuation are expected to fall within the considered model time step of 1 day. Routing and transformation routines for total runoff are therefore not required (personal communication with experts at IGF).

The model uses five storage boxes, connected by various fluxes. Storages and fluxes are described per routine in the following sections. Model input are time series of daily precipitation P [mm], daily temperature T [°C] and daily potential evapotranspiration PET [mm]. Total catchment area and the fraction of the catchment with forest cover are used as variables. The model calculates all fluxes and storage terms in unit [mm] with a daily time step, which allows the input series P , T , PET and parameters $CFMAX$ ($[mm\ ^\circ C^{-1}\ d^{-1}]$), $CFLUX$ ($[mm\ d^{-1}]$), K_f ($[d^{-1}]$), and K_s ($[d^{-1}]$) to be used without difficulty. Model output is a time series of simulated discharge Q_{sim} [m^3/s], converted from the daily total runoff flux [mm].

3.2. HBV model description

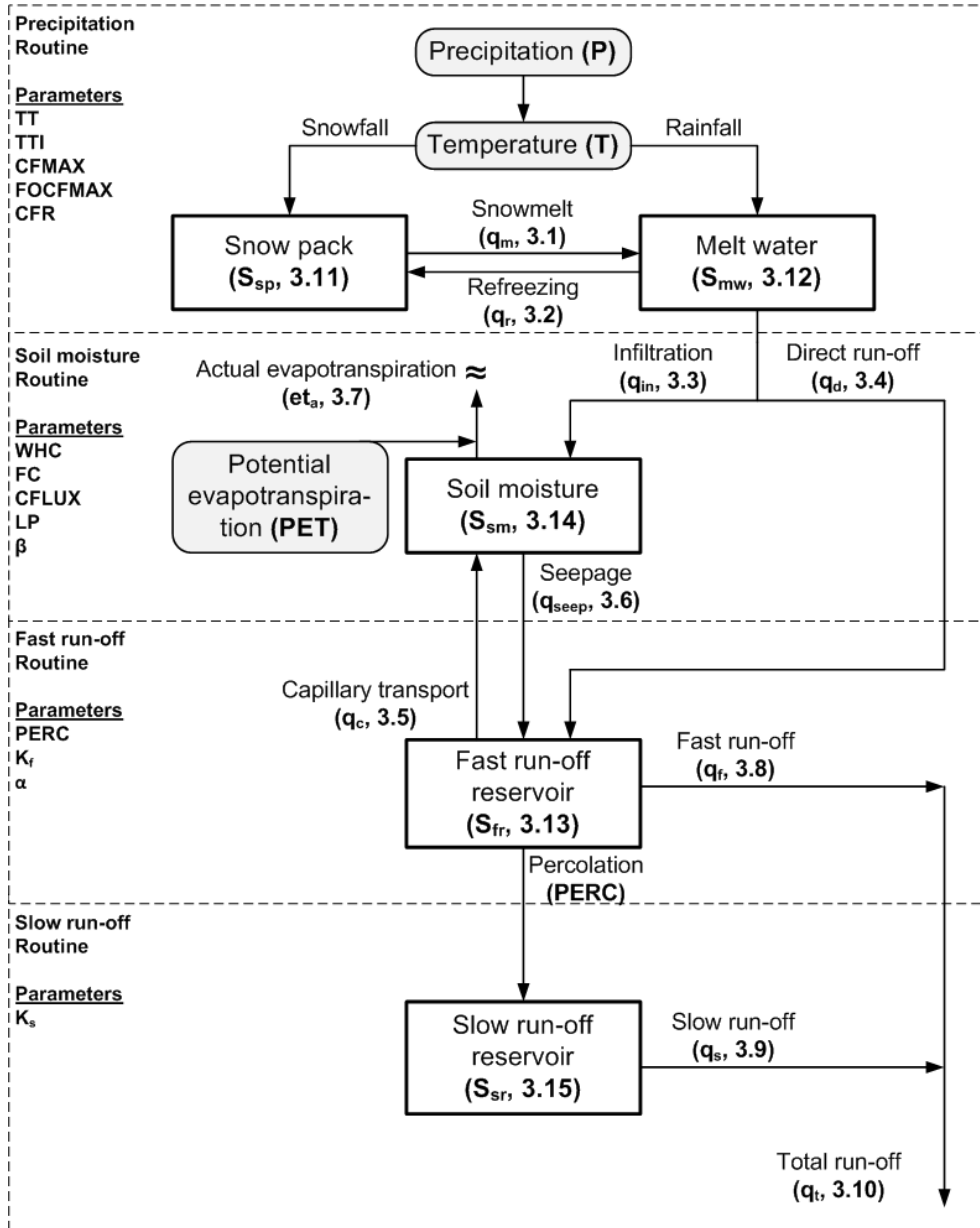


Figure 3.1: Structure of the HBV model applied in this study. Model inputs (P , T and PET) are shown in grey rounded boxes, storages in regular boxes and fluxes as arrows. Numbers correspond to equations in section 3.2.1

3.2. HBV model description

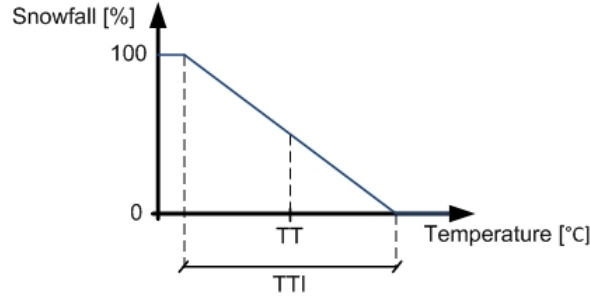


Figure 3.2: Visualisation of the rain-snow interval, including parameters TT and TTI

Precipitation routine

The precipitation routine determines whether precipitation occurs as rainfall, snowfall, or a combination of both. Precipitation at a daily time step t , $P(t)$, is divided into rainfall $P_r(t)$ and snowfall $P_s(t)$ based on daily temperature $T(t)$. Parameters TT [$^{\circ}\text{C}$] and TTI [$^{\circ}\text{C}$] define an interval in which precipitation is assumed to be a mix of snow and rain, decreasing linearly from 100% snow at the lower end to 0% snow at the upper end. TT is the threshold temperature where 50% of precipitation occurs as snow and 50% as rain. TTI specifies the interval length (figure 3.2).

Snow and rain are directed into different storage boxes; snow pack S_{sp} [mm] and melt water S_{mw} [mm] respectively. Interaction between snow pack and melt water boxes is given by snow melt q_m [mm] (eq. 3.1) and refreezing fluxes q_r [mm] (eq. 3.2):

$$q_m(t) = CFMAX * (T(t) - TT) \quad (3.1)$$

$$q_r(t) = CFR * CFMAX * (TT - T(t)) \quad (3.2)$$

- $CFMAX$ = degree-day factor; rate of snow melt [$mm \ ^{\circ}\text{C}^{-1} \ d^{-1}$]
- CFR = refreezing factor of water released from melting snow [-]
- TT = threshold temperature [$^{\circ}\text{C}$]

Soil moisture routine

Water enters the soil moisture routine from the precipitation and fast runoff routines. Water from the precipitation routine is divided into infiltration q_{in} [mm] (eq. 3.3) into the soil moisture storage S_{sm} and direct runoff into the fast runoff routine q_d [mm] (eq. 3.4). In the coding, the infiltration equation gives the total influx from the precipitation routine. The direct runoff equation makes the distinction between infiltration and direct runoff, where part of the melted water is temporarily retained in the snow pack (if

3.2. HBV model description

present) through parameter WHC (simulating the water holding capacity of snow). Retained water is assumed to infiltrate into the soil moisture routine on $t + 1$:

$$q_{in}(t) = S_{mw}(t) + q_m(t) + P_r(t) - q_r(t) - WHC * S_{sp}(t) \quad (3.3)$$

$$q_d(t) = q_{in}(t) + S_{sm}(t) - FC \quad (3.4)$$

WHC = water holding capacity of snow [$mm \ mm^{-1}$]
 FC = field capacity, maximum storage in S_{sm} [mm]

Capillary rise q_c [mm] (eq. 3.5) from the fast runoff routine replenishes soil moisture storage, providing that soil moisture storage is not yet saturated:

$$q_c(t) = CFLUX * \frac{FC - S_{sm}(t)}{FC} \quad (3.5)$$

$CFLUX$ = rate of capillary rise [$mm \ d^{-1}$]

Soil moisture storage releases water as seepage q_{seep} [mm] (eq. 3.6) into the fast runoff routine and actual evapotranspiration et_a [mm] (eq. 3.7) which leaves the model completely:

$$q_{seep}(t) = \left(\frac{S_{sm}(t)}{FC} \right)^\beta * (q_{in}(t) - q_d(t)) \quad (3.6)$$

$$\begin{aligned} et_a(t) &= et_p(t) * \frac{S_{sm}(t)}{LP * FC} && \text{if } S_{sm}(t) < LP * FC \\ et_a(t) &= et_p(t) && \text{if } S_{sm}(t) \geq LP * FC \end{aligned} \quad (3.7)$$

β = non-linearity parameter [-]
 et_p = model input series PET, corrected for different evapotranspiration rate in forests [mm]
 LP = factor limiting potential evapotranspiration [-]

Fast runoff routine

The fast runoff reservoir S_{fr} [mm] receives water from direct runoff and seepage. Three outflows exist; capillary transport to soil moisture q_c [mm] (eq. 3.5), percolation to the slow runoff routine (which is not expressed as an equation, but rather calibrated as a model parameter $PERC$ [$mm \ d^{-1}$]) and fast runoff out of the model q_f [mm] (eq. 3.8):

$$q_f(t) = K_f * S_{fr}(t)^{1+\alpha} \quad (3.8)$$

3.2. HBV model description

$$\begin{aligned} K_f &= \text{fast runoff parameter } [d^{-1}] \\ \alpha &= \text{non-linearity parameter } [-] \end{aligned}$$

Slow runoff routine

The slow runoff reservoir S_{sr} [mm] has a single influx from percolation (*PERC*) and a single outflow as slow runoff q_s [mm] (eq. 3.9):

$$q_s(t) = K_s * S_{sr}(t) \quad (3.9)$$

$$K_s = \text{slow runoff parameter } [d^{-1}]$$

Slow and fast runoff are combined into total runoff q_t [mm] (eq. 3.10):

$$q_t(t) = q_f(t) + q_s(t) \quad (3.10)$$

Changes in storage terms

The storage terms are updated based on daily fluxes. Safeguards are included for cases where total outflow fluxes exceed the total of current storage and inflow fluxes. In this case the storage term is set at zero, rather than letting it reach physically impossible negative storage values, which also prevents numerical issues in the model equations.

Snow pack storage:

$$S_{sp}(t+1) = S_{sp}(t) + P_s(t) + q_r(t) - q_m(t) \quad (3.11)$$

Melt water storage:

$$S_{mw}(t+1) = S_{mw}(t) + P_r(t) + q_m(t) - q_r(t) - q_{in}(t) \quad (3.12)$$

Soil moisture storage:

$$S_{sm}(t+1) = S_{sm}(t) + q_{in}(t) - q_d(t) - q_{seep}(t) + q_c(t) - et_a(t) \quad (3.13)$$

Fast runoff reservoir storage:

$$S_{fr}(t+1) = S_{fr}(t) + q_d(t) + q_{seep}(t) - PERC - q_f(t) - q_c(t) \quad (3.14)$$

Slow runoff reservoir storage:

$$S_{sr}(t+1) = S_{sr}(t) + PERC - q_s(t) \quad (3.15)$$

3.2. HBV model description

3.2.2 Model parameters and ranges

The HBV model without routing and transformation routines includes eight calibration parameters (FC , LP , α , β , K_f , K_s , $PERC$ and $CFLUX$). For this catchment however, certain parameters in the snow routine might need to be calibrated for proper simulations as well. Following Kollat et al. (2012), the following parameters in the snow routine are included as calibration parameters: TT , TTI , CFR , WHC and $CFMAX$. Parameter $FOCFMAX$ ($CFMAX$ corrected for reduced snow melt rate in forests) is included as well, because nearly a quarter of the catchment is covered by forests and the reduced snow melt rate might be important for overall model functioning. This gives a total of 14 calibration parameters.

Parameters are evaluated within pre-set ranges, based on literature and practical experience with this specific combination of catchment and model (table 3.1).

Table 3.1: Parameter ranges for the 14 parameters used in the sensitivity analysis. Source: ¹Deckers (2006), ²Romanowicz et al. (s.d.), ³Kollat et al. (2012)

Parameter	Min	Max	Unit	Description
¹ FC	0	500	[mm]	Field capacity, maximum soil moisture storage
¹ β	1	6	[-]	Non-linearity parameter
¹ LP	0.1	1	[-]	Factor limiting actual evapotranspiration
¹ α	0	3	[-]	Non-linearity parameter
¹ K_f	0.0005	0.3	[d^{-1}]	Fast runoff parameter
¹ K_s	0.0005	0.3	[d^{-1}]	Slow runoff parameter
¹ $PERC$	0	6	[$mm d^{-1}$]	Rate of percolation
² $CFLUX$	0	4	[$mm d^{-1}$]	Rate of capillary rise
³ TT	-3	3	[$^{\circ}C$]	Threshold temperature
³ TTI	0	7	[$^{\circ}C$]	Threshold temperature interval length
³ $CFMAX$	0	20	[$mm ^{\circ}C^{-1} d^{-1}$]	Degree day factor, rate of snow melt
$FOCFMAX$	0.1	1	[-]	$CFMAX$ corrected for forests
³ CFR	0	1	[-]	Refreezing factor
³ WHC	0	0.8	[$mm mm^{-1}$]	Water holding capacity of snow

3.3 Sensitivity analysis

Section 3.2.2 specifies 14 free parameters for the HBV model. Calibrating 14 parameters will take a very long time, because of the large number of possible combinations of parameter values involved. A sensitivity analysis is applied to reduce the number of calibration parameters and thus prepare the model for use in this study.

Sensitivity analysis shows the influence of each parameter on a measure of model performance, the so-called objective function (section 3.3.1). The reaction of the objective function to sources apart from parameter values, such as input data and model structure, is considered beyond the scope of this study. Section 3.3.2 details the choice of the sensitivity analysis method and gives a description of the method and its application in this study. Results are presented in section 3.3.3, conclusions in section 3.3.4.

3.3.1 Objective function

An objective function or target functions is a common approach to quantify model performance, by calculating a certain measure for the difference between observed and modelled discharge. An objective function focusses on a specific aspect of the hydrograph and therefore for different modelling goals, different objective functions should be used (Romanowicz et al., s.d.).

The Nash-Sutcliffe coefficient (NS) is commonly used as a goodness-of-fit-indicator for hydrological modelling (Romanowicz et al., s.d.). However, for researching model performance under changing catchment conditions, many authors prefer a combination of goodness-of-fit indicator with a measure for the volume error produced by the model; examples include Refsgaard and Knudsen (1996, NS, flow duration index and water balance), Seibert (2003, NS, groundwater coefficient, R_{peak}), Chiew et al. (2009, NS and Relative Volume Error), Xu (1999, NS and Relative Error), Wilby (2005, NS and bias indicator relative absolute mean error E), Vaze et al. (2010, weighted combination of NS and logarithmic bias function), Bastola et al. (2011, NS and Volume Error), Merz et al. (2011, function based on NS of runoff, NS of logarithmic runoff and Volume Error) and Coron et al. (2012, function based on Root-Mean-Square-Error of runoff and bias).

Furthermore, calibration experiments in this study have shown that when using only NS as objective function (which has an inherent bias towards medium and high flows) large volume errors can result with relatively good NS values (e.g. NS=0.83, 10% volume error for calibration, NS=0.70, 20% volume error for validation). Therefore an objective function is used that combines goodness-of-fit from NS with a measure for the volume error in the simulated runoff (Relative Volume Error, RVE); referred to as Y (Akhtar et al., 2009):

3.3. Sensitivity analysis

$$Y = \frac{NS}{1 + |RVE|} \quad (3.16)$$

With:

$$NS = 1 - \frac{\sum_{i=1}^{i=N} [Q_{sim}(i) - Q_{obs}(i)]^2}{\sum_{i=1}^{i=N} [Q_{obs}(i) - \bar{Q}_{obs}]^2} \quad (3.17)$$

$$RVE = \frac{\sum_{i=1}^{i=N} [Q_{sim}(i) - Q_{obs}(i)]}{\sum_{i=1}^{i=N} Q_{obs}(i)} \quad (3.18)$$

- Q_{sim} = discharge simulated by the HBV model
- Q_{obs} = observed discharge
- \bar{Q}_{obs} = mean of observed discharge

Equation 3.17 shows that when $Q_{sim} = \bar{Q}_{obs}$, $NS = 0$. In this case the simulated discharges perform the same as simply using the average discharge for predictions. When $Q_{sim} = Q_{obs}$, meaning perfect simulation, $NS = 1$. The numerator in Y can therefore have values from minus infinity to 1, where only positive values indicate that using the model results in better predictions than not using the model.

The optimal value for $RVE = 0$, meaning that no difference exists between observed and simulated volumes. Differences between observation and simulation can be both positive and negative. However, since the absolute value for RVE is used, the denominator of Y will always have a value equal to, or greater than, 1.

Since optimal values for NS and RVE are $NS = 1$ and $RVE = 0$, the optimal value for Y is equal to 1.

3.3.2 Sobol' sensitivity analysis

Method selection

Multiple methods for sensitivity analysis exist and are typically based on different assumptions on how to properly assess sensitivity. This can cause different methods to produce different results and thus rank parameters in a different order of importance (Frey and Patil, 2002). While the Sobol' method (Saltelli et al., 2004) is considered quite robust (e.g. Pappenberger et al. (2008); Tang et al. (2007)), it is generally advised to apply multiple methods to increase confidence in the importance of the various model parameters (Frey and Patil, 2002; Pappenberger et al., 2008).

An exploratory application of different methods, including the Sobol' method, identifiability analysis (e.g. Abebe et al. (2010); Saltelli et al.

(2004)), correlation coefficients and univariate sensitivity analysis (e.g. Tillaart (2010)), pointed out that there are drawbacks to each method. Comparing results of various sensitivity analyses is a subjective and time consuming task. Therefore just the Sobol' method is used, because of its robustness compared to other methods, especially with regard to the interaction between model parameters.

Description of Sobol' sensitivity index

The Sobol' method uses variance-based sensitivity indices. The goal is to determine the influence of each parameter on total variance in the model output. The model can then be simplified by assigning the parameters with low to no influence a fixed value and excluding them from calibration (Saltelli et al., 2004). The influence of an arbitrary parameter X_i on the variance of model output $V(Y)$ consists of the main effect ...

$$V_i = V[E(Y|X_i)] \quad (3.19)$$

... and total effect

$$V_{Ti} = V[E(Y|X_{-i})] \quad (3.20)$$

which are respectively the amount of variance removed from the total output variance if the true value of X_i were known, and the total amount of variance left unexplained if only X_i is left to vary and the true values of all other parameters, X_{-i} , are known. Main and total effect can be normalized by dividing them by total output variance:

$$S_i = \frac{V[E(Y|X_i)]}{V(Y)} \quad (3.21)$$

$$S_{Ti} = \frac{V[E(Y|X_{-i})]}{V(Y)} \quad (3.22)$$

The normalized total sensitivity index S_{Ti} consists of the main effect and the effect of the interaction of X_i with the other parameters:

$$S_{Ti} = S_i + S_{interactions} \quad (3.23)$$

$S_{interactions}$ is a bucket term containing the $2^{number\ of\ parameters} - 1$ sensitivity terms for X_i that describe the relationships between all possible combinations of parameters. If no interaction occurs between the parameters, $S_i = S_{Ti}$ for all X_i 's. This is called an additive model. In a non-additive model $S_i < S_{Ti}$ for at least one X_i (Ratto et al., 2007).

The Sobol' method is model independent, meaning that it does not depend on any assumptions between model input and output (such as linearity) (Saltelli et al., 2000), making it suited for application with the HBV model.

Application

A sensitivity package for Matlab was provided by the Polish Academy of Sciences, Institute of Geophysics, which returns S_i and S_{T_i} based on an extensive sampling simulation (75000 samples are used, the computational limit because of available RAM). The sensitivity analysis is performed for the full 30 years of observed data, with the target function Y (section 3.3.1).

The interaction between a specific parameter and the others follows from rewriting equation 3.23. In case of 14 free parameters, $S_{interactions}$ includes 16383 possible terms. It is not possible to determine which of all the possible interactions between parameters are responsible for the value of $S_{interactions}$ for any given parameter, because of the long computation times involved.

It is difficult to properly define a threshold above which a parameter is considered to have an important influence on generation of model output. Examples of thresholds of importance in literature are often not explained (e.g. Pappenberger et al., 2008) or self-proclaimed as subjective (e.g. Tang et al., 2007). The decision about which parameters to calibrate and which to fix at default values is thus inherently a subjective one.

This study aims to clarify the possible relationships between climate variables and optimal model parameter values. Interactions between parameters are not explicitly taken into account. Parameters that show a high total effect S_{T_i} will be calibrated, with a preference for parameters that also have a high main effect S_i (i.e. parameters that independently from others have a high influence on output variance). This preference stems from the fact that interactions between parameters are not taken into account during the establishing of relationships between individual parameters and climate variables.

3.3.3 Results

Figure 3.3 shows resulting sensitivity indices for all 14 parameters. Blue columns show the total sensitivity index S_{T_i} (eq. 3.22), while green and red columns split this up in main effect S_i (eq. 3.21) and interactions with other parameters respectively $S_{interactions}$ (eq. 3.23). Table 3.2 shows the quantitative results of the Sobol' method. The first column presents the total effect, while the second and third column split this in main effect and interactions with other parameters respectively. Parameters are ranked per column, in descending order of importance.

Figure 3.3 and the results quantified in table 3.2 show that the HBV model is a non-additive model (i.e. interactions between parameters are present, since $\sum S_i < 1$ and $\sum S_{T_i} > 1$, Saltelli et al., 2004). Approximately 60% of the total output variance is explained by the main effects, and approximately 40% is explained by interactions between parameters.

Several parameters show very small negative sensitivity indices, which

3.3. Sensitivity analysis

should not exist. This is a known issue with the Sobol' method; “readers should note that the truncation and Monte Carlo approximations of the integrals required in Sobol’s method can lead to small numerical errors [...] such as slightly negative indices” (Tang et al., 2007). Negative indices encountered here do not influence results.

3.3.4 Discussion and parameter selection

Just five parameters have discernible main effects S_i (table 3.2, first column): FC , $PERC$, α , TT and LP . FC has the most influence by far, the other four parameters only influence a marginal part of output variance through their respective main effects. Combined, main effects of these five parameters explain approximately 60% of total output variance. The remaining nine parameters all have negligible main effects.

Most parameters show larger interaction effects with other parameters $S_{interactions}$, than main effects (table 3.2, second column). While parameter FC is again the most influential, the difference between FC and the other parameters is less than when comparing their main effects. The five parameters with visible main effects (FC , α , $PERC$, TT and LP) explain nearly the entire effect of interactions on the total output variance.

The total influence of each parameter on the total output variance is shown in the third column of table 3.2. This shows the great influence of parameter FC , and the relative influence of parameters α , $PERC$, LP and

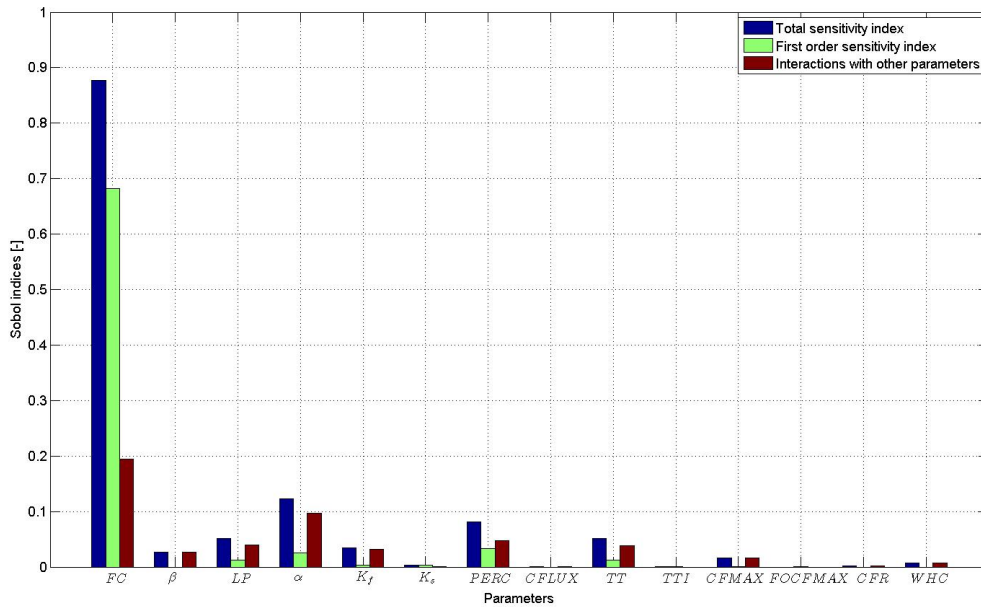


Figure 3.3: Results of variance decomposition for the HBV model applied to the Welna catchment, based on 30 years of observed data

3.3. Sensitivity analysis

Table 3.2: Results of variance decomposition for the HBV model of Weina, based on 30 years of observed data. Results are ranked per category based on unrounded values for sensitivity indices. Bold values show the selected parameters. The negative indices result from numerical errors in the method and do not influence the conclusions

	Main effect		Effect of interactions		Total effect	
1	<i>FC</i>	0.74	<i>FC</i>	0.20	<i>FC</i>	0.94
2	<i>PERC</i>	0.03	α	0.12	α	0.14
3	α	0.02	<i>PERC</i>	0.06	<i>PERC</i>	0.08
4	<i>LP</i>	0.02	K_f	0.05	K_f	0.05
5	<i>TT</i>	0.01	<i>TT</i>	0.04	<i>LP</i>	0.05
6	β	0.00	<i>LP</i>	0.03	<i>TT</i>	0.04
7	K_f	0.00	β	0.02	β	0.03
8	K_s	0.00	<i>CFMAX</i>	0.01	<i>CFMAX</i>	0.01
9	<i>FOCFMAX</i>	0.00	<i>WHC</i>	0.01	<i>WHC</i>	0.01
10	<i>TTI</i>	0.00	K_s	0.00	K_s	0.00
11	<i>CFR</i>	0.00	<i>CFLUX</i>	0.00	<i>FOCFMAX</i>	0.00
12	<i>CFLUX</i>	-0.00	<i>FOCFMAX</i>	0.00	<i>CFR</i>	0.00
13	<i>WHC</i>	-0.00	<i>CFR</i>	0.00	<i>CFLUX</i>	0.00
14	<i>CFMAX</i>	-0.00	<i>TTI</i>	0.00	<i>TTI</i>	0.00
Sum	(61%)	0.77	(39%)	0.50	(100%)	1.27

TT: these five parameter explain nearly all model output variance.

Because interactions between parameters are not explicitly accounted for in the remainder of this research, the main effect of parameters is considered more important for determining which parameters to calibrate. Initially, the five parameters (*FC*, *PERC*, α , *LP* and *TT* were selected for calibration, with the remaining parameters fixed at default values (influence of K_f , β , *CFMAX* and *WHC* through interactions can be neglected, appendix A, section A.1). However, the attempt to find suitable values at which to fix K_f and K_s showed the importance of calibrating K_s when shorter time periods are considered than the 30-year period used for the sensitivity analysis (appendix A, section A.2). Therefore six parameters are selected for calibration, the remaining parameters are assigned fixed values (table 3.3).

3.3. Sensitivity analysis

Table 3.3: Default values for parameters (Swedish Meteorological and Hydrological Institute [SMHI] 2004) that can be fixed according to the sensitivity analysis. Value for K_f is the result from earlier calibration of the HBV model for the Weina catchment, since a default value is not available

Parameter	Value	Unit
β	2.00	[-]
K_f	0.0005	[d^{-1}]
$CFLUX$	1.00	[$mm\ d^{-1}$]
TTI	2.00	[$^{\circ}C$]
$CFMAX$	3.50	[$mm\ ^{\circ}C^{-1}\ d^{-1}$]
$FOCFMAX$	0.60	[-]
CFR	0.050	[-]
WHC	0.1000	[$mm\ mm^{-1}$]

Chapter 4

Methodology

This chapter describes the various steps undertaken in this study. Section 4.1 describes the calibration procedure used to calibrate both the base model and multiple 5-year periods. Section 4.2 explains the method for calculating correlations and how it is used in this study. These results provide the information to answer research question 1.

Section 4.3 describes linear regression analysis and its application in this study. Results are regression equations for certain model parameters, that estimate the parameter value based on climate variables. Section 4.4 then details how these regression equations are implemented in the HBV code as regression models, and how each regression equation is expected to perform during climate change impact assessment. The regression model with the best expected performance is selected for further use. Sections 4.3 and 4.4 combined give the necessary information to answer research question 2.

Section 4.5 explains how the difference between using the base and regression model for climate change impact assessment is determined. These results answer research question 3.

4.1 Calibration procedure

Calibration is the procedure of adjusting values of model parameters, until output time-series are sufficiently similar to observed time-series in a catchment (Wagener et al., 2003).

Calibration can be done manually, with automated routines or a combination of both. Automatic calibration utilizes searching algorithms that optimize one or several objective functions without interference of the modeller. This provides increased objectivity and requires less experience of the modeller compared to manual calibration and therefore an automatic calibration procedure is used in this study.

Typical automatic calibration consists of four major elements: (1) an objective function, (2) calibration data, (3) an optimisation algorithm and (4) termination criteria for the algorithm (Sorooshian and Gupta, 1995).

The objective function is explained in section 3.3.1. Section 4.1.1 details which data periods are used (data itself is shortly explained in section 2.2). Section 4.1.2 details the calibration algorithm and its termination criterion.

4.1.1 Calibration data

This section details how the available 30 years of observations are used during calibration of the model. Model initialisation time is discussed, and a distinction is made between calibration of the base model (which is the baseline for later comparison) and calibration of multiple 5-year periods on which the regression models will be based.

Model initialisation

In principle the HBV model can transform input (precipitation, temperature and potential evapotranspiration data) into output (discharge series) from the moment when input data is available. However, it is unlikely that storage terms start at zero storage and actual storages are unknown. Initial values of storage terms are therefore arbitrarily set by the modeller and this influences simulation accuracy.

It is common practice to let the model “warm up”; allowing it to run for a certain number of time steps until the effect of the initial conditions is no longer noticeable and the model reaches a natural state. A period of at least two months (with daily time steps) is recommended (e.g. Carpenter and Georgakakos (2004); Vrugt et al. (2003a)) as warm-up time, depending on the response time of catchment processes.

In this study, data are available from 01-01-1971 to 31-12-2000. Analyses are based on hydrological years, starting November 1st and ending on October 31th. Hydrological years are used to capture winter runoff in a single year and not split this over two calendar years. This leaves ten unused months at the start of the data series as warm-up time for the model, easily exceeding the minimal recommended time. For computational ease, a warm-up period of a full year is used for calculations that do not start in the first hydrological year present in the data. The objective function is not evaluated during model warm-up, because resulting Y-values would be inaccurate.

Base model

A common approach to model calibration is to use a large part of the available data for calibration (to use as much information as possible during the calibration process), while keeping part of the data separate from calibration for validation purposes (table 4.1). There is no consensus whether the model should be calibrated on the most recent part of data and validated on older observations, or vice versa. Therefore the base model is calibrated twice, the oldest and most recent 20 years of data (referred to as models A and B, with 10 months and 1 year warm-up time respectively) and validated on the remaining period (figure 4.1). The model with the best validation

4.1. Calibration procedure

performance (i.e. the model with the best performance on data independent from calibration) is selected as base model.

Table 4.1: Overview of calibration and validation periods in various studies. Calibration and validation length and order differ between the various studies and seem to depend largely on the availability of data and the study purpose

Source	Calibration length [y]	Validation length [y]	Notes
Lindström et al. (1997)	10	10	order unknown
Romanowicz et al. (s.d.)	10	10	order unknown
Booij and Krol (2010)	16	13	calibration first
Madsen (2003)	4	2	calibration first
Chiew et al. (2009)	31	112	calibration last
Görgen et al. (2010)	17	17	both ways
Booij et al. (2011)	19	20	calibration first

5-year periods

Following Coron et al. (2012), the entire data set is divided into overlapping 5-year periods, resulting in 25 periods with different climate characteristics (figure 4.1). The HBV model is calibrated for each 5-year period (with a 1 year warm-up period preceding the calibration period), to find optimal parameter sets for the climatic conditions during each period.

4.1.2 Calibration algorithm

The Shuffled Complex Evolution Metropolis algorithm (Vrugt et al., 2003b, SCEM-UA) is used to optimize the objective function Y . SCEM-UA is an automatic searching algorithm that converges to a global optimum in the parameter space, based on the earlier SCE-UA algorithm (Duan et al., 1992). It combines controlled random search, competitive evolution and complex shuffling to find the optimum parameter set in the parameter space.

Calibration experiments in this study have shown that the parameter space is quite complex, and extensive sampling is required for proper calibration. Table 4.2 shows the settings used for the calibration runs. These settings are based on the recommendations of Vrugt et al. (2003b) for complex problems. The minimal recommended population size $s_{scem} = 250$ proved sufficient to calibrate the base model on 20 years of observed data. The calibration blocks of 5 hydrological years required a larger population size $s_{scem} = 1000$. This might be related to the fact that the 20 year calibration results in a more average parameter set (reasonably suited to a variety of climatic conditions), while each 5-year period has a very specific parameter set optimized for those specific climatic conditions.

4.2. Correlations

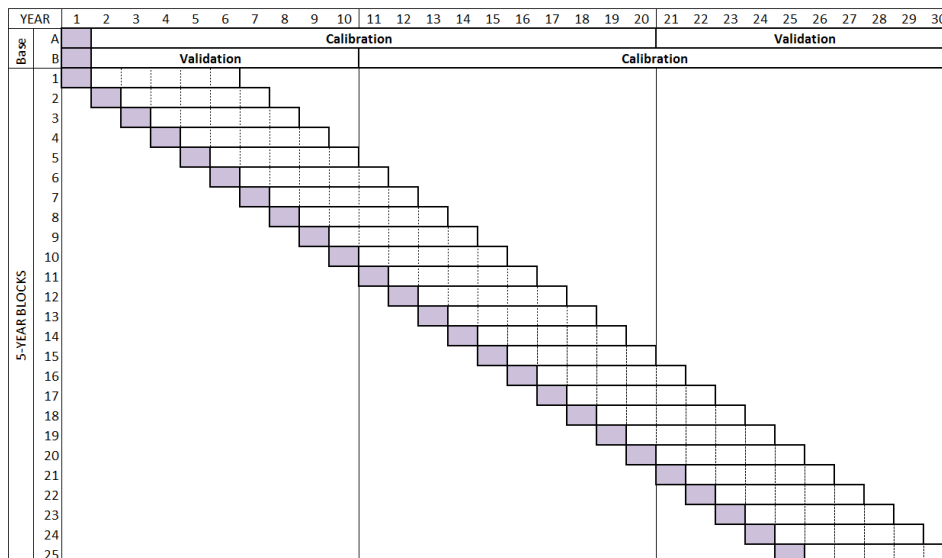


Figure 4.1: Overview of calibration periods for base model A and B, and overlapping 5-year periods. Model warm-up periods are shown with purple boxes, warm-up periods for validation period of base model A and calibration period of base model B are not shown, because they overlap with the end of the calibration and validation periods respectively

SCEM-UA sampling is capped at a user-defined maximum number of iterations. It is not possible to use convergence criteria to end calibration. Therefore convergence plots are made after each calibration run, that show whether the used number of iterations was sufficient for the algorithm to converge to a single value for each parameter. Calibration is repeated with more iterations until the plots show sufficient convergence.

Table 4.2: Settings of SCEM-UA algorithm, based on recommendations for complex problems (Vrugt et al., 2003b)

Variable	Description	Value
n_{scem}	# of parameters	6
q_{scem}	# of complexes	10
s_{scem}	population size	250 (base model) / 1000 (windows)
$C_{n,scem}$	jump rate	$2.4/\sqrt{n_{scem}}$
T_{scem}	likelihood ratio	$1e^6$

4.2 Correlations

This section details how correlations between parameter values and climate characteristics are determined and how these correlations are evaluated. Sec-

4.2. Correlations

tion 4.2.1 describes the applied correlation method. A short description of climate characteristics is given in section 4.2.2. Section 4.2.3 specifies which correlations are investigated and describes significant correlations between parameter values and climate characteristics from a hydrological point of view where possible.

4.2.1 Pearson correlation coefficient

The Pearson correlation coefficient (r ; Davis, 2002) is used to determine the linear correlations between parameter values and climate characteristics, using calibration results and climate characteristics from the 5-year windows as data set. A linear approach is used because it is unknown which relationships exist between model parameters and climate variables. A linear relation is the most simple option and there is no justification to attempt more complex relationships (e.g. rank correlation).

The Pearson correlation coefficient is determined by dividing the covariance between two variables x and y by the product of their standard deviations σ . $r = 1$ indicates a perfect positive correlation, $r = -1$ indicates a perfect negative correlation:

$$r = \frac{cov_{x,y}}{\sigma_x \sigma_y} \quad (4.1)$$

Correlation significance is determined with a T-test and a table of critical values depending on sample size (Davis, 2002). A significance level of 5%, or $p < 0.05$ is used as a threshold to determine which correlations are statistically significant.

4.2.2 Climate characteristics

This study is limited to simple characteristics related to the climatic variables P (precipitation), T (temperature) and PET (potential evapotranspiration). These variables serve as input for the HBV model and are thus used to estimate the optimal values for the model parameters through calibration. Precipitation intensity on days with $P > 0.1$ mm (P_{wet}) is also considered. Runoff Q is not considered because this is model output and the variable of interest in climate change impact assessment.

Climate characteristics are determined for each block of 5 hydrological years. 5-year averages of daily values are denoted with subscript μ (e.g. P_μ). Average daily observations during winter months (December, January, February, [DJF]) are denoted with μ, w (e.g. $T_{\mu,w}$) and with μ, s (e.g. $P_{wet,\mu,s}$) during summer months (June, July, August, [JJA]). Last, average aridity (ar_μ) is considered, which is average PET divided by average P.

Variability of various climate characteristics can be considered by looking at their respective standard deviations. However, significant correlations

4.2. Correlations

between standard deviation and parameters are difficult to explain from a hydrological point of view. Moreover, significant correlations with standard deviations occur solely as a coincidental side effect of significant correlation between the average value of a climate characteristic and a parameter, and a strong correlation between average value and standard deviation of this climate characteristic.

4.2.3 Application

This section details between which variables correlations are determined and how these correlations are used to explain relationships between parameter values and climate characteristics.

Interrelation climate characteristics

First, correlation between logical combinations of climate characteristics are investigated. Correlations of summer and winter P, T, PET and P_{wet} with their respective average values are determined. Correlations between T and PET, correlations between P and P_{wet} and correlations between aridity and P and PET are also calculated. This assists in stating which correlations between climate characteristics and model parameters have a hydrological basis, and which are simply the result of correlations between interdependent climate characteristics. For instance, a parameter might show significant correlations with P_μ and ar_μ . Assuming that a relationship exists between the parameter and P_μ , the correlation with ar_μ might be a different relationship, or a result of the high correlation between P_μ and ar_μ .

Climate characteristics and runoff

Second, correlations between climate characteristics and runoff are determined. In the model, parameter values form the connection between climatic input and runoff output. Knowledge about correlation between climate and observed runoff gives insight in the result of the processes that the model parameters try to simulate. This information assists in describing correlations between climate and parameters from a hydrological point of view.

Climate characteristics and parameter values

Third, correlations between climate characteristics and parameter values are calculated. Significant correlations form the basis of further regression analysis, which ultimately leads to a regression equation that quantifies the relationship between certain parameters and climate characteristics.

Given a significant correlation, a chance still exists that this correlation is present by coincidence, rather than as a result of a physically meaningful relationship between two variables. Therefore a hydrological explanation of

significant correlations is given where possible, to increase the confidence in later regression equations (i.e. to increase confidence that a regression equation describes an actual relationship rather than coincidence). Any individual parameter is however not responsible for the correct modelling of a single hydrological process, but rather for the combined effect of several hydrological processes. This makes the relationship between climate indicators and optimal parameter values a complex one, because a multitude of physical processes might be involved in any potential relationship.

4.3 Linear regression analysis

Regression analysis is used to establish equations for parameter values, based on the significant correlations a parameter has with climate characteristics. This section describes two regression methods used in this study. Single linear regression aims to explain the relationship between one independent and one dependent variable with a linear equation. Multiple linear regression expands on this, using multiple independent variables to explain one dependent variable in a linear way. In this case the six model parameters are dependent variables or predictands, while the various climate characteristics are the independent variables or predictors.

4.3.1 Single and multiple linear regression

The Matlab function “polyfit” is used in the regression analysis. The function finds the coefficients ($c_{1,2,\dots}$) of a polynomial $y_r(x)$ of degree z that provides the best relationship between the dependent and independent variable(s):

$$y_r = c_1x^z + c_2x^{z-1} + \dots + c_zx + c_{z+1} \quad (4.2)$$

An error term SS_E is introduced in order to find the best fit for the equation, by minimizing the sum of the squared difference between the observed values ($y_{r,i}$) and those estimated by the regression line ($\hat{y}_{r,i}$). This is known as the least square approach (Davis, 2002):

$$SS_E = \sum_{i=1}^n (\hat{y}_{r,i} - y_{r,i})^2 = \text{minimum} \quad (4.3)$$

It is unlikely that a perfect linear relationship will be found between a certain climate characteristic and the optimal value for a model parameter, given the complexity of the problem. However, what the actual relationship looks like is unknown. Therefore the most simple option of a linear fit is used, as to not overcomplicate matters. Higher order polynomial regression might fit observed data better, but this fit will likely deteriorate quickly outside the

4.3. Linear regression analysis

fitted data range. This stays in line with the correlation approach (section 4.2).

For a single linear fit $z = 1$ (eq. 4.2):

$$y_r = c_1x + c_2 \quad (4.4)$$

This equation uses a single independent variable to predict the dependent variable, which in this case means that a single climate characteristic is used to predict the optimal parameter value. Since it is possible that the optimal parameter value is dependent on more than a single climate characteristic, the regression analysis also includes multiple linear regression.

Multiple linear regression assess the influence of multiple independent variables on the dependent variable, by assessing the contribution of the individual variables. It expands on the single linear regression equation (equation 4.4) by adding multiple linear terms to the regression equation:

$$y_r = c_1x_1 + c_2x_2 + \dots + c_zx_z + c_{z+1} \quad (4.5)$$

Adding more linear terms to the regression equation does not necessarily lead to a better estimate of the independent variable. Methods exist that selectively add terms (i.e. climate characteristics that are positively correlated with the parameter under consideration) to the regression equation. However, due to the relatively low number of possible combinations ($2^{\text{number of significant correlations}} - 1$) it is in this study possible to simply assess all possible regression equations for each parameter.

Regression strength

The strength or goodness of fit of the regression line is given by the R^2 value, found by dividing the sum of squares due to regression (SS_R) by the total sum of squares (SS_T):

$$R^2 = \frac{SS_R}{SS_T} = \frac{\sum_{i=1}^n (\hat{y}_{r,i} - \bar{y}_{r,i})^2}{\sum_{i=1}^n (y_{r,i} - \bar{y}_{r,i})^2} \quad (4.6)$$

SS_R measures the sum of squares of the difference between the estimates from the regression equation ($\hat{y}_{r,i}$) and the average of the observed values ($\bar{y}_{r,i}$). SS_T gives the sum of squares of the difference between the observed values ($y_{r,i}$) and the average of these values. The fraction R^2 becomes 1 when the regression equation provides a perfect fit with the observations, i.e. when $\hat{y}_{r,i} = y_{r,i}$ (Davis, 2002).

In the case of single linear regression, where the dependent variable is linked to a single independent variable, R^2 is equal to the squared value of the Pearson correlation coefficient r between both variables.

Regression significance

This section details two different tests that help determine whether established regressions are significant in a statistical sense. The F-test is a mathematical test, whereas confidence bands give a visual indication of significance.

F-test: in principle, a significant Pearson correlation coefficient indicates that significant single linear regression is present. The significance of the regression shows, in the case of single linear regression, if the slope coefficient c_1 (eq. 4.4) is significantly different from zero. If this is not the case, the scatter in values around the regression line is the same as the scatter around the mean $\bar{y}_{r,i}$; i.e. the regression does not provide a better relationship between the two variables than the mean value $\bar{y}_{r,i}$ does.

In case of multiple linear regression, adding more individually significant terms to the equation does not necessarily lead to a significant combined equation. An F-test is used to determine regression significance, based on the hypothesis and its alternative:

$$\begin{aligned}H_0 &: c_{1,2,\dots,z} = 0 \\H_1 &: c_{1,2,\dots,z} \neq 0 \text{ for at least 1 } c_z\end{aligned}$$

The H_0 hypothesis is rejected when F exceeds a certain value that varies based on the desired significance level. It uses the mean sums of squares due to regression MS_R and error MS_E , which are the sums of squares divided by their respective degrees of freedom. The general equation for F depends on the number of terms in the regression equation m :

$$F = \frac{MS_R}{MS_E} = \frac{\frac{SS_R}{m}}{\frac{SS_E}{n-m-1}} \quad (4.7)$$

For single linear regression $m = 1$, whereas for multiple linear regression the number of terms can be larger. Table 4.3 shows F-values for varying degrees of freedom, with $n = 25$ from the data points that result from the 25 calibration blocks.

Confidence bands: a 95% confidence limit is constructed around the regression line, as a visual control of the significance test. The true population regression lies between the confidence bands with probability of 95% (Davis, 2002). Therefore for 25 data points (following from the 25 calibration blocks), approximately $((1 - 0.95) * 25 =)$ 1.25 data points can be expected to be outside the confidence interval. If more than 1.25 points are outside the confidence interval, the regression is not statistically significant at a 95% significance level.

4.4. Implementation of regression relations

Table 4.3: F-values for varying degrees of freedom at a 95% significance level (Davis, 2002, Table A.3a)

m	F	
1	4.28	single linear regression
2	3.44	Multiple linear regression
3	3.07	Multiple linear regression
4	2.87	Multiple linear regression
5	2.74	Multiple linear regression

4.3.2 Selection of regression equations

Regression equations are determined for each parameter that shows significant and meaningful correlation with at least one of the climate characteristics (called flexible parameters here). From all possible regression equations, only those that fulfil the significance criterion will be considered for use in the hydrological model. A single equation is selected for each parameter, based on a trade-off is made between regression strength (goodness-of-fit R^2) and the complexity of the equation (adding more terms to the equation will most likely increase the fit R^2 but might be a case of data-fitting rather than describing an actual relation).

4.4 Implementation of regression relations

Several different regression models are made that each estimate a different combination of parameter values with the selected regression equations (section 4.3.2). The first regression model estimates the value of the parameter that is best estimated by its regression equation (best goodness-of-fit the selected regression equations). For following regression models, more regression equations are included ranked on their respective goodness-of-fit.

The following sections explain the process of parameter estimation and implementation of regression equations in HBV in more detail. The performance of all models with GCM-RCM projections as input is shortly described. Last, a short description is given about how from all established regression models one is selected to be used for climate change impact assessment.

4.4.1 Recalibration and validation performance

Parameters that can not properly be estimated with regression equations, have fixed values in the HBV model (called fixed parameters here, these parameters come from the six calibration parameters that are the result of the sensitivity analysis). To account for possible interactions between all model parameters, the fixed parameters in each regression model are recalibrated.

4.4. Implementation of regression relations

The goal is to calibrate these fixed parameters towards values that are compatible with a variety of estimated values for the flexible parameters. The total amount of fixed parameters is 6 – *flexible parameters*. Parameters that have been assigned a default value after the sensitivity analysis keep this default value.

Recalibration and validation periods are the same periods as are used for the base model (figure 4.2). Calibration spans year 11 to 30, while validation uses years 1 to 10. Value estimates of flexible parameters are changed per hydrological year during calibration and validation. The estimates are based on 5-year averages of the required climate characteristics, with the year under consideration as middle point (e.g. parameter estimates for year 13 are based on the average climate characteristics calculated over years 11 to 15). Figure 4.2 shows in coloured blocks the 5-year periods on which parameter estimates for a specific year are based. These 5-year blocks consist of 5 consecutive hydrological years, of which the first starts towards the end of calendar year 1.

This approach to parameter estimates has consequences for the periods that can be used for calibration of the fixed parameters and validation of the resulting regression models. Calibration and validation should be independent periods, to provide objective testing of the calibrated model. Since yearly parameter estimates are based on average climate statistics, some overlap between calibration and validation can occur (i.e. figure 4.2, red blocks).

While year 11 falls in the calibration period, its parameter estimates are partly based on climate characteristics stemming from the validation period. This compromises the independence of the validation period. Therefore calculation of the objective function during calibration does not start until year 13, the year for which parameter estimates are solely based on years within the calibration period. Year 28 is the last year included in calculation of the objective function, since for years 29 and 30 only 4-year and 3-year climate averages are available. Similarly, the objective function during validation is calculated for years 4 to 8; the only years for which complete, independent parameter estimates can be made. Warm-up times are included for calibration and validation. Warm-up periods use the same estimates for flexible parameters as the first years of validation and calibration periods (years 4 and 13 respectively). For proper comparison, the base model is revalidated on years 4-8 as well, to provide a baseline for evaluating the performance of the regression models.

4.4.2 Regression model performance with GCM-RCM input

One of the regression models is used for climate change impact assessment. The procedure for climate change impact assessment involves running the hydrological model with flexible and recalibrated fixed parameters with in-

4.4. Implementation of regression relations

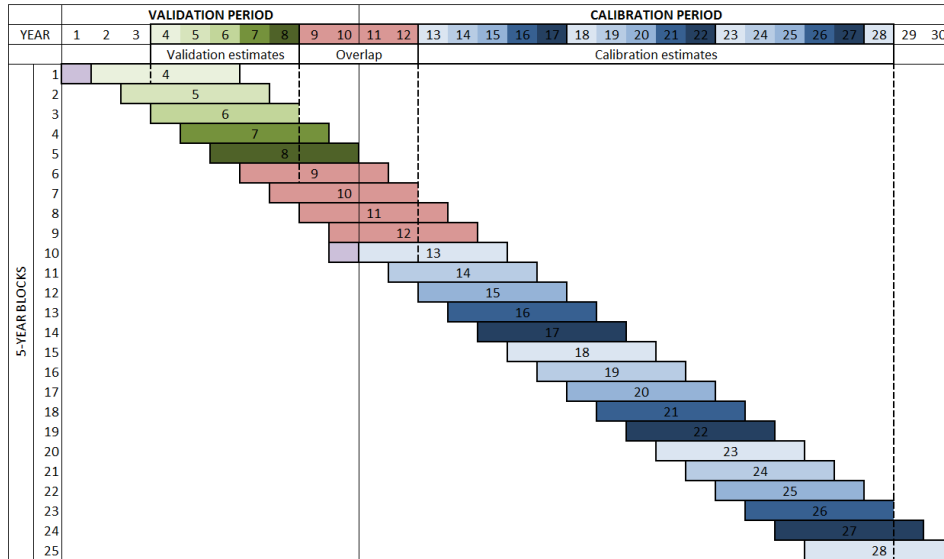


Figure 4.2: Approach towards parameter estimation during recalibration of fixed parameters and validation of this recalibration. Purple: model warm-up time, green: validation period, red: overlap between validation and calibration, blue: calibration period

put from GCM-RCM combinations. Before making the choice for a single regression model, the performance of all regression models with GCM-RCM input for both current and future conditions is evaluated.

A regression equation for an arbitrary parameter is based on calibrated values for that parameter for multiple 5-year periods (section 4.1). These calibrated values are based on observed values of P, T and PET. This is also the case for estimated values for the parameter during recalibration and validation of the regression models (section 4.4.1). Estimated values are therefore quite close to the range of parameter values observed during calibration of the 5-year periods.

It is possible that estimated values of flexible parameters will deviate from this observed range. While interpolation within the range is unlikely to lead to modelling issues, extrapolating values outside this range can cause problems (e.g. 0 values for FC effectively remove soil moisture storage and evapotranspiration from the model). Therefore all regression equations are tested with GCM-RCM input, to determine if these issues occur.

4.4.3 Selection and evaluation of regression model

The final choice for the regression model is based on the combined assessment of validation performance, and expected performance of the regression model with GCM-RCM input.

4.5 Influence on climate change impact assessment

This section describes the process of climate change impact assessment (section 4.5.2) and how the final comparison between base and regression model is made (section 4.5.3). Proper parameter estimates can only be made for 25 years out of the full 30 years in the data set (section 4.4.1). This limits the period for which the regression model can be applied (figure 4.2) to years 1974-1998. Similarly, future projections with the regression model can only be made for period 2074-2098. All statistics discussed in the following sections are calculated for these two time periods.

4.5.1 Projected climate change

GCM-RCM projections (section 2.2.2) are used as input for both base and selected regression model, to project runoff for periods 1971-2000 and 2071-2100. A short summary of expected changes per GCM-RCM is made, to show which climatic changes are modelled with the base and regression models.

4.5.2 Climate change impact assessment method

Projections of future runoff can not be directly compared with historical runoff observations, as this would discount the uncertainty stemming from the use of GCM-RCM combinations and the hydrological model, several steps constitute the climate change impact assessment. First, simulated runoff based on observed P, T and PET data is compared with observed runoff for both the base and regression model. This shows the accuracy of both hydrological models. Second, simulated runoff based on GCM-RCM projections for period 1971-2000 is compared with simulated runoff based on observed P, T and PET data from base and regression model. This shows the influence of the various GCM-RCM combinations on runoff predictions.

Third, simulated runoff based on GCM-RCM projections for period 2071-2100 is compared with simulated discharge based on GCM-RCM projections for period 1971-2000 from both base and regression model. This shows the actual expected climate change.

Daily GCM-RCM predictions of P and T, resulting from simulated climatology, include relevant variability and a random component. Climate change impacts are therefore derived from changes in runoff statistics, since simulated hydrographs for present and future periods can not be directly compared, due to the inherent randomness of the GCM-RCM projections used as hydrological model input. Flow-duration-curves are used to visualise changes in frequency of simulated flows. Changes in overall and seasonal flows are determined by comparing mean and average values of overall and seasonal flows between both simulated periods.

4.5.3 Comparison of predicted changes

The final step in this study is comparison of the predicted changes in runoff by the base model with changes predicted by the regression model. Validation values of both models (section 4.4.1) give an indication of which model is likely better suited for climate conditions that differ from calibration conditions. However, ultimately a qualitative comparison of predicted changes is the best that can be achieved, since it is impossible to know which of both simulations of future runoff is more accurate.

Chapter 5

Results

5.1 Calibration results

This section presents the results of calibration procedure (section 4.1). Section 5.1.1 concerns calibration and selection of the base model, section 5.1.2 shows the results of calibration of the 5-year windows that form the basis for correlation and regression analysis.

5.1.1 Base model

Two models A and B are calibrated and the model with best validation performance is selected as base model (section 4.1). Calibration of both models is capped at 5000 iterations. Parameter progression plots show that this is sufficient to properly identify optimum values of all six parameters in both cases. Table 5.1 shows calibration and validation results for models A and B (calibrated on 20 years of data, validated on 9 years).

Model performance during validation is somewhat worse than calibration for both models, mostly due to incorrect modelling of the water balance (seen as an increase in Relative Volume Error during validation). Model B seems better suited for use outside its calibration period, judging from Y-values during validation. Model B is therefore selected as base model.

Figure 5.2 shows model performance of both model A and B when their respective parameter sets are used to simulate runoff for all 5-year periods. Model B has a higher Y-value than model A for 19 out of 25 periods, reinforcing the choice to use model B as base model.

Table 5.1: Calibration and validation results of base model. Base model A is calibrated on the first 20 years of data and validated on the remaining 9, base model B is calibrated on the last 20 years and validated on the first 9 years

	Base model A		Base model B	
	Calibration	Validation	Calibration	Validation
Y [-]	0.74	0.64	0.73	0.68
NS [-]	0.74	0.70	0.73	0.73
RVE [%]	0.52	9.7	0.53	7.4

5.1.2 5-year windows

Calibration of the 5-year blocks is capped at 50000 iterations. Parameter convergence plots show that most parameters converge quickly in any time period, although in some specific cases this large number of iterations is necessary. The most influential parameter FC is properly identified in all cases, and the same goes for α and $PERC$ which are the next most important ones (section 3.3.3). The algorithm sometimes struggles to find the optimal value for LP and TT and keeps switching back and forth between several similar values. This shows that the objective function is relatively insensitive to the values of these parameters in certain time periods. Parameter K_s can be identified in all periods, although in some cases thorough sampling is required. Overall, parameter identifiability for the 5-year periods seems satisfactory.

However, initial calibration results of the 5-year windows were unsatisfactory for the time periods 14, 16, 19 and 23 (appendix B, figure B.1, red circles), where the calibration algorithm determined optimal parameters in such a way that the roles of slow and fast runoff reservoirs were reversed. This has been corrected with a recalibration of the specific periods with restricted parameter ranges (appendix B, figure B.1, blue stars). Figure 5.1 shows the resulting Y-values of all 5-year periods, and a decomposition of the objective function Y in specific parts related to NS and RVE (section 3.3.1). The calibrated parameters for each 5-year window are such that the relative volume error is nearly zero and therefore variations in the NS coefficient almost exclusively determine the final Y-value (figure 5.1).

Calibration period 18 shows a low Y-value compared to the pattern before and after this period. Gradual changes in Y-value might be expected since each calibration period differs in only one of its 5 calibration years from the period before. Period 18 consists of 5 years with very low and constant runoff, without any clear runoff peaks; a situation that is not encountered in any other 5-year period. Daily runoff varies little from the average runoff in this period and therefore the lower part of the NS coefficient has a low value (figure 5.1). Since the upper part of the NS equation also has a low value compared to the other periods, the total fraction of the NS equation is high. This leads to a lower Y-value for this period than would be expected based on the pattern in Y-values.

Figure 5.2 compares Y-values of the 5-year periods with Y-values for those periods determined with models A and B. This shows that parameter sets calibrated for each 5-year period perform better than either model A or B. The 5-year parameter sets thus simulate runoff closer to observed runoff than either model A or B, based on climate input.

5.2. Correlation results

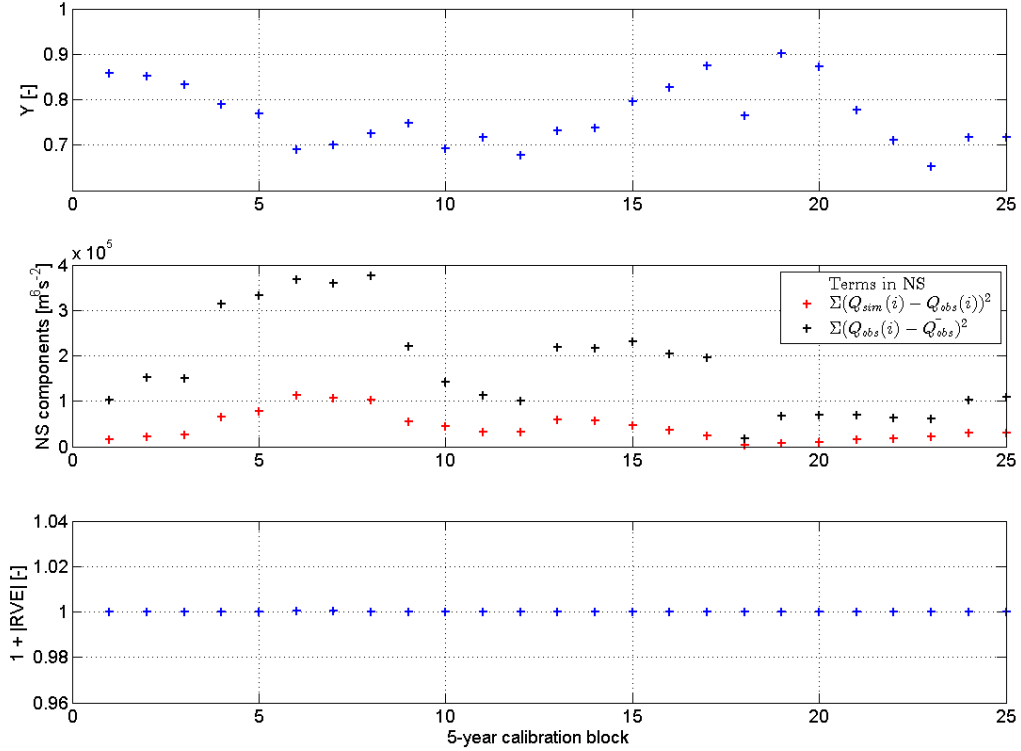


Figure 5.1: Calibration results for blocks of 5 hydrological years specified as the individual components of Y (equation 3.16): the Nash-Sutcliffe coefficient (NS, equation 3.17), consisting of modelling error (difference between daily simulated and observed discharge) and natural discharge variability (variability in discharge measured as the sum of the difference between daily observed and average observed discharge), and the Relative Volume Error (RVE, equation 3.18)

5.2 Correlation results

This section presents correlation results as described in section 4.2. Interrelation of climate characteristics is given and shortly discussed, as are correlations between climate characteristics and observed runoff (section 5.2.1). Following this, correlations between climate characteristics and optimal parameter values are presented and discussed (section 5.2.2).

5.2.1 Explanatory correlations

Table 5.2 shows Pearson correlation coefficients between dependent climate characteristics and correlations between all climate characteristics and observed discharge, used to give a hydrological explanation of correlations between climate characteristics and parameter values (section 4.2).

5.2. Correlation results

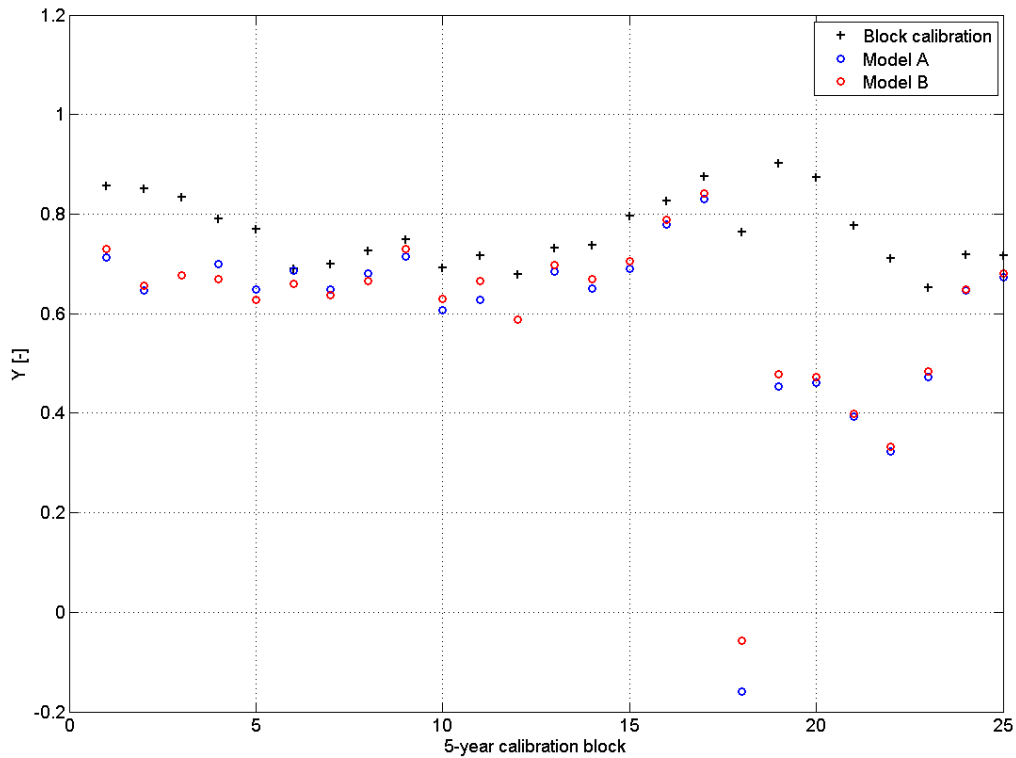


Figure 5.2: Calibration results for blocks of 5 hydrological years (black crosses) and performance per calibration block of models A and B, that have been calibrated on the first and last 20 years of data respectively

Interrelation climate characteristics

All investigated interrelations of climate characteristics show significant positive correlations (table 5.2).

This has some consequences for estimating parameter values with regression equations, because certain climate characteristics are not completely independent from each other. Estimating a parameter value from two climate characteristics where one is dependent on the other, obscures the actual relationship between the parameter value and the first climate characteristic. A regression equation based on two climate characteristics with this type of relationship between them would be a case of overfitting the data, rather than describing an actual relationship. It is however difficult to determine the difference between overfitting of the data, and a weak relation between a specific characteristic and parameter value. Because in both cases adding this characteristic to the regression equation only improves the fit slightly, but for very different reasons.

5.2. Correlation results

Correlation between climate and observed runoff

Average values of P, T, PET, P_{wet} show logical correlations with runoff (table 5.2). Increased P leads to increased runoff due to overall availability of water. Increased P_{wet} likely leads to increased runoff through earlier saturation of soil moisture as a result of increased precipitation intensity. Increased T and PET lead to increased evaporation and thus less runoff.

The lack of correlation between winter runoff and winter climate is likely the influence of snow, which delays part of winter precipitation until snow melt occurs in early spring. The positive correlation between winter P_{wet} and runoff is difficult to explain from a hydrological sense. This might be a meteorological effect, related to high precipitation combined with above zero temperature, leading to high direct runoff instead of snow forming.

Summer characteristics and runoff show similar correlations as average values of climate and runoff, apart from P_{wet} . This might be the result of increased evapotranspiration during summer, which leaves more space in the soil moisture reservoir. Therefore increased precipitation intensity does not automatically lead to increased direct runoff (which is the result from saturated soil moisture).

Winter (summer) climate and summer (winter) runoff are independent events, and correlations are likely not a reflection of real relationships. Similarly, correlations between average runoff and seasonal characteristics represent a damped effect of the respective seasonal correlation and thus do not provide additional information.

Aridity is the combined effect of daily PET divided by daily P.

Table 5.2: Pearson correlation coefficients (r) and p-values between dependent climate characteristics, and correlation between climate characteristics and observed runoff. Green: $p \leq 0.05$ (significant at 95% level), red: $p > 0.05$ (not significant at 95% level), white: unused

Interrelation climate characteristics		
5 year average of ..		r p
daily P	daily Pwet	0.96 0.00
daily T	daily PET	0.96 0.00
winter (DJF) P	daily P	0.55 0.00
winter (DJF) T	daily T	0.81 0.00
winter (DJF) PET	daily PET	0.72 0.00
winter (DJF) Pwet	daily Pwet	0.53 0.01
winter (DJF) Pwet	winter (DJF) P	0.78 0.00
winter (DJF) T	winter (DJF) PET	0.95 0.00
summer (JJA) P	daily P	0.75 0.00
summer (JJA) T	daily T	0.80 0.00
summer (JJA) PET	daily PET	0.89 0.00
summer (JJA) Pwet	daily Pwet	0.75 0.00
summer (JJA) Pwet	summer (JJA) P	0.83 0.00
summer (JJA) T	summer (JJA) PET	0.99 0.00
aridity index	daily P	-0.96 0.00
aridity index	daily PET	0.82 0.00

Correlation climate characteristics and run-off							
5 year average of ..		Q		Q_winter		Q_summer	
		r	p	r	p	r	p
daily	P	0.62	0.00	0.49	0.01	0.55	0.00
	T	-0.75	0.00	-0.53	0.01	-0.73	0.00
	PET	-0.79	0.00	-0.61	0.00	-0.75	0.00
	Pwet	0.63	0.00	0.60	0.00	0.48	0.01
winter (DJF)	P	0.32	0.13	0.31	0.13	0.23	0.26
	T	-0.61	0.00	-0.25	0.22	-0.69	0.00
	PET	-0.65	0.00	-0.23	0.26	-0.79	0.00
	Pwet	0.26	0.21	0.40	0.05	0.15	0.49
summer (JJA)	P	0.56	0.00	0.45	0.03	0.54	0.01
	T	-0.67	0.00	-0.68	0.00	-0.53	0.01
	PET	-0.69	0.00	-0.69	0.00	-0.54	0.01
	Pwet	0.24	0.24	0.31	0.14	0.17	0.41
aridity index		-0.73	0.00	-0.58	0.00	-0.66	0.00

5.2. Correlation results

5.2.2 Climate and parameter correlation

Table 5.3 shows Pearson correlation coefficients between calibrated parameter values and climate characteristics. Correlations are considered significant for $p \leq 0.05$ (based on unrounded values, shown in green). Correlations in red do not meet the significance criterion. In following subsections only correlations significant at the 95% level are discussed, which are present for parameters FC , LP , α , K_s and $PERC$. TT does not show any significant correlations with climate characteristics.

Table 5.3: Pearson correlation coefficients (r) and p-values between climate characteristics and model parameters. Green: $p \leq 0.05$ (significant at 95% level), red: $p > 0.05$ (not significant at 95% level)

5 year average of ..		FC		LP		α		K_s		PERC		TT	
		r'	p	r'	p	r'	p	r'	p	r'	p	r'	p
daily	P	0.50	0.01	-0.11	0.59	0.58	0.00	0.41	0.04	0.51	0.01	-0.15	0.47
	T	-0.12	0.56	-0.06	0.79	-0.28	0.18	-0.24	0.26	-0.30	0.14	0.15	0.48
	PET	-0.10	0.62	-0.01	0.98	-0.32	0.12	-0.31	0.14	-0.34	0.09	0.14	0.52
	Pwet	0.41	0.04	-0.07	0.75	0.55	0.00	0.38	0.06	0.52	0.01	-0.16	0.45
winter (DJF)	P	0.49	0.01	-0.14	0.50	0.53	0.01	0.05	0.81	0.25	0.22	0.21	0.32
	T	-0.07	0.75	-0.39	0.05	0.08	0.69	0.06	0.78	0.09	0.67	0.22	0.30
	PET	-0.10	0.63	-0.33	0.11	0.05	0.83	0.07	0.75	0.09	0.68	0.13	0.53
	Pwet	0.34	0.09	-0.51	0.01	0.68	0.00	0.34	0.09	0.60	0.00	0.17	0.43
summer (JJA)	P	0.20	0.33	0.32	0.12	0.13	0.54	0.07	0.74	0.12	0.58	-0.18	0.39
	T	0.16	0.45	0.00	1.00	-0.19	0.37	-0.22	0.28	-0.25	0.23	0.08	0.69
	PET	0.16	0.44	-0.05	0.82	-0.16	0.44	-0.25	0.24	-0.23	0.26	0.14	0.50
	Pwet	0.22	0.30	0.03	0.90	0.31	0.13	0.15	0.48	0.37	0.07	-0.17	0.42
aridity index		-0.42	0.03	0.08	0.70	-0.56	0.00	-0.42	0.04	-0.51	0.01	0.18	0.38

FC

FC shows positive correlation with P_μ , $P_{wet,\mu}$ and $P_{\mu,w}$, and negative correlation with ar_μ .

Increased FC means more space in the soil moisture reservoir, which for independent precipitation events means that a relatively bigger part of the precipitation can be stored. Therefore when more space is available in the soil moisture reservoir, less water from precipitation events is directly available for runoff. For low and medium precipitation events, the increased soil moisture storage can lead to lower runoff. For high precipitation the soil moisture reservoir will be saturated at some point, and the effect of increased FC on high flows is thus diminished.

P_μ has a positive correlation with both runoff and FC . Since higher FC should lead to lower low to medium runoff peaks, FC could be expected to have negative correlation with precipitation characteristics (since increased P would lead to increased runoff and decreased FC ensures this). However, correlation between P_μ and FC is positive. This might indicate that the model is overly sensitive for changes in this characteristic (e.g. model overestimates runoff for increases P_μ) and the optimal FC value might increase

5.2. Correlation results

to dampen this effect.

Correlation of FC with $P_{wet,\mu}$ might have a similar explanation (since $P_{wet,\mu}$ also has a positive correlation with runoff): higher FC means more storage in soil moisture, which is able to store a larger part of precipitation events (leading to lower runoff) and so dampen the effect of increases in $P_{wet,\mu}$ on runoff generation by the model. Alternatively, correlation with $P_{wet,\mu}$ could be the result of high positive correlation between P_μ and $P_{wet,\mu}$.

$P_{\mu,w}$ has a positive correlation with FC , but not a significant correlation with average runoff. Therefore this correlation might be the result of the positive correlation between $P_{\mu,w}$ and P_μ .

Correlation with ar_μ might follow from the evaporation controlling properties of FC . A decrease in FC would lead to an increase of actual evapotranspiration.

LP

LP is negatively correlated with $P_{wet,\mu,w}$. No other significant correlations are present.

An increase in LP leads to a decrease in actual evapotranspiration, given constant values of FC , PET and soil moisture storage, up to a maximum of all available soil moisture. This leads to a higher amount of water as runoff. $P_{wet,\mu,w}$ has a significant positive correlation with runoff during the winter months, indicating that with higher $P_{wet,\mu,w}$, higher runoff occurs. Positive correlation between LP and $P_{wet,\mu,w}$ simulates this effect.

The lack of other significant correlations between LP and other climate characteristics is unexpected, given the high correlation between $P_{wet,\mu,w}$ and $P_{\mu,w}$ and $P_{wet,\mu}$. Furthermore, the increase in LP leading to lower actual evapotranspiration seems an artificial way in which the model reaches acceptable runoff. From a physical point of view, it makes little sense that a higher average precipitation intensity on wet days during winter would go together with lower actual evapotranspiration. Therefore the correlation between LP and $P_{wet,\mu,w}$ is a possible coincidence with no basis in a true relationship between the two.

α

α is positively correlated with P_μ , $P_{wet,\mu}$, $P_{\mu,w}$ and $P_{wet,\mu,w}$. It shows negative correlation with ar_μ .

An increase in α leads to increased runoff from the fast runoff reservoir. Since P_μ and $P_{wet,\mu}$ are both positively correlated with average runoff, it is understandable that α assumes a higher value for higher values of both climate characteristics.

$P_{wet,\mu,w}$ shows positive correlation with runoff during winter months, but $P_{\mu,w}$ does not. Soil is generally saturated during winter, leading to more

5.2. Correlation results

direct runoff from precipitation events. This is more so for high intensity events (which would lead to runoff peaks) than for steady low precipitation (which keeps the soil saturated). Since α controls the magnitude of peak flows, it is understandable that α increases with increasing $P_{wet,\mu,w}$. The correlation between α and $P_{\mu,w}$ can not be directly related to correlation of $P_{\mu,w}$ and winter runoff, and might be the result of high correlation between $P_{\mu,w}$ and $P_{wet,\mu,w}$.

ar_{μ} depends on P_{μ} and thus shows correlation with α as well. A higher aridity index indicates more potential evapotranspiration compared to precipitation. This potentially leads to more actual evapotranspiration and thus lower saturation of soil moisture. This means a decrease in fast runoff, since more space is available in soil moisture storage. A negative correlation between ar_{μ} and α would lead to lower fast runoff due to lower α occurring with higher ar_{μ} and is thus understandable.

K_s

K_s is positively correlated with P_{μ} and has a negative correlation with ar_{μ} .

K_s controls runoff from the slow runoff reservoir, and slow runoff increases as K_s increases. Since both P_{μ} is positively correlated with runoff, it is understandable that the runoff controlling parameter K_s is positively correlated with P_{μ} .

Negative correlation between K_s and ar_{μ} is understandable, since an increase in ar_{μ} indicates less available water for runoff (either due to lower precipitation, increased potential evapotranspiration or both) and vice-versa. K_s shows this effect in runoff from the slow runoff reservoir.

$PERC$

$PERC$ shows positive correlations with P_{μ} , $P_{wet,\mu}$ and $P_{wet,\mu,w}$, and negative correlation with ar_{μ} .

The positive correlations indicate that when average precipitation increases, part of this increase is directed to the groundwater reservoir and thus slow runoff increases. Since P_{μ} and $P_{wet,\mu}$ are all positively correlated with average runoff, and $P_{wet,\mu,w}$ with average runoff in winter, this is a reasonable relation.

Negative correlation with the average aridity reinforces this relationship. When less water is available, groundwater is recharged more slowly, as shown by decreased flow to the groundwater reservoir through decreased $PERC$.

Intercorrelation of climate characteristics

The correlations discussed above can directly or indirectly be traced back to intercorrelation with P_{μ} (table 5.2). Correlations between P_{μ} and $P_{wet,\mu}$ and

5.3. Regression analysis

ar_μ are very high. $P_{\mu,w}$ also shows high correlation with P_μ . $P_{wet,\mu,w}$ shows high correlation with $P_{wet,\mu}$ and $P_{\mu,w}$, which both are strongly correlated with P_μ . This provides an alternative explanation for most correlations, since there is still the possibility that these correlation do not result from a relationship between the parameters and climate. This reflection is used during the regression analysis, and aids in choosing whether to add another term to the regression equation (trade-off between increased fit R^2 and equation complexity).

5.3 Regression analysis

This section gives the results of the regression analysis used to describe the relationships between parameter values and climate characteristics. Section 5.3.1 shortly describes single linear regression results, section 5.3.2 gives more elaborate results from multiple linear regression and a conclusion about the regression approach for each individual parameter.

5.3.1 Single linear regression

This section discusses the single linear regression of correlations between model parameters and climate characteristics that were found significant at the 95% level (table 5.3). The correlation between LP and $P_{wet,\mu}$ is excluded because this was deemed to be the result of coincidence (section 5.2.2). All single linear regressions of a significant linear correlations are significant as well. Resulting fit (R^2) of each single linear regression can be found in table 5.4. Regression plots can be found in appendix C.

α is estimated the best with single linear regression, with fits varying from $R^2 = 0.28$ to $R^2 = 0.46$. $PERC$ is next best, with fits varying from $R^2 = 0.26$ to $R^2 = 0.36$. FC and K_s are not estimated particularly well with single regression, with fits varying from $R^2 = 0.17$ to $R^2 = 0.25$, and $R^2 = 0.17$ or $R^2 = 0.18$ respectively.

Table 5.4: Fit R^2 of single linear regression of significant correlations between model parameters and climate characteristics

Parameter	Climate characteristic				
	P_μ	$P_{wet,\mu}$	$P_{\mu,w}$	$P_{wet,\mu,w}$	ar_μ
FC	0.25	0.17	0.24	-	0.18
α	0.33	0.3	0.28	0.46	0.32
K_s	0.17	-	-	-	0.18
$PERC$	0.27	0.27	-	0.36	0.26

5.3.2 Multiple linear regression

Multiple linear regression is used in an attempt to improve the fits found with single linear regression (table 5.4) and establish regression equations that better estimate parameter values. Tables 5.5 to 5.8 show the significant results of multiple linear regression analysis for parameters FC , α , K_s and $PERC$ respectively, summarized as the best fit (R^2) per number of terms in the regression equations (full results can be found in appendix C.2). Only the climate characteristics that show significant correlation with the various parameters are used in the multiple linear regression analysis.

FC

Table 5.5 shows the result of multiple linear regression analysis for FC , as the equations with the best fit R^2 per number of terms in the equation. The best equation from single linear regression is based on P_μ and this characteristic is present in all possible best equations. This fit can significantly be improved by adding $P_{\mu,w}$ as term in the regression equation, and again by adding $P_{wet,\mu}$ as well. Expanding the equation further to include four terms improves overall fit only a little, and this might be a case of overfitting. Since correlations between FC and P_μ , $P_{wet,\mu}$ and $P_{\mu,w}$ can be explained from a hydrological point of view, the equation based on these three terms is used to estimate FC values.

Table 5.5: Best multiple linear regression results for parameter FC , measured by the regression fit R^2 per number of terms included in the regression equation. Selected regression equation underlined

# of terms	Included characteristic(s)	R^2	F	p
1	P_μ	0.25	7.63	0.01
2	$P_\mu, P_{\mu,w}$	0.32	5.10	0.02
3	$P_\mu, P_{wet,\mu}, P_{\mu,w}$	0.40	4.66	0.01
4	$P_\mu, P_{wet,\mu}, P_{\mu,w}, ar_\mu$	0.43	3.76	0.02

α

The best fit achieved with single linear regression for α occurs in the equation that depends on $P_{wet,\mu,w}$. The fit can be significantly improved by adding the term P_μ in a multiple regression equation. This builds on the physical interpretation of the correlations (section 5.2.2): the increase in α for periods with high winter P (reflecting the increased direct runoff due to saturation of the soil) is included in the regression equation through the term $P_{wet,\mu,w}$. The influence of increased aridity, more space for precipitation to add to soil moisture, is included due to the term P_μ . This term is directly used in the calculation of the aridity index ar_μ .

5.3. Regression analysis

Adding terms to the equation containing P_μ and $P_{wet,\mu,w}$ has very little effect: the fit increases only marginally. While the additional terms can be explained from a hydrological point of view, they can also be traced back to their relation with P_μ and $P_{wet,\mu,w}$. Therefore it makes little sense to include more than two terms in the regression equation, because the added complexity from additional terms likely offsets the marginal gains obtained from a better fit.

Table 5.6: Best multiple linear regression results for parameter α , measured by the regression fit R^2 per number of terms included in the regression equation. Selected regression equation underlined

# of terms	Included characteristic(s)	R^2	F	p
1	$P_{wet,\mu,w}$	0.46	19.31	0.0002
2	$P_\mu, P_{wet,\mu,w}$	0.54	12.7	0.0002
3	$P_\mu, P_{wet,\mu}, P_{wet,\mu,w}$	0.55	8.58	0.0007
	$P_\mu, P_{wet,\mu,w}, ar_\mu$	0.55	8.44	0.0007
4	$P_\mu, P_{wet,\mu}, P_{\mu,w}, P_{wet,\mu,w}$	0.56	6.33	0.0018
	$P_\mu, P_{wet,\mu}, P_{\mu,w}, ar_\mu$	0.56	6.32	0.0019
	$P_\mu, P_{wet,\mu}, P_{wet,\mu,w}, ar_\mu$	0.56	6.34	0.0018
5	$P_\mu, P_{wet,\mu}, P_{\mu,w}, P_{wet,\mu,w}, ar_\mu$	0.57	5.04	0.0041

K_s

The best fit achieved with single linear regression for K_s occurs in the equation that depends on ar_μ , which is only marginally better than the equation based on P_μ . The regression equation including both terms does not meet the significance standard (Appendix C.2, table C.5). Since single linear regression does not provide a convincing equation for estimating K_s , attempting to estimate the proper value of K_s very likely only leads to more uncertainty than calibrating this parameter. K_s is therefore not estimated with a regression equation and recalibrated when the various regression models are established.

Table 5.7: Best multiple linear regression results for parameter K_s , measured by the regression fit R^2 per number of terms included in the regression equation. No regression equation selected

# of terms	Included characteristic(s)	R^2	F	p
1	ar_μ	0.18	4.93	0.04

5.4. Establishment of regression model

PERC

The best fit achieved with single linear regression for *PERC* occurs in the equation that depends on $P_{wet,\mu,w}$. This fit can significantly be improved by adding either P_μ or $P_{wet,\mu}$ to the regression equation. Using more than two terms in the regression does not provide a significantly better fit.

Both P_μ and $P_{wet,\mu}$ have a reasonable hydrological explanation (section 5.2.2). Regression with P_μ has a slightly higher F-statistic and is also similar to the regression equation for α . Therefore this regression equation is chosen to estimate *PERC*.

Table 5.8: Best multiple linear regression results for parameter *PERC*, measured by the regression fit R^2 per number of terms included in the regression equation. Selected regression equation underlined

# of terms	Included characteristic(s)	R^2	F	p
1	$P_{wet,\mu,w}$	0.36	12.98	0.00
2	$P_\mu, P_{wet,\mu,w}$	0.42	8.11	0.00
	<u>$P_{wet,\mu}, P_{wet,\mu,w}$</u>	0.42	7.90	0.00
3	$P_\mu, P_{wet,\mu,w}, ar_\mu$	0.43	5.23	0.01
4	$P_\mu, P_{wet,\mu}, P_{wet,\mu,w}, ar_\mu$	0.43	3.74	0.02

5.4 Establishment of regression model

This section explains the implementation of the multiple linear regression relationships for *FC*, α and *PERC* in the HBV model and evaluates the new models' performance by validation (section 5.4.1) and for use with GCM-RCM input (section 5.4.2). One regression model is then selected for climate change impact assessment (section 4.3.2).

5.4.1 Recalibration and validation performance

Relationships for *FC*, α and *PERC* are implemented in the HBV code. Four different regression models are established. The first model estimates only the value of α , since the multiple linear regression for α has the highest fit of the three. In subsequent models, values for *FC* and *PERC* are also estimated from their regression equations. Since *FC* and *PERC* have similar fits for their respective regression equations, either is a good option to estimate along with α . Therefore the second and third model estimate values of α and *PERC*, and α and *FC* respectively. Finally, the fourth model estimates values of α , *FC* and *PERC* all. Parameters that are not estimated with a regression equation are recalibrated (section 4.4.1). Table 5.9 summarizes multiple linear regression results (goodness-of-fit of the selected regression equations) and which regression models are created.

5.4. Establishment of regression model

Table 5.9: Summary of multiple linear regression results and implementation in the HBV model

Multiple regression results		Implementation	
Parameter	R^2	Model	Included equations
α	0.54	1	α
$PERC$	0.42	2	$\alpha, PERC$
FC	0.40	3	α, FC
		4	$\alpha, PERC, FC$

Table 5.10: Calibration and validation results of four models with multiple linear regression equations (section 4.4.1), compared with base model. Model (1): α , (2): $\alpha, PERC$, (3): α, FC , (4): $\alpha, PERC, FC$

	Base model	Regression models			
		1	2	3	4
Calibration					
Y [-]	0.73	0.73	0.71	0.73	0.71
NS [-]	0.73	0.73	0.71	0.73	0.71
RVE [-]	0.00	0.00	0.00	0.00	0.00
Validation					
Y [-]	0.69	0.52	0.50	0.56	0.56
NS [-]	0.78	0.60	0.65	0.63	0.69
RVE [-]	0.13	0.15	0.27	0.12	0.23

Calibration performance

The base model can be considered as the optimal model for the entire calibration period, since the parameter set is optimized for this specific period ($Y = 0.73$, based on $NS = 0.73$ and $RVE = 0.0053$). The regression models have performance equal to, or very similar as, the base model. Regression models 2 and 4 include estimates for $PERC$, and these show slightly lower values for Y than either base model or regression models 1 and 3.

Validation performance

Validation performance of all regression models is lower than validation performance of the base model. Differences between the regression models seem to originate from whether $PERC$ is calibrated or estimated. Models 1 and 3 use a calibrated value for $PERC$ and have a better value for RVE . Models 2 and 4 estimate the values of $PERC$ and have a somewhat better value for NS .

5.4.2 Regression model performance with GCM-RCM input

This section investigates expected regression model functioning with GCM-RCM input, by using the regression equations for parameters FC , α and $PERC$ to estimate their values based on GCM-RCM climate projections. Parameter values are estimated for periods 1971-2000 and 2071-2100 (appendix C.2, figures C.5, C.6 and C.7 show parameter values, figures C.8 and C.9 show projections of used climate characteristics).

FC

FC values are not estimated within plausible ranges (compared to ranges encountered during calibration of 5-year windows) with GCM-RCM input. Values for the period 1971-2000 are generally negative, due to an overestimation of average precipitation intensity ($P_{wet,\mu}$) and underestimation of average winter precipitation (P_μ) by the GCM-RCM combinations. In contrast, estimated FC values for period 2071-2100 are very high, mainly due to a projected decrease in precipitation intensity ($P_{wet,\mu}$) and increase in winter precipitation (P_μ).

With a value of zero for FC , the HBV model would effectively disable the soil moisture reservoir. Using a lower limit higher than zero is not felt to be a reasonable alternative because a value can not objectively be determined. Moreover, this would effectively fix FC at this value for most simulations, leading to a situation where FC is treated like a recalibrated parameter most of the time, only with a worse-than-calibrated value.

α

α values are estimated within plausible ranges (compared to ranges encountered during calibration of 5-year windows) with GCM-RCM input. An exception is future projections of GCM-RCM 1, which give very high estimates of winter precipitation intensity ($P_{wet,\mu,w}$) leading to relatively high values of α .

Estimates of future values for α seem somewhat high with input from GCM-RCM 1. The other estimates do not seem unreasonable.

$PERC$

$PERC$ values are estimated within plausible ranges (compared to ranges encountered during calibration of 5-year windows) for the period 1971-2000 with all GCM-RCM input. Most GCM-RCM combinations project a decrease in average winter precipitation intensity ($P_{wet,\mu,w}$) for the period 2071-2100, which leads to negative values for $PERC$ in many cases (capped at a very low positive value in the regression equation, to prevent complete

groundwater drainage). This leads to the infeasible situation of very low groundwater recharge and thus a decrease in base flow. The low estimates of *PERC* values coincide with low GCM-RCM projections of $P_{wet,\mu,w}$. Low precipitation intensity leads to lower runoff peaks and increased importance of base flow (due to lower direct runoff). Therefore it seems unlikely that *PERC* will assume very low values in these cases.

Estimates of future values for *PERC* are thus somewhat doubtful: draining of the slow runoff reservoir with little to no replenishment seems unlikely to happen from a hydrological point of view.

5.4.3 Regression model selection and evaluation

Due to problems with *FC* estimates with GCM-RCM input, regression models 3 and 4 can not be used for climate change impact assessment. Regression model 1 does not include *PERC* estimates (that have unlikely low values for the future period) and has a slightly better validation value than model 2, and is thus selected to be used for climate change impact assessment.

5.5 Climate change impact assessment

This section shows the results of the climate change impact assessments performed with base and regression models. Outcomes are compared to determine the difference between both modelling approaches. Section 5.5.1 gives a short overview of changes in P and T projected by various GCM-RCM combinations (full tables in appendix D). Section 5.5.2 gives the results of climate change impact assessments with base and regression model. Section 5.5.3 compares the projected changes by both model types.

5.5.1 Projected climate change

Most GCM-RCM combinations project an increase in average precipitation, coupled with a decrease in precipitation variability (averaged over the full 30 years of GCM-RCM projections). Projected precipitation changes vary from 0% to +16.5% (appendix D, table D.1) with an increased frequency of wet days (leading to a decrease in average precipitation intensity, table 6.1). With GCM-RCM combinations 1 and 5, precipitation changes are such that functioning of the base model might not be optimal (due to transposing the calibrated parameter set to very different climatic conditions, section 1.1.2).

Temperature is expected to increase with at least 2°C with slight variations in variability, averaged over the full 30 years of GCM-RCM projections (appendix D, table D.2).

Potential evapotranspiration (estimated with Penman-Monteith method) is expected to increase with minimal changes in variability, in most GCM-RCM projections (averaged over the full 30 years of GCM-RCM projections).

GCM-RCM 2 projects a slight decrease in PET (appendix D, table D.3). For both period 1971-2000 and period 2071-2100, average PET is higher than average P. However, in projections of GCM-RCM 1, 2 and 5, P increases more (percentage-wise) than PET. In projections from GCM-RCM 3 and 4, PET shows the higher percentage-wise increase.

The overall picture is that of a warmer climate, with less variability in precipitation and temperature than before. Precipitation and potential evapotranspiration are both expected to increase, but in different magnitudes which makes the net result of available water uncertain.

5.5.2 Climate change impact assessment

This section gives the results of climate change impact assessment with base and regression models. First, simulated runoff based on observed P, T and PET is compared with observed runoff to determine hydrological model accuracy. Next, simulated runoff based on observed P, T and PET is compared with simulated runoff based on GCM-RCM projections to determine GCM-RCM influence. Last, simulated runoff based on GCM-RCM projections for 1971-2000 is compared with runoff based on projections for 2071-2100, to determine the projected climate change impact. Runoff characteristics are determined for winter (December, January, February; DJF), spring (March, April, May; MAM), summer (June, July, August; JJA) and autumn (September, October, November; SON).

Due to the way parameter estimates are based on 5-year average climate characteristics, all calculated statistics and flow duration curves are made for periods 1974-1998 and 2074-2098 (section 4.5).

Influence of hydrological models

Table 5.11 shows seasonal and annual statistics of observed discharge and simulated discharges by base and regression models with observed P, T and PET as input (full table in appendix D.2). Figure 5.3 shows flow duration curves of these discharges.

Table 5.11 shows that the base model slightly overestimates average runoff during the period 1974-1998, compared to observed values. The regression model simulates very similar average runoff as what has been observed. For both models this value is much lower than the RVE during validation (table 5.10, base model 13%, regression model 15%), since this period also includes a large part of their calibration period. Both base and regression model however, underestimate winter (DJF) and spring (MAM) flows, and overestimate summer (JJA) and autumn (SON) flows. Seasonal distribution of discharge is thus different from observations, even if overall discharge is similar to observations.

Figure 5.3 shows the lower variability simulated by both models: simu-

5.5. Climate change impact assessment

Table 5.11: Overview of differences between observed discharge and simulated discharge by base and regression model with observed P, T and PET as input, for period 1974-1998. I: observed discharge [m^3/s], II.a-I: difference between observed and simulated discharge by base model [%], III.a-I: difference between observed and simulated discharge by regression model [%]. Green: estimates are higher than I, red: estimates are lower than I

	Baseline [m^3/s]	DJF		MAM		JJA		SON		Overall	
		μ	σ	μ	σ	μ	σ	μ	σ	μ	σ
I		12.4	3.9	13.6	5.8	5.4	2.3	5.8	2.1	9.3	10.0
	Changes [%]	μ	σ	μ	σ	μ	σ	μ	σ	μ	σ
II.a		-7.5	-13.9	-14.5	-37.0	51.7	51.0	16.3	14.3	2.5	-20.3
III.a		-9.6	-3.0	-17.9	-29.1	47.4	35.4	16.7	16.1	0.1	-16.0

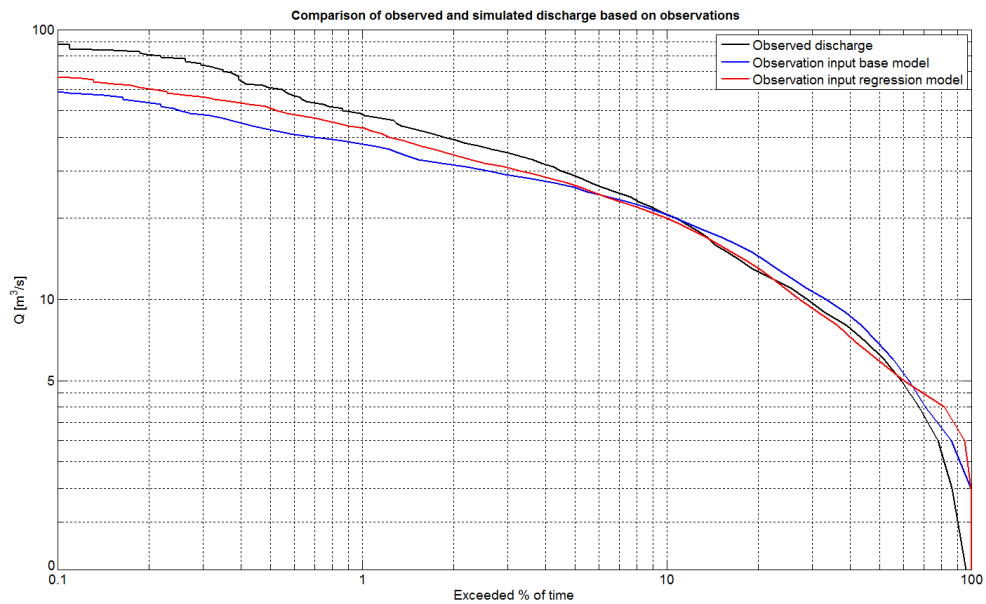


Figure 5.3: Flow duration curves of observed discharge, and discharge simulated with observations of P, T and PET as model input, for period 1974-1998

lated discharges from both base and regression model cover a smaller range of flows than have been observed. Base and regression model simulate lower peak flows than observed. The base model simulates flows with an exceedance frequency of 10% lower than have been observed. Flows with a higher exceedance frequency than 10% are simulated higher than observations. The regression model is somewhat more accurate. Simulated flows with an exceedance frequency of 15% are lower than observed, but generally closer to observations than simulations from the base model. Flows with exceedance frequencies between 15% and 60% are simulated very similar to observations by the regression model. Flows with exceedance frequencies higher than 60% are simulated higher than observed.

The base and regression models are not perfect in their simulation of runoff statistics. The base model has a much higher value for validation than the regression model ($Y = 0.69$ compared to $Y = 0.52$). However, comparing runoff statistics and flow-duration curves, the regression model performs slightly better than the base model with regard to average and seasonal flows, and seems to give a closer approximation of the observed flow duration curve for high flows. It has to be noted however, that these values are the result of using both models over the full data set, which has for a part been used to calibrate the base model and has in its entirety been used to establish the regression model.

Influence of GCM-RCM input

Table 5.12 shows seasonal and annual statistics of simulated discharges by base and regression models with observed P, T and PET as input. These are compared to simulated discharges by base and regression models with GCM-RCM projections of P, T and PET as input, for the period 1974-1998 (full table in appendix D.3). Figure 5.4 shows flow duration curves of these discharges.

Table 5.12 shows that (with some exceptions) using GCM-RCM projections as model input leads to lower average and seasonal runoff than using observations. This is reflected in the flow-duration curves in figure 5.4.

The base and regression model show similar reactions to GCM-RCM input, in the sense that resulting differences in table 5.12 are generally in the same direction (e.g. decrease in annual average runoff is visible in both models. Exceptions are found in differences in standard deviations during winter (DJF) and spring (MAM)). Both base and regression model show the biggest differences during summer (JJA) and autumn (SON), where the base model simulates bigger runoff differences than the regression model. Differences in winter (DJF) and spring (MAM) are smaller for both models, where the regression model generally simulates slightly bigger differences than the base model. This might be caused by changes in α in the regression model, which influences fast runoff, which in turn is more prevalent during

5.5. Climate change impact assessment

Table 5.12: Overview of differences between simulated discharges by base and regression model with observed P, T and PET and GCM-RCM projected P, T and PET as input, for period 1974-1998. II.a: simulated discharge by base model with observations as input [m^3/s], II.b-II.a: differences between simulated discharge with observations and GCM-RCM 1971-2000 input by base model [%], III.a: simulated discharge by regression model with observations as input [m^3/s], III.b-III.a: differences between simulated discharge with observations and GCM-RCM 1971-2000 input by regression model [%]. Green: estimates are higher than II.a and III.a respectively, red: estimates are lower than II.a and III.a respectively

	Baseline [m^3/s]	DJF		MAM		JJA		SON		Overall		
		μ	σ	μ	σ	μ	σ	μ	σ	μ	σ	
II.a		11.4	3.4	11.6	3.7	8.3	3.4	6.8	2.4	9.5	8.0	
	Changes [%]	μ	σ	μ	σ	μ	σ	μ	σ	μ	σ	
II.b-II.a	GCM-RCM	1	3.8	22.2	-1.1	12.2	-39.4	-53.9	-28.4	-50.4	-12.6	-13.9
		2	-13.2	-14.4	-8.6	13.5	-39.1	-44.1	-38.6	-57.5	-22.0	-25.9
		3	5.3	19.1	-4.8	7.0	-39.5	-42.6	-28.7	-38.7	-13.9	-14.6
		4	-19.9	9.2	-2.1	17.6	-52.3	-70.4	-49.9	-82.3	-26.5	-26.1
		5	-13.0	10.2	0.9	16.1	-50.5	-69.0	-50.9	-77.2	-23.2	-26.4
III.a	Baseline [m^3/s]	μ	σ	μ	σ	μ	σ	μ	σ	μ	σ	
III.a		11.2	3.8	11.1	4.1	8.0	3.1	6.8	2.4	9.3	8.4	
	Changes [%]	μ	σ	μ	σ	μ	σ	μ	σ	μ	σ	
III.b-III.a	GCM-RCM	1	2.8	12.1	-4.5	-1.1	-33.7	-56.5	-20.9	-52.5	-11.6	-17.1
		2	-16.1	-23.4	-10.6	6.2	-33.2	-54.1	-30.1	-68.0	-20.8	-23.6
		3	9.1	22.2	-11.1	-7.2	-32.3	-50.3	-19.5	-37.0	-11.5	-15.3
		4	-18.8	-8.4	-1.2	10.7	-43.3	-80.9	-37.7	-87.9	-22.0	-30.8
		5	-14.9	-2.0	4.3	20.6	-44.3	-81.3	-40.2	-86.9	-19.8	-28.2

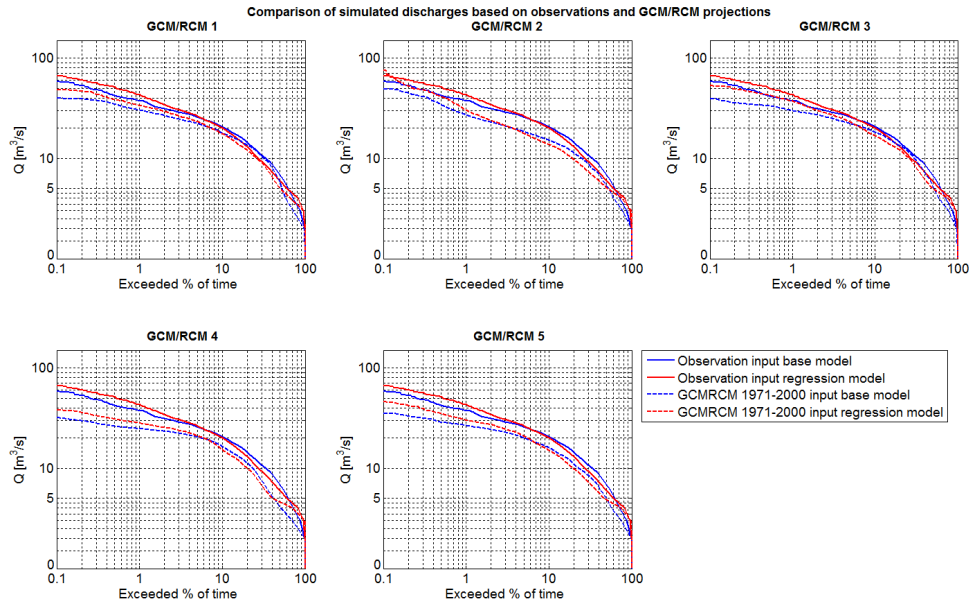


Figure 5.4: Flow duration curves of simulated discharge with observations of P, T and PET and GCM-RCM projections as model input, for period 1974-1998

winter and spring.

The flow duration curves show a tendency for both the base and regression model to simulate lower flows with GCM-RCM input than with observations as input. Of the two, the regression model simulates higher flows for exceedance frequencies lower than approximately 10% and for exceedance frequencies higher than approximately 50%. The base model simulates higher flows for exceedance frequencies between 10% and 50%.

GCM-RCM precipitation projections are, even after bias-correction, quite different from observations (projections are 11% lower than observations, section 2.2). This is most likely the cause of the big differences between simulated runoff with observed data and GCM-RCM projections by both the base and regression model. Moreover, the choice of GCM-RCM affects simulated discharges much more than the choice for either the base or regression model (e.g. differences resulting from varying GCM-RCM input are larger than differences resulting from using either base or regression model with the same GCM-RCM projections as input).

Projected impact of climate change

Table 5.13 shows seasonal and annual statistics of simulated discharges by base and regression models with GCM-RCM projections as input, for the periods 1974-1998 and 2074-2098 (full table in appendix D.4). Figure 5.5 shows flow duration curves of these discharges.

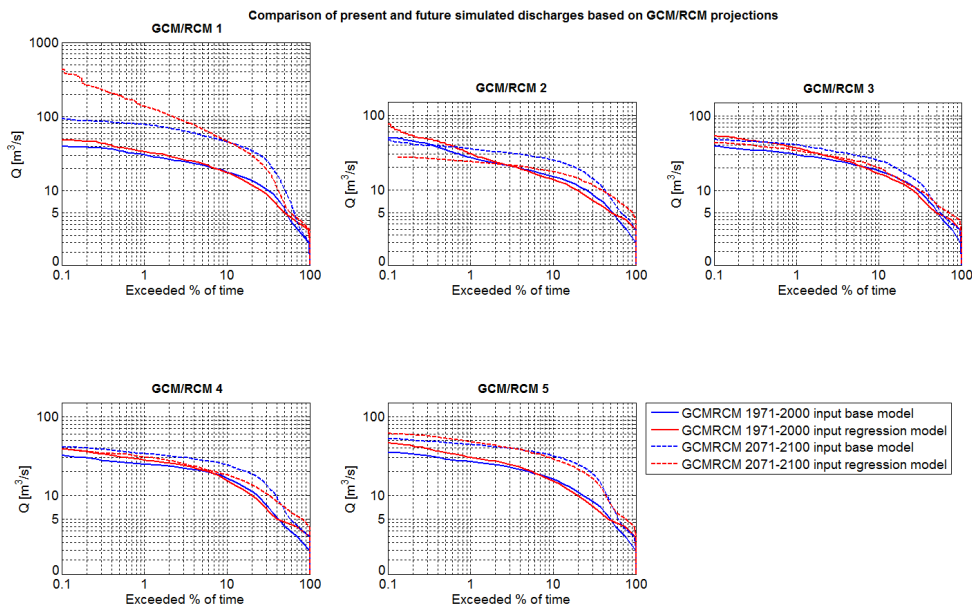


Figure 5.5: Flow duration curves of simulated discharge with GCM-RCM projections for period 1974-1998 and 2074-2098 as model input

5.5. Climate change impact assessment

Table 5.13: Overview of differences between simulated discharges by base and regression model with GCM-RCM projected P, T and PET for period 1974-1998 and 2074-2098 as input. II.b: simulated discharge by base model with GCM-RCM 1974-1998 input [m^3/s], II.c-II.b: differences between simulated discharge with GCM-RCM 1974-1998 and GCM-RCM 2074-2098 input by base model [%], III.b: simulated discharge by regression model with GCM-RCM 1974-1998 input [m^3/s], III.c-III.b: differences between simulated discharge with GCM-RCM 1974-1998 and GCM-RCM 2074-2098 input by regression model [%]. Green: estimates are higher than II.b and III.b respectively, red: estimates are lower than II.b and III.b respectively

		DJF		MAM		JJA		SON		Overall		
Baseline [m^3/s]		μ	σ	μ	σ	μ	σ	μ	σ	μ	σ	
II.b	GCM-RCM	1	11.9	4.1	11.5	4.1	5.0	1.6	4.8	1.2	8.3	6.9
		2	9.9	2.9	10.6	4.1	5.0	1.9	4.2	1.0	7.4	5.9
		3	12.0	4.0	11.0	3.9	5.0	2.0	4.8	1.5	8.2	6.8
		4	9.1	3.7	11.3	4.3	3.9	1.0	3.4	0.4	7.0	5.9
		5	9.9	3.7	11.7	4.2	4.1	1.1	3.3	0.5	7.3	5.9
Changes [%]		μ	σ	μ	σ	μ	σ	μ	σ	μ	σ	
II.c-II.b	GCM-RCM	1	175.1	213.8	156.6	185.5	40.2	152.1	7.7	164.8	124.1	173.1
		2	74.5	96.3	61.4	29.0	16.6	-6.2	26.3	2.1	53.8	47.1
		3	11.3	44.8	60.3	17.8	47.4	58.9	-20.0	-41.5	29.9	35.8
		4	81.2	57.2	44.8	36.1	27.7	26.9	31.9	153.5	52.5	44.5
		5	136.4	107.8	74.7	68.4	27.1	69.5	39.7	266.2	84.5	98.9
Baseline [m^3/s]		μ	σ	μ	σ	μ	σ	μ	σ	μ	σ	
III.b	GCM-RCM	1	11.5	4.3	10.6	4.1	5.3	1.3	5.4	1.2	8.2	7.0
		2	9.4	2.9	9.9	4.4	5.4	1.4	4.7	0.8	7.3	6.4
		3	12.2	4.7	9.9	3.8	5.4	1.5	5.5	1.5	8.2	7.1
		4	9.1	3.5	11.0	4.6	4.5	0.6	4.2	0.3	7.2	5.8
		5	9.5	3.8	11.6	5.0	4.5	0.6	4.1	0.3	7.4	6.0
Changes [%]		μ	σ	μ	σ	μ	σ	μ	σ	μ	σ	
III.c-III.b	GCM-RCM	1	275.9	877.2	106.5	343.8	14.1	232.2	44.7	565.7	140.6	455.2
		2	22.6	-1.7	44.5	-50.8	45.8	1.9	33.0	-36.7	36.2	-23.0
		3	-19.4	-26.3	52.3	-31.6	52.9	58.3	-11.1	-65.9	16.5	-2.1
		4	34.2	-0.8	25.9	-34.8	47.5	96.4	27.3	72.6	32.0	3.5
		5	124.3	97.1	66.5	27.2	39.2	159.4	33.0	366.3	76.0	80.3

Table 5.13 shows a projected increase in average runoff for all GCM-RCM combinations, and an increase for nearly all seasonal flows. With the regression model, standard deviations do not show a uniform change: both increases and decreases are visible. The base model generally foresees an increase in standard deviation. For both models, spring (MAM) and to a somewhat lesser extent winter (DJF), see a larger runoff increase than summer (JJA) and autumn (SON). This seems the result of increased projected precipitation during winter ($P_{\mu,w}$, appendix C.2, figure C.9).

Runoff changes are especially large when projections from GCM-RCM 1 are used as model input, which seems consistent with its large projected increase in precipitation (appendix D, table D.1). GCM-RCM 1 also has the highest projections of precipitation intensity during winter ($P_{wet,\mu,w}$, appendix C.2, figure C.9) which leads to high values for α in the regres-

5.5. Climate change impact assessment

sion model. This occasionally results in very high simulated discharges, as reflected in figure 5.5. Both base and regression model simulate very high future flows compared to the present period, with input from this GCM-RCM.

The base model projects an increase in flows for nearly all situations with GCM-RCM projected input. Only with input from GCM-RCM 2, the base model projects lower very high flows (exceedance frequency lower than 0.3%) than with projected present input. The regression model however, only projects increased flows for GCM-RCM combinations 1, 4 and 5. For GCM-RCM combinations 2 and 3, the regression model actually simulates lower very high flows (with exceedance frequency lower than 2.5%), and higher higher, medium and low flows (with exceedance frequency greater than 2.5%) in future, compared to the present. This is likely related to projections of future $P_{wet,\mu,w}$ which are lower than present projections of $P_{wet,\mu,w}$ for most GCM-RCM combinations. This leads to lower α values and more spread out runoff peaks.

5.5.3 Comparison of projected runoff changes

Table 5.14 shows the difference between changes projected by base and regression model. Green values indicate that the regression model projected the bigger change, red values show that the base model projected the bigger change. Note that the colouring does not indicate the direction of projected changes, which can be found in table 5.13.

Table 5.14: IV: differences in runoff changes projected by base and regression model [%] (table 5.13). For example: with input from GCM-RCM 1, the regression model projects a change in overall runoff that is 13.3% larger than the change in overall runoff projected by the base model. Green: regression model projects higher change than base model, red: regression model projects lower change than base model. Note: colouring does not reflect direction of projected changes

	Changes [%]	DJF		MAM		JJA		SON		Overall		
		μ	σ	μ	σ	μ	σ	μ	σ	μ	σ	
IV	GCM-RCM	1	57.6	310.2	-32.0	85.3	-64.8	52.7	480.4	243.4	13.3	163.0
		2	-69.7	-101.8	-27.4	-275.1	176.1	-130.6	25.7	-1878.9	-32.8	-148.9
		3	-271.5	-158.7	-13.4	-277.2	11.8	-1.1	-44.8	59.0	-44.9	-105.9
		4	-57.9	-101.4	-42.2	-196.4	71.3	257.6	-14.4	-52.7	-39.1	-92.1
		5	-8.8	-9.9	-11.0	-60.2	44.4	129.2	-17.0	37.6	-10.1	-18.8

On an annual average basis, simulated runoff is very similar for base and regression model with GCM-RCM projections for the period 1974-1998 as input (appendix D, table D.6). Differences between the base and regression model range from -1.2% to +3.6% for this period. Differences in simulated runoff for the period 2074-2098 are more pronounced, ranging from -12.2% to +6.1%. Whether the base or regression model is used thus matters little

for the period 1974-1998, but makes a significant difference for predictions of future runoff.

Concerning projected changes, the regression model projects smaller changes in average runoff than the base model, with input from four of the GCM-RCMs. The exception is input from GCM-RCM 1, which leads the regression model to project a larger change than the base model. This is likely related to the very high flows simulated with future GCM-RCM input. In almost all cases, the regression model projects smaller changes than the base model during winter (DJF), spring (MAM) and autumn (SON), and larger changes than the base model during summer (JJA).

While the regression model shows a tendency to simulate higher high flows than the base model when simulating discharge for the period 1974-1998 (with both observations and GCM-RCM projections as input), this behaviour is not seen for projected future discharge with GCM-RCM 2-4 as input (figure 5.5). With these three GCM-RCM combinations as input the base model projects larger high flows than the regression model.

Earlier research into model performance under changing climate conditions found that model performance deteriorates for periods with large changes in average precipitation, compared to the calibration period (e.g. (Bastola et al., 2011; Chiew et al., 2009; Coron et al., 2012; Merz et al., 2011; Vaze et al., 2010)). Authors mention lower ranges varying from -7.5% to -15% , and upper ranges from $+7.5\%$ to 20% for changes in precipitation for which model performance is still acceptable. In this research, the base model stays at acceptable performance (measured as a value for the objective function) during validation, for a $+8.5\%$ change in average precipitation (comparing average precipitation during calibration with average precipitation during validation). Average precipitation projected by the GCM-RCMs of both present and future (table D.1) differs from average precipitation during calibration between -10.4% and $+6.7\%$. This is within, or close to, the range specified by various authors. There is therefore little reason to assume that base model functioning will be negatively affected by using GCM-RCM projected precipitation input.

Concluding, differences exist between both models when they are used for climate change impact assessment. Since the base model shows better validation than the regression model, and estimated precipitation by GCM-RCM combinations is not very different from precipitation during calibration of the base model, projected changes by the base model seem more trustworthy than changes projected by the regression model. However, differences in projected changes are much bigger between the various GCM-RCM combinations than between base and regression model for a specific GCM-RCM. GCM-RCM input therefore appears to be an important source of projection uncertainty.

Chapter 6

Discussion

6.1 Place in recent developments

This study follows on recent research on parameter non-stationarity (e.g. Coron et al. (2012); Merz et al. (2011), section 1.1.3). To the author's best knowledge, this study is new to explore the second option presented in Merz et al. (2011): predicting parameter values based on their correlation with climate characteristics. The first option of expanding the model structure to include relevant catchment processes affected by climate change is outside the scope of this study.

Much of this study's value can be found in the general applicability of the methodology. The methodology is independent of the model and catchment used here, and can easily be applied to different catchments (with the recommendation to select a catchment for which long and high-quality data sets are available) and/or conceptual models, given that certain changes to the methodology are recommended (further discussion).

HBV parameters aim to capture the result of various hydrological processes occurring in the catchment. The methodology in this study assumes that, from the location in the model and the numerical influence of parameter values, can be deduced which processes the parameter captures. For example, parameter α is located in the fast runoff routine in the HBV model, and influences the magnitude of peak flows. It is therefore assumed that α simulates the effect of hydrological processes related to peak-flow generation. This explanation is used to select significant correlations on which to base further regression analysis. However, in the HBV model this link between parameter values and hydrological processes can be doubted (since the model is conceptual rather than process-based) and this can be even more so for different models (i.e. models with less parameters and thus even less clear relations with hydrological processes). Therefore the way of assessing which significant correlations to use for regression analysis might have to be changed, when applying the methodology to different models.

6.2 Data

In this study, values for the objective function are not high for both calibration and validation, compared to other catchments (e.g. $Y_{cal} = 0.93$,

$Y_{val} = 0.84$ for the Ourthe basin in the Meuse catchment, Tillaart, 2010). This might be related to data quality of observed P, T, PET and Q.

Precipitation data have been constructed for this catchment using Thiessen polygons based on multiple measuring stations in and near the catchment. The catchment is relatively flat, so orographic effects are minimal. This method does however rely on accurate measurements from 15 locations.

Temperature is measured at a station outside of the catchment. The catchment is relatively small, so temperature differences are probably not large, but this can not be confirmed.

Potential evapotranspiration is calculated based on the temperature time series with the Hamon-method. This method is one of the simplest evapotranspiration estimates available, and generally used for monthly or annual values. The method is used here to estimate daily PET values. It is likely that the method underestimates PET during cold periods (e.g. winter months) and overestimates PET during warm periods (e.g. summer). Calibrated parameters might thus be compensating for structural bias in the PET estimates. GCM-RCM projections of PET are however made with the more advanced Penman-Monteith method, which should provide more accurate PET estimates. It is therefore possible that the calibrated parameters are compensating for PET estimation errors that are not present when using GCM-RCM input, thus reducing model accuracy.

The GCM-RCM projections are bias-corrected, but based on a reanalysis of precipitation and temperature data. This leads to differences between average observed and average GCM-RCM projected P, T and PET for the period 1971-2000 (which, in the case of PET is also caused by different estimation methods).

The catchment contains many control structures and storage systems. This disrupts the natural catchment response to precipitation. Therefore calibration is difficult, since the calibration algorithm tries to fit model parameters to account for unpredicted anthropogenic effects.

Calibration results of all 5-year periods are used as a basis for correlations and regression equations. The fact that the data sets used for calibration of this periods are not optimal, influences the accuracy of later analyses. In a catchment with a more natural relation between climate input and runoff and for which data of better quality is available, it will be easier to establish accurate regression equations.

6.3 Sensitivity analysis

The sensitivity analysis marked FC as the most important parameter by far. Compared to the main effect of FC , all other effects (both main and interactions) are small. Parameters α and $PERC$ are the next two most important parameters, based on their total effect.

FC , α and $PERC$ are the only parameters for which statistically sig-

nificant regression equations with a reasonable fit R^2 can be established. However, only the equation for α can be used in combination with GCM-RCM input. FC and $PERC$ are fixed during the final climate change impact assessment. Results would likely have been very different if the regression equation for FC could be properly included during climate change impact assessment.

The sensitivity analysis also indicates that for many parameters, interactions with other parameters have more influence on overall model output variance, than their respective main effects. These interactions are however not included in the established regression equations, which only include climate characteristics. Fixed parameters in the regression model are recalibrated to partly account for these interactions (recalibration is intended to provide parameter values that perform reasonably well with a variety of values of the estimated parameters). However, for the exact same period, a fully calibrated model will always be equal as, or better than, a regression model that can not account for parameter interactions.

The sensitivity analysis defined parameters FC , LP , α , $PERC$ and TT as the parameters with the most influence on model output variance, based on sampling of the full 30 years of data (section 3.3.3). However, for certain 5-year periods, the model seems sensitive to K_s to an extent not shown by the sensitivity analysis. This might be caused by the differences in climatic variability between the 5-year periods, and resulting differences in relative importance of baseflow simulation and thus K_s . It might therefore be worthwhile in future research to perform the sensitivity analysis multiple times: once for the full period, and once for each 5-year period to ensure that no “incidental” sensitivities (such as K_s in this case) are missed.

6.4 Methodology

6.4.1 Research background

Conceptual model parameters aim to capture the results of various hydrological processes occurring in a catchment. Theoretically, parameters are catchment dependent and should be independent from climate. In practice however, optimal parameter values vary in time and are correlated with certain climate characteristics. This might reflect an actual relation between parameter values and climatic conditions, or the parameters might compensate for errors in model structures. The methodology in this study assumes that a relationship exists (e.g. changes in average temperature might affect vegetation in any number of ways, which in turn might change evapotranspiration, interception and runoff processes) and attempts to quantify this relationship with regression analysis.

However, if the assumption of a relationship between parameter value and climatic conditions were not true, this study is potentially an exercise in

data-fitting of the 5-year variability in P . The correlations of parameters with various climate characteristics could be the result of intercorrelation of those characteristics with average P . This is not necessarily bad, since a regression model might still improve model functioning for climatic conditions different from those present during calibration. However, if the regression equations do simulate an actual relationship, confidence in model performance for different climatic conditions will be higher.

It is very difficult to determine the difference between a true relationship and data-fitting. It might be possible to test this by selecting multiple similar catchments (e.g. similar catchment characteristics and similar climate characteristics) and establishing regression equations for these catchments. Similar catchments showing very different correlations between parameter values and climatic conditions might indicate that no relationship is present between parameters and climate.

6.4.2 Calibration procedure

Three different calibration algorithms were investigated for this study, each with its own pros and cons, with the final choice being the SCEM-UA algorithm. During calibration, the algorithm is found not to be perfect. Restricted parameter ranges are necessary for certain 5-year periods to ensure proper model functioning with regard to fast and slow runoff reservoirs. However, restricting the parameter ranges also leads to better values for objective function Y for these periods, while the parameter space is simply restricted and not expanded. This means that the algorithm was unable to locate a better alternative parameter set during the first calibration attempt, and thus does not always end up in the global optimum of the available parameter space. Convergence plots of parameter progression show that the algorithm converges to the sub-optimal value, so this is not a case of using too few iterations.

The entire 30-year data set is divided into 5-year periods for calibration. This has the downside however, that truly independent validation of the regression model is not possible, since regression equations are for a part based on data points from the validation period. For further research, it is recommended to use a catchment for which a long data set is available, to both ensure enough (preferably more than used in this study) points for correlation and regression analyses, and a completely independent validation period.

Equifinality (the fact that different parameter sets might result in the same value for the objective function) possibly presents a problem. It is possible that, while parameter values might be correlated with climate characteristics, a different, random parameter set performs equally well by mere coincidence. This seems unlikely to influence the 5-year calibration results, since parameter progression throughout the 5-year windows is rather

smooth. Knowing that each 5-year period is only 1 year different from the year before, and assuming that calibrated parameter values are an average value for the entire period, the smooth parameter progression would indicate that equifinality is not an issue here. However, this assumption is not in all cases true. For example, parameter α has an unexpected low value for calibration period 18, which has only low flows and no runoff peaks. This is likely caused by the objective function which is biased towards peak flows. This directs calibration of α in the periods that do include pronounced peak flows (e.g. period 17 and 19, where α is not an average value for the entire period, but directly aimed at representing the single peak present in both time periods). It is therefore difficult to be completely certain about equifinality.

6.4.3 Suitability of objective function

The objective function follows a relatively smooth pattern during calibration of all 5-year windows, with an unexpected value for period 18 (lower objective function value than would fit the pattern, section 5.1.2). The objective function can be split up into three distinct parts (section 3.3.1): upper NS (related to modelling error), lower NS (related to observed daily variability in discharge) and RVE (related to difference between modelled and observed discharge volume).

Runoff during period 18 has been very low and constant, without any prominent discharge peaks (lowest natural variability of all periods). Absolute modelling error during this period is the lowest of all 5-year periods as well (figure 5.1). However, relative to the observed discharge variability, modelling error is quite high, which results in a low value for NS and thus Y.

In the objective function Y, RVE has a penalty function: an incorrect volume error lowers the overall objective function value. RVE is nearly zero for all 5-year periods and variations in NS therefore almost exclusively determine the value of Y. However, NS is inherently biased towards correct simulation of medium and high flows, because it uses the square of absolute difference between daily modelled and observed discharge. This makes NS not very well suited as a target function for periods without any peak flows. The effect of peak flows on the NS coefficient can be seen for periods 17 and 19 (figure 5.1): these periods differ only one year from period 18, but the variability component of NS is several factors larger, due to the occurrence of clear runoff peaks in the single year that both periods differ from period 18.

Parameter values that result from calibration of period 18 are however no outliers compared to calibrated values from all other periods. Therefore, while the objective function might not be very well suited for this specific period, this does not affect the further analyses much.

6.4.4 Correlation procedure

Linear relations are assumed for all investigated correlations. It seems likely that actual relationships are more complex, but there is little evidence to enforce this via rank correlation coefficients. A longer data set with more data points, might provide a clearer picture of the shape of potential relationships.

Correlation between various parameters is not investigated, and these relations are ignored in the regression equations as well for sake of simplicity (because it is not easily determined which parameter is dependent on which others, as is required knowledge for the regression analysis. Most likely parameter values are interdependent in an iterative way). The sensitivity analysis shows however that interactions between parameters play an important role in model outcome variability. Parameter interactions are not easily defined in the HBV model, and the Sobol' sensitivity method is unable to define which specific interactions lead to the sensitivity results. Either a model for which these interactions are explicitly described, or a sensitivity analysis that can define parameter interactions, or a catchment showing only (or mostly) sensitivity for a single parameter (that can properly be estimated with a regression equation) are therefore recommended for further research.

6.4.5 Regression analysis

Linear regression equations are established for FC , α and $PERC$. The various regression fits are not optimal with values of $R_{\alpha}^2 = 0.54$, $R_{PERC}^2 = 0.42$ and $R_{FC}^2 = 0.40$. This is partly related to data issues, and partly to the overall length of the data set. A longer data set would give more points on which to base correlation and regression analyses, and might give a better description of the relationship between parameter and climate. This could give a reason to change linear regression into a more complex regression, possibly with asymptotes for parameter values (removing the extrapolation issues encountered with FC and $PERC$ estimates in this study).

6.4.6 Implementation of regression equations

With the current methodology, regression coefficients of regression equations are determined based on the best fit R^2 on the available data points. Alternatively, regression equations could be integrated in the model as changes to the model structure, and the regression coefficients could be calibrated along with other parameters. This will add several degrees of freedom to the calibration procedure (e.g. in this study three coefficients for α , three for $PERC$ and four for FC) leading to a much larger parameter space. This

has the downside of increasing calibration time, and decreasing the chances of finding a global optimum with a calibration algorithm. It has the benefit of directly calibrating the regression equation against the objective function, rather than fitting the regression equation to multiple calibrated parameter values with varying accompanying values for the objective function (i.e. the values of the objective function for the various 5-year periods).

6.4.7 Climate change impact assessment

Due to the differences in average values between observed P, T and PET, and bias-corrected GCM-RCM projections of P, T and PET, the model simulates lower flows with GCM-RCM input than with observations as input. Therefore the climate change impact assessment in this study should only be used as a tool to determine the differences between the base and regression model, and not as an accurate projection of possible changes in the catchment.

Delta-method for estimating precipitation changes

An alternative to the climate change impact assessment approach used here is the so-called “Delta-method” in which not the actual GCM-RCM projections are used for projections of present and future runoff. Rather the projected changes (“change fields”) are derived from present and future GCM-RCM projections and applied to the observed data sets to give an estimate of future climate conditions (IPCC, 2001b, ch. 4.3.6.2). This method generally uses absolute changes for temperature and relative changes for precipitation and potential evapotranspiration. It provides easier comparison of runoff characteristics than directly using GCM-RCM projections as model input, since with the Delta-method only climatic observations and estimated changed observations are used as model input. This skips the step where simulated runoff based on observations is compared with simulated runoff based on GCM-RCM projections.

This method is difficult to apply in this research because of the difference between frequency of wet days as observed and projected by the GCM-RCM combinations (table 6.1). All GCM-RCM combinations foresee an increase in wet days, that can not be taken into account with the Delta-method since observations are multiplied with the derived projected change. This will lead to differences between the average precipitation intensity on wet days as projected by GCM-RCM combinations and as used in the hydrological model from adjusted observations (e.g. a projected average increase in precipitation will lead to an increased precipitation intensity in the adjusted observations, while the GCM-RCM combinations actually project a decrease in intensity due to the increased number of wet days).

Since precipitation intensity is used in the regression equations that es-

6.5. Results

timiate future parameter values, inaccurate representation of this climate characteristic is undesirable and the Delta-method is therefore not applied. The consequence of this is that the regression equation for parameter FC can not be used and FC is recalibrated (section 4.4.1). The sensitivity analysis pointed FC as the most important parameter, so conclusions would be more convincing if FC could have been estimated with a regression equation as well.

Table 6.1: Observed and estimated frequency of wet days ($P > 0.1 \text{ mm}$)

	Present	Future
Observed	0.53	
GCM-RCM		
1	0.45	0.72
2	0.43	0.54
3	0.43	0.70
4	0.44	0.64
5	0.44	0.66
6	0.42	0.63

6.5 Results

The results in this research are arguably more important for further research, than the practical applicability for the Wehna catchment. It is impossible to know for certain whether the base or regression model performs better for future conditions, but validation results are better for the base model than for the regression model. This indicates that the base model is potentially better suited for climatic conditions outside the calibration period.

In hindsight, this catchment was not the ideal test case for a new modelling approach, given data quality, anthropogenic effects obscuring the relation between climate and runoff and the rather short available data series. It is shown however, that the regression model performs similar to the base model when modelling discharge for the entire period 1971-2000 (including both calibration and validation periods). Furthermore, calibration results for all regression models are similar to that of the base model, even in the case that the three most sensitive parameters (FC , α and $PERC$) are estimated and not calibrated. This gives confidence in the regression approach as a whole.

Chapter 7

Conclusions and recommendations

7.1 Conclusions

The goal of this study is to establish relationships between optimal model parameters and climate variables, to quantify how well these relationships perform during validation and to assess how these relationships perform during climate change impact assessment, compared to a traditional hydrological approach towards calibrated parameters. To achieve this goal, first linear correlations between calibrated parameter values and various climate characteristics are determined. Next, significant correlations that also make sense from a hydrological point of view are used in a linear regression analysis. This results in regression equations that estimate the value of certain parameters. The regression equations are then implemented in the hydrological model and validated. Last, the performance of the new regression model during climate change impact assessment is compared to that of the base model.

Correlations between the six calibration parameters and various climate characteristics are determined. Since this study looks for relationships between parameter values and climatic conditions, each significant correlation is analysed to determine whether the correlation could be the result of an actual relationship, or that it results from coincidence. *LP* is only correlated with precipitation intensity during winter months. This seems a coincidence and parameter *LP* is thus not used in the regression analysis. *TT* shows no significant correlations with the investigated climate characteristics. Parameters *FC*, α , K_s and *PERC* show significant and explainable correlations and these are used during the regression analysis.

Both single and multiple linear regression are used to establish regression equations for *FC*, α , K_s and *PERC*. Multiple regression shows an improvement of the equation fit (R^2) over single regression for *FC*, α , and *PERC*. K_s only shows significant correlations with two climate characteristics and these can not be combined in a single significant regression equation for K_s . The best relationship for *FC* includes climate characteristics P_μ , $P_{wet,\mu}$ and $P_{\mu,w}$, with a fit of $R^2 = 0.40$. The best relationship for α includes P_μ and $P_{wet,\mu,w}$, with a fit of $R^2 = 0.54$. The best relationship for K_s uses ar_μ , with a fit of $R^2 = 0.18$. The best relationship for *PERC* includes

7.1. Conclusions

P_μ and $P_{wet,\mu,w}$, with a fit of $R^2 = 0.42$. None of the regression equations estimate their respective parameter values particularly well (see R^2 values). However, in light of the complexity of the problem and the simplicity of the regression approach, the equations still include a big part of the variability in values of α , $PERC$ and FC . The fit for K_s is too low to consider using this equation; the resulting uncertainty will likely lead to much more outcome uncertainty than simply recalibrating this parameter. Therefore only the regression equations of α , $PERC$ and FC are implemented in the regression models.

Four regression models are established that estimate values of only α , of α and $PERC$, of α and FC , and of α , $PERC$ and FC . Each regression model is tested with GCM-RCM projections as input. Due to biases in GCM-RCM projections of precipitation, the regression equations of FC and $PERC$ do not perform satisfactory. Estimated values of FC are generally negative (capped at zero in the equation) for the present period, effectively disabling the soil moisture routine in the HBV model. Estimated values of $PERC$ are very low and often negative for the future period, which affects the functioning of the groundwater routine and generation of base-flow. The situations resulting from estimated FC and $PERC$ values are considered hydrologically unlikely. Therefore the regression model that estimates only the value of α is selected for climate change impact assessment.

The base model is calibrated on the last 20 years of data ($Y = 0.73$). Parameters in the regression model that are not estimated with regression equations are recalibrated on this same period ($Y = 0.73$). The base and regression model are validated using the remaining part of the data set, with $Y = 0.69$ for the base model and $Y = 0.52$ for the regression model. Measured over the entire data period however, the regression model simulates average discharge closer to observed values than the base model does. Again seen over the entire data period, both the base and regression model underestimate winter and spring discharges, and overestimate summer and autumn discharges. The regression model simulates high flows (exceedance frequency $<60\%$) more accurate than the base model, compared to observations. The base model is closer to observations for low flows (exceedance frequency $>60\%$).

Due to bias in GCM-RCM precipitation projections, both base and regression model structurally simulate lower overall discharge, compared to simulations with observed P, T and PET as input. Especially for summer and autumn, both models simulate lower discharges, although the base model simulates larger differences than the regression model. Runoff simulations are closer to simulations with observed P, T and PET as input for winter and spring months, where the regression model seems to simulate somewhat larger differences than the base model. The regression model has a tendency to simulate higher peak (exceedance frequency approximately $<5\%$) and low flows (exceedance frequency approximately $>50\%$). The base

model simulates higher medium flows. Overall however, the base and regression model react similarly to GCM-RCM input, and differences between the GCM-RCM projections create larger differences in runoff than the choice for either base or regression model.

Comparing runoff simulations with GCM-RCM projections for the present and future, both base and regression model simulate increased overall runoff. With a few exceptions, this increase is also visible in all seasonal flows for both the base and regression model. Again, different GCM-RCM projections influence simulated runoff more than the choice for either base and regression model. The base model simulates higher future flows for all exceedance frequencies, compared to simulated present flows (with the exception of the top 0.3% flows with GCM-RCM 2 input, which are projected slightly lower in future). The regression model shows this behaviour with input from GCM-RCM 1, 4 and 5. With input from GCM-RCM 2 and 3 however, the regression model simulates lower high flows (exceedance frequency $<2\%$) and higher medium and low flows (exceedance frequency $>2\%$).

Comparing the projected changes by the base and regression model, the base model projects larger changes for four of the five GCM-RCM combinations. The exception is GCM-RCM 1, where the regression model projects the bigger change. This is likely due to its projected high precipitation intensity during winter, which causes the regression model to use high values for α . This in turn leads to incidental very high runoff peaks simulated by the regression model. For the other four GCM-RCM combinations, the regression model projects changes that are between 10% and 45% lower than the changes projected by the base model. In most cases, the regression model predicts lower changes in winter, spring and autumn average discharge, and higher change in summer discharge than the base model does. Projected average variability measured over the entire period is generally lower in regression model simulations as well. The regression model thus simulates lower and more steady runoff (lower average variability) than the base model for the future period.

Concluding, differences between both climate change impact assessments are visible. However, the base model has better validation than the regression model and it is therefore uncertain how accurate the observations about regression model functioning compared to base model functioning during climate change impact assessment are. The methodology applied in this study seems promising however, and it could be worthwhile to investigate regression models further. A better functioning regression model (i.e. equal or better validation than the base model) will give a clearer conclusions about the differences in projected climate change impacts by both model types. In this study however, the choice of GCM-RCM input influences climate change impact assessment more than whether the base or regression model is used.

7.2 Recommendations

For further research into the use of regression models, five recommendations are made that address the major issues encountered in this study:

1. This study assumes that a relationship between optimal parameter values exists and the research methodology is applied according to this assumption. It is however very difficult to differentiate between modelling an actual relationship and curve-fitting of the available data. If it would be certain that there is an actual relationship between parameter values and climatic conditions, the established relations can be applied to future periods with more confidence than is the case now.

It might be possible to test for actual relationships by applying this methodology to multiple similar catchments (in terms of catchment and climate characteristics) and comparing the results. This will most likely not provide a conclusive answer, but rather indicate if it is plausible that these relationships might be true.

2. Test case(s) for later research should be selected with care. It is strongly recommended to use one or more natural catchments with no to minimal human interference, for which longer data sets are available. This leads to a less obscured connection between runoff and climate, and thus between parameter values used for simulating runoff and climate.

Furthermore, a longer data set provides more possible points for correlation and regression analysis (potentially allowing selection of parameter sets with an objective function value threshold, e.g. only use those parameter sets with $Y > 0.90$ for further analysis) and allows to save a period for completely independent validation, without reducing the number of data points for correlation and regression analysis overly much.

Additionally, a longer data set might include climate variations that can be used as an analogy for climate change. This would allow calibration and validation of a base model and establishing of a regression model on those parts of data that represent current and future climate.

3. It seems unwise to neglect parameter interactions. If it can be determined which interactions occur in the model, and which parameter depends on which other parameter, these relations might be included in the regression equations. This assumes however, that parameter interaction is a one-way process and not the result of an iterative process during calibration, which seems more likely.

An easier alternative would be to use a catchment with a very high sensitivity for a single parameter (providing this parameter can be estimated with a regression equation), which makes interaction effects relatively less important.

4. The followed approach with regard to using GCM-RCM estimates for climate change assessment is not optimal, because parameter estimates are influenced by bias in the GCM-RCM estimates. The Delta-method

for climate change impact assessment provides an alternative to using actual GCM-RCM projections as model input, by changing the observed data series of P, T and PET relative to changes predicted by the used GCM-RCM combinations. However, limitations to the Delta-method are that it does not alter the order of wet and dry days, nor the frequency of days with precipitation. By extent, the average intensity of precipitation events in the altered observation series will be different from the GCM-RCM projections, given that the GCM-RCM combinations project a change in the frequency of wet days. Given these limitations, the correlation and regression methodology has to be adjusted to include only those climate characteristics that are not affected by application of the Delta-method.

5. Explicitly accounting for parameter changes by determining regression coefficients from multiple regression analysis can be exchanged for changing the model structure to include parameter equations and calibration of these coefficients. This potentially leads to long calibration times due to the increased degrees of freedom, so it is recommended to keep the number of other calibrated parameters to a minimum. This would potentially lead to a better model fit and performance during validation.

Experimental calibration (50000 iterations) of the regression coefficients is attempted for the four regression models established in this study (table 7.1). Calibration results are slightly lower than the results obtained from using the regression coefficients from regression analysis and validation values are clearly worse with calibrated coefficients. This shows the need for much longer calibration (because a higher degree of freedom during calibration should result in a better calibration fit), the need for an algorithm suited for searching the increased solution space (since the SCEM-UA algorithm was unable to find the regression coefficient as they are established in the regression analysis, while these coefficients are included in the calibration interval) and that equifinality is very likely to influence results (since calibrated regression coefficients are very different from coefficients found with regression analysis).

7.2. Recommendations

Table 7.1: Results of calibrated regression coefficients (“Cal. coef.”) compared to regression coefficients established with regression analysis (“Reg. coef.”) for the four regression models

		Model 1		Model 2	
		Reg. coef.	Cal. coeff.	Reg. coef.	Cal. coeff.
Degrees of freedom		5	8	4	10
Calibration	Y	0.73	0.66	0.71	0.67
Validation	Y	0.52	0.01	0.50	0.22
		Model 3		Model 4	
		Reg. coef.	Cal. coeff.	Reg. coef.	Cal. coeff.
Degrees of freedom		4	11	3	14
Calibration	Y	0.73	0.69	0.71	0.67
Validation	Y	0.56	0.13	0.56	-7.35

Bibliography

- Abebe, N.A., F.L. Ogden, and N.R. Pradhan (2010), "Sensitivity and uncertainty analysis of the conceptual HBV rainfallrunoff model: Implications for parameter estimation." *Journal of Hydrology*, 389, 301–310. doi: 10.1016/j.jhydrol.2010.06.007.
- Akhtar, M., N. Ahmad, and M. J. Booij (2009), "Use of regional climate model simulations as input for hydrological models for the Hindukush-Karakorum-Himalaya region." *Hydrology and Earth System Sciences*, 13, 1075–1089. doi: 10.5194/hess-13-1075-2009.
- Andersson, L., J. Wilk, M.C. Todd, D.A. Hughes, A. Earle, D. Kniveton, R. Layberry, and H.H.G. Savenije (2006), "Impact of climate change and development scenarios on flow patterns in the Okavango River." *Journal of Hydrology*, 331, 43–57. doi: 10.1016/j.jhydrol.2006.04.039.
- Bastola, S., C. Murphy, and J. Sweeney (2011), "Evaluation of the transferability of hydrological model parameters for simulations under changed climatic conditions." *Hydrology and Earth System Sciences Discussions*, 8, 5891–5915. doi: 10.5194/hessd-8-5891-2011.
- Bergström, S., B. Carlsson, and M. Gardelin (2001), "Climate change impacts on runoff in Sweden-assessments by global climate models, dynamical downscaling and hydrological modelling." *Climate Research*, 16, 101–112.
- Booij, M.J. (2002), *Appropriate modelling of climate change impacts on river flooding*. Ph.D. thesis, University of Twente, Enschede.
- Booij, M.J. (2005), "Impact of climate change on river flooding assessed with different spatial model resolutions." *Journal of Hydrology*, 303, 176–198. doi: 10.1016/j.jhydrol.2004.07.013.
- Booij, M.J. and M.S. Krol (2010), "Balance between calibration objectives in a conceptual hydrological model." *Hydrological Sciences Journal*, 55, 1017–1032. doi: 10.1080/02626667.2010.505892.
- Booij, M.J., D. Tollenaar, E. van Beek, and J.C.J. Kwadijk (2011), "Simulating impacts of climate change on river discharges in the Nile basin." *Physics and Chemistry of the Earth, Parts A/B/C*, 36, 696–709. doi: 10.1016/j.pce.2011.07.042.
- Carpenter, T.M. and K.P. Georgakakos (2004), "Impacts of parametric and radar rainfall uncertainty on the ensemble streamflow simulations of a distributed hydrologic model." *Journal of Hydrology*, 298, 202–221. doi: 10.1016/j.jhydrol.2004.03.036.
- Chiew, F.H.S., J. Teng, J. Vaze, D.A. Post, J.M. Perraud, D.G.C. Kirono, and N.R. Viney (2009), "Estimating climate change impact on runoff across southeast Australia: Method, results, and implications of the modeling method." *Water Resources Research*, 45, W10414. doi: 10.1029/2008WR007338.
- Christensen, O.B., M. Drews, J.H. Christensen, K. Dethloff, K. Ketelsen, I. Hebestadt, and A. Rinke (2007), "The HIRHAM Regional Climate Model

Bibliography

- Version 5 (β)." Technical report, Danish Meteorological Institute.
- Coron, L., V. Andréassian, C. Perrin, J. Lerat, J. Vaze, M. Bourqui, and F. Hendrickx (2012), "Crash testing hydrological models in contrasted climate conditions: An experiment on 216 Australian catchments." *Water Resources Research*, 48, W05552. doi: 10.1029/2011WR011721.
- Davis, J.C. (2002), *Statistics and Data Analysis in Geology*, 3th edition. John Wiley and Sons, New York, NY, USA.
- Deckers, D. (2006), *Predicting discharge at ungauged catchments: parameter estimation through the method of regionalisation*. MSc. thesis, University of Twente, Enschede.
- Déqué, M, C Dreveton, A Braun, and D Cariolle (1994), "The ARPEGE/IFS atmosphere model: a contribution to the French community climate modelling." *Climate Dynamics*, 10, 249–266. doi: 10.1007/BF00208992.
- Déqué, M., D.P. Rowell, D. Lüthi, F. Giorgi, J.H. Christensen, B. Rockel, D. Jacob, E. Kjellström, M. Castro, and B. Hurk (2007), "An intercomparison of regional climate simulations for Europe: assessing uncertainties in model projections." *Climatic Change*, 81, 53–70. doi: 10.1007/s10584-006-9228-x.
- Duan, Q., S Sorooshian, and V. Gupta (1992), "Effective and efficient global optimization for conceptual rainfallrunoff models." *Water resources research*, 28, 1015–1031.
- European Environment Agency [EEA] (2011), "Corine land cover 2000." Technical report, European Environment Agency.
- Frey, H.C. and S.R. Patil (2002), "Identification and review of sensitivity analysis methods." *Risk analysis : an official publication of the Society for Risk Analysis*, 22, 553–78.
- Furevik, T., M. Bentsen, H. Drange, I.K.T. Kindem, N.G. Kvamstø, and A. Sorteberg (2003), "Description and evaluation of the bergen climate model: ARPEGE coupled with MICOM." *Climate Dynamics*, 21, 27–51. doi: 10.1007/s00382-003-0317-5.
- Görgen, K., J. Beersma, G. Brahmer, H. Buiteveld, M. Carambia, O. de Keizer, P. Krahe, E. Nilson, R. Lammersen, C. Perrin, and D. Volken (2010), *Assessment of climate change impacts on discharge in the Rhine River Basin: Results of the RheinBlick2050 Project*. I.
- Gudmundsson, L., J. B. Bremnes, J. E. Haugen, and T. Engen Skaugen (2012), "Technical Note: Downscaling RCM precipitation to the station scale using quantile mapping a comparison of methods." *Hydrology and Earth System Sciences Discussions*, 9, 6185–6201. doi: 10.5194/hessd-9-6185-2012.
- Hamon, W.R. (1961), "Estimating potential evapotranspiration." *Journal of Hydraulics Division, Proceedings of the American Society of Civil Engineers*, 871, 107–120.
- International Panel on Climate Change [IPCC] (2001a), *Climate change 2001: the scientific basis*. Cambridge University Press, New York, NY, USA.
- International Panel on Climate Change [IPCC] (2001b), *Climate change 2001: Impacts, Adaptation, and Vulnerability*. Cambridge University Press, New York, NY, USA.
- International Panel on Climate Change [IPCC] (2007), *Climate change 2007: synthesis report*. November, Cambridge University Press, Cambridge, United kingdom and New York, NY, USA.
- International Panel on Climate Change [IPCC] (2011), "Climate model out-

Bibliography

- put.” URL http://www.ipccdata.org/ddc_gcm_intro.html. Online, accessed: 05/11/2012.
- Jacob, D. (2001), “A note to the simulation of the annual and inter-annual variability of the water budget over the Baltic Sea drainage basin.” *Meteorology and Atmospheric Physics*, 77, 61–73. doi: 10.1007/s007030170017.
- Jiang, T., Y.D. Chen, C. Xu, X. Chen, and V.P. Singh (2007), “Comparison of hydrological impacts of climate change simulated by six hydrological models in the Dongjiang Basin, South China.” *Journal of Hydrology*, 336, 316–333. doi: 10.1016/j.jhydrol.2007.01.010.
- Kjellström, E., L. Bärring, S. Gollvik, U. Hansson, C. Jones, P. Samuelsson, M. Rummukainen, U. Ullerstig, A. Willén, and K. Wyser (2005), “A 140-year simulation of European climate with the new version of the Rossby Centre regional atmospheric climate model (RCA3).” Technical Report 108, SMHI Reports Meteorology and Climatology No. 108, SE-60176 Norrköping, Sweden.
- Kollat, J. B., P. M. Reed, and T. Wagener (2012), “When are multiobjective calibration trade-offs in hydrologic models meaningful?” *Water Resources Research*, 48. doi: 10.1029/2011WR011534.
- Lindström, G., B. Johansson, M. Persson, M. Gardelin, and S. Bergström (1997), “Development and test of the distributed HBV-96 hydrological model.” *Journal of hydrology*, 201, 272–288.
- Madsen, Henrik (2003), “Parameter estimation in distributed hydrological catchment modelling using automatic calibration with multiple objectives.” *Advances in Water Resources*, 26, 205–216. doi: 10.1016/S0309-1708(02)00092-1.
- Merz, R., J. Parajka, and G. Blöschl (2011), “Time stability of catchment model parameters: Implications for climate impact analyses.” *Water Resources Research*, 47, W02531. doi: 10.1029/2010WR009505.
- Nakicenovic, N., J. Alcamo, G. Davis, B. de Vries, J. Fenhann, S. Gaffin, K. Gregory, A. Grubler, T.Y. Jung, T. Kram, E.L. La Rovere, L. Michaelis, S. Mori, T. Morita, W. Pepper, H.M. Pitcher, L. Price, K. Riahi, A. Roehrl, H.-H. Rogner, A. Sankovski, M. Schlesinger, P. Shukla, S.J. Smith, R. Swart, S. van Rooijen, N. Victor, and Z. Dadi (2000), *Special report on emissions scenarios*. Cambridge University Press, New York, NY (US).
- National Climatic Data Center (2011), “State of the climate, global analysis annual 2011.” URL <http://www.ncdc.noaa.gov/sotc/global/2011/13>. Online, accessed: 13/11/2012.
- Pappenberger, F., K.J. Beven, M. Ratto, and P. Matgen (2008), “Multi-method global sensitivity analysis of flood inundation models.” *Advances in Water Resources*, 31, 1–14. doi: 10.1016/j.advwatres.2007.04.009.
- Pechlivanidis, I.G., B.M. Jackson, N.R. McIntyre, and H.S. Wheater (2011), “Catchment scale hydrological modelling: a review of model types, calibration approaches and uncertainty analysis methods in the context of recent developments in technology and applications.” *Global NEST*, 13, 193–214.
- Radu, R., M. Déqué, and S. Somot (2008), “Spectral nudging in a spectral regional climate model.” *Tellus A*, 60, 898–910. doi: 10.1111/j.1600-0870.2008.00341.x.
- Ratto, M., P.C. Young, R. Romanowicz, F. Pappenberge, A. Saltelli, and A. Pagano (2007), “Uncertainty, sensitivity analysis and the role of data based mechanistic modeling in hydrology.” *Hydrology and Earth System Sciences*, 11, 1249–1266.
- Refsgaard, J.C. and J. Knudsen (1996), “Operational Validation and Intercomparison of Different Types of Hydrological Models.” *Water Resources Research*, 32,

2189. doi: 10.1029/96WR00896.
- Roeckner, E., G. Bäuml, L. Bonaventura, R. Brokopf, M. Esch, M. Giogetta, S. Hagemann, I. Kirchner, L. Kornblueh, E. Manzini, A. Rhodin, U. Schlese, U. Schulzweida, and A. Tompkins (2003), “The atmospheric general circulation model ECHAM5 - part 1.” Technical Report 349, Max-Planck-Institut für Meteorologie, Hamburg.
- Romanowicz, R.J. and M. Osuch (s.d.), “Statistical analysis of low flow indices under varying climatic conditions.” *Unpublished, in progress.*
- Romanowicz, R.J., M. Osuch, and M. Grabowiecka (s.d.), “On the choice of calibration periods and objective functions: a practical guide to model identification.” *Acta Geophysica, ?*
- Saltelli, A., S. Tarantola, F. Campolongo, and M. Ratto (2004), *Sensitivity analysis in practice - a guide to assessing scientific models*. John Wiley and Sons Ltd, Chichester.
- Saltelli, A., S. Tarantola, and F. Campolongo (2000), “Sensitivity Analysis as an Ingredient of Modeling.” *Statistical Science*, 15, 377–395.
- Seibert, J. (2003), “Reliability of Model Predictions Outside Calibration Conditions.” *Nordic Hydrology*, 34, 1–13.
- Siniecki, C. (2009), “The role of small retention and water cooperatives in water management illustrated by the River Wena case study.” In *Ecological issues in the River Wena catchment*, 83–88 (in Polish).
- SMHI (2004), “Integrated Hydrological Modelling System (IHMS) Manual Version 4.5.”
- Sorooshian, S. and V.K. Gupta (1995), “Model calibration.” In *Computer models of watershed hydrology* (V.P. Singh, ed.), Water Resources Publications, USA.
- Tang, Y., P. Reed, T. Wagener, and K. van Werkhoven (2007), “Comparing sensitivity analysis methods to advance lumped watershed model identification and evaluation.” *Hydrology and Earth System Sciences*, 11, 793–817. doi: 10.5194/hess-11-793-2007.
- Tillaart, S.P.M. (2010), *Influence of uncertainties in discharge determination on the parameter estimation and performance of a HBV model in Meuse sub basins*. MSc. thesis, University of Twente, Enschede.
- van der Linden, P and J.F.B. Mitchell (2009), *ENSEMBLES: Climate Change and its Impacts: Summary of research and results from the ENSEMBLES project*. Met Office Hadley Centre, Exeter.
- van Meijgaard, E, L.H. van Ulft, W.J. van de Berg, F.C. Bosveld, B.J.J.M. van den Hurk, G. Lenderink, and A.P. Siebesma (2008), “The KNMI regional atmospheric climate model RACMO version 2.1.” Technical report, Koninklijk Nederlands Meteorologisch Instituut, De Bilt.
- Vaze, J., D.A. Post, F.H.S. Chiew, J.-M. Perraud, N.R. Viney, and J. Teng (2010), “Climate non-stationarity Validity of calibrated rainfallrunoff models for use in climate change studies.” *Journal of Hydrology*, 394, 447–457. doi: 10.1016/j.jhydrol.2010.09.018.
- Vrugt, J.A., H.V Gupta, L.A. Bastidas, W. Bouten, and S. Sorooshian (2003a), “Effective and efficient algorithm for multiobjective optimization of hydrologic models.” *Water Resources Research*, 39, 5–1 5–18. doi: 10.1029/2002WR001746.
- Vrugt, J.A., H.V. Gupta, W. Bouten, and S. Sorooshian (2003b), “A Shuffled Complex Evolution Metropolis algorithm for optimization and uncertainty assessment of hydrologic model parameters.” *Water Resources Research*, 39. doi:

Bibliography

- 10.1029/2002WR001642.
- Wagener, T., N. McIntyre, M.J. Lees, H.S. Wheater, and H.V. Gupta (2003), "Towards reduced uncertainty in conceptual rainfall-runoff modelling: dynamic identifiability analysis." *Hydrological Processes*, 17, 455–476. doi: 10.1002/hyp.1135.
- Wagener, T., M. Sivapalan, P.A. Troch, B.L. McGlynn, C.J. Harman, H.V. Gupta, P. Kumar, P.S.C. Rao, N.B. Basu, and J.S. Wilson (2010), "The future of hydrology: An evolving science for a changing world." *Water Resources Research*, 46. doi: 10.1029/2009WR008906.
- Wilby, R.L. (2005), "Uncertainty in water resource model parameters used for climate change impact assessment." *Hydrological Processes*, 19, 3201–3219. doi: 10.1002/hyp.5819.
- Wira, J. (2011), "Ocena wpływu wybranych wskaźników fizycznych i biologicznych na jakość wód rzeki Weny (Evaluation of impact of selected physical and biological indices upon quality of water in the Wena)." *Zeszyty Naukowe Inżynieria Lądowa i Wodna w Kształtowaniu Środowiska (Scientific papers of civil engineering on shaping the environment)*, 3, 71–76.
- Xu, C. (1999), "Operational testing of a water balance model for predicting climate change impacts." *Agricultural and Forest Meteorology*, 98-99, 295–304. doi: 10.1016/S0168-1923(99)00106-9.

Appendix A

Sensitivity analysis

This appendix provides more insight into the process around the sensitivity analysis. Section A.1 explains why the influence of parameters *CFMAX*, *WHC*, β and K_f on model output variance can be neglected. Section A.2 explores the influence of parameters K_f and K_s on calibration performance per 5-year window.

A.1 Interaction between parameters

This appendix expands on the interaction effect of parameters *CFMAX*, *WHC*, β and K_f (section 3.3.3). These parameters show a certain influence on model output variance through their respective interactions with other parameters. These four parameter are however not calibrated but kept at fixed values.

Parameters *CFMAX* and *WHC* can be safely fixed because both have only minimal effect on total model output variance (table 3.2). Fixing their respective values should therefore have little influence on model performance.

Monte Carlo sampling (200000 samples) of all parameters is used to determine which parameters interact with β and K_f . Parameter values of the top 5% parameter sets (5% of the samples with highest model performance as measured with objective function Y) are plotted against the values β and K_f , to see if any important relations between the parameters become apparent (figures A.1 and A.2 respectively).

β only shows a clear interaction with *LP*. High values for β seem to coincide with high values for *LP* and the same goes for low values. This balances the actual evapotranspiration and seepage terms.

K_f shows slight interaction with K_s and *PERC*. K_f is responsible for fast runoff, while *PERC* and K_s regulate slow runoff. Higher values for *PERC* drain the reservoir from which K_f simulates the fast runoff. Since fast runoff is based on the current storage level in the fast runoff reservoir, K_f has to assume higher values to keep the fast runoff component at the same level. K_s and K_f are together responsible for the total runoff due to addition of the fast and slow runoff components. High values for K_s indicate high values for the slow runoff. This only occurs at low values of K_f in order not to overestimate the total runoff.

The interaction of β is limited to *LP*, while the interactions of K_f is limited to K_s . Since these are only weak interactions (table 3.2), the effects of fixing K_f and β to a single value on overall model performance are assumed to be small.

A.2 Influence of K_f and K_s on calibration

This analysis was originally intended to define values on which to fix parameters K_f and K_s , since the sensitivity analysis indicates that these parameters have low

A.2. Influence of K_f and K_s on calibration

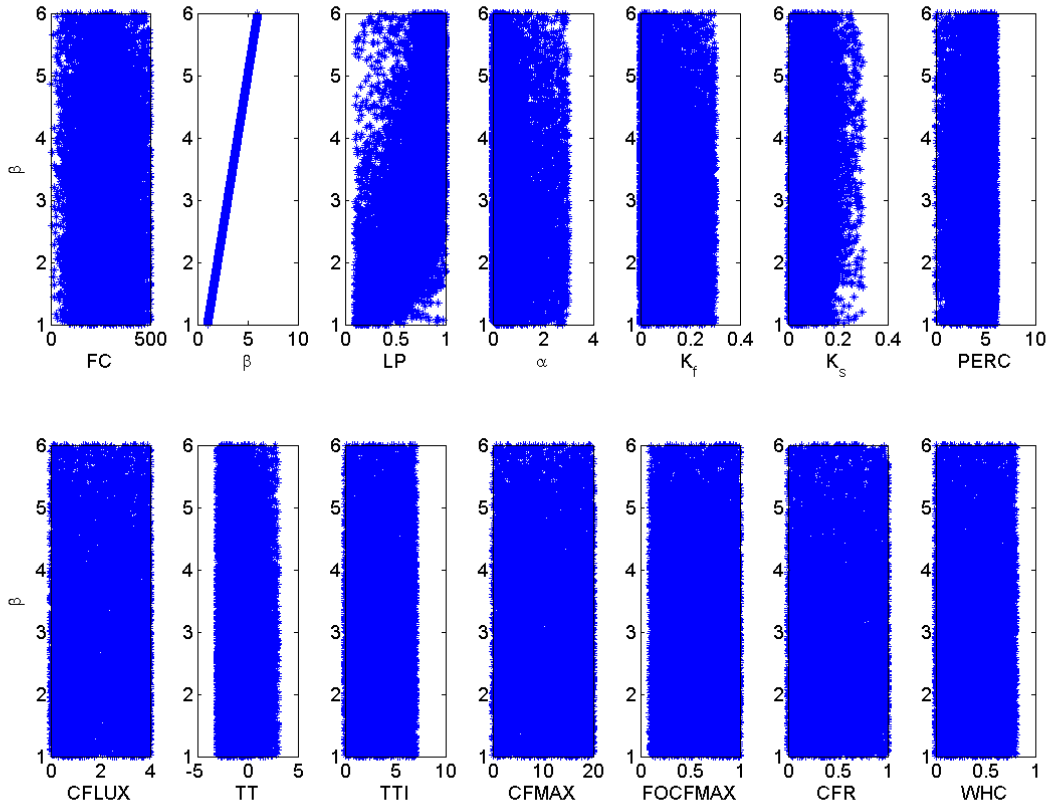


Figure A.1: Values of β plotted against the values of the other parameters for the top 5% parameter sets from Monte Carlo sampling

influence on total model output variance. The sensitivity analysis is however based on the full 30-year period, and especially the influence of parameter K_s varies throughout the years.

Figure A.3 shows Y values for calibration with three different parameter sets, for different 5-year periods. The first set consists of the five parameters determined by the sensitivity analysis (FC , LP , α , $PERC$ and TT , section 3.3.4). The second and third set contain these five parameters and K_s and K_f respectively.

As the figure shows, including K_f as a calibrated parameter improves model performance somewhat during period 2 ($Y + 0.02$) and hardly matters for the other periods. Calibrating K_s has a more noticeable effect, especially for periods 21-24 ($Y + 0.02 - 0.07$).

Since this study aims at clarifying the potential relationship between parameter values and climatic variables, it seems prudent to include parameter K_s as a calibrated parameter. K_f can be assigned a fixed value without difficulty.

A.2. Influence of K_f and K_s on calibration

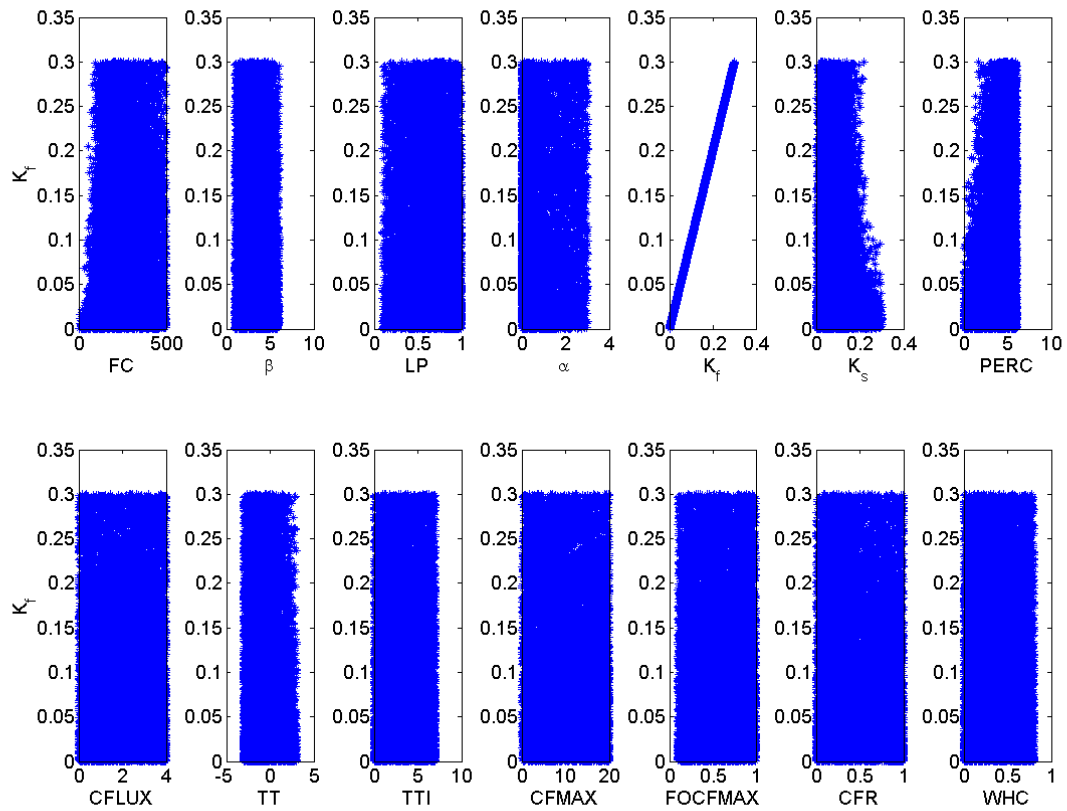


Figure A.2: Values of K_f plotted against the values of the other parameters for the top 5% parameter sets from Monte Carlo sampling

A.2. Influence of K_f and K_s on calibration

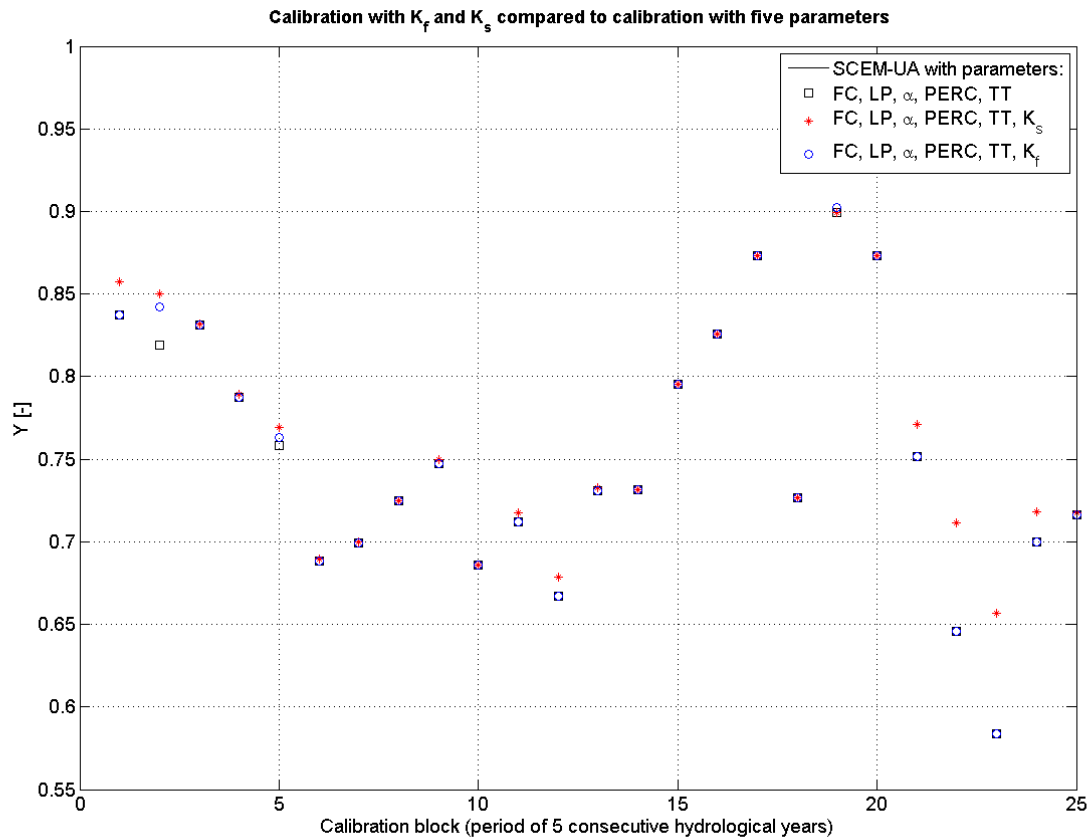


Figure A.3: Calibration results for parameters FC , LP , α , $PERC$ and TT , with parameters K_f and K_s included in calibration as well

Appendix B

Calibration process

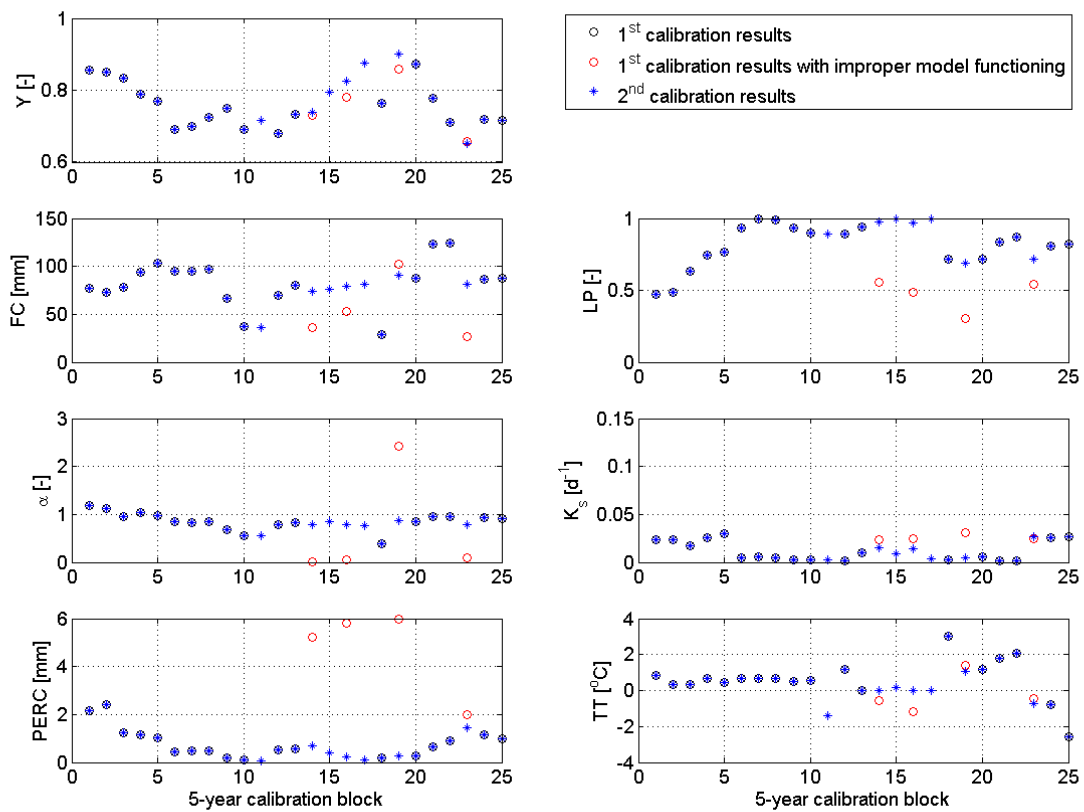


Figure B.1: Calibration results for the periods of 5 consecutive hydrological years. Upper figure shows the values for the objective function Y , the lower six figures show the optimal parameter sets as determined by the SCEM-UA algorithm

Figure B.1 shows both the resulting objective function value and the optimal parameter values from the first calibration run (circles). The red circles indicate periods with unsatisfactory model behaviour (i.e. time periods 14, 16, 19 and 23).

The HBV model is based on the theory that the total runoff is comprised of runoff from the fast runoff reservoir (peak flow after rain events) and runoff from the slow runoff reservoir (steady base flow). Figure B.2 (top plot) shows this principle for time period 20, with the parameter set calibrated for this period. Figure B.2 (middle plot) shows the fast and slow runoff as simulated with the

optimal parameter set for period 19; the total runoff is almost completely modelled by the slow-runoff reservoir. The influence of the fast runoff reservoir is only visible at some peaks (e.g. $t = 1920$).

However, when the performance of both parameter sets is measured against the objective function Y , both parameter sets perform very similar: $Y_{20} = 0.87$ and $Y_{19} = 0.86$. Clearly, good values for the objective function do not necessarily imply proper model functioning.

K_s for period 20 is equal to $6e^{-3}$, while the fixed $K_f = 5.4e^{-4}$. Intuitively it feels strange that the slow runoff parameter K_s has a higher value than the fast runoff parameter K_f . However, proper calibration ensures that the effective value of K_f is higher than that of K_s and the model functions properly. The calibrated parameter values for the periods 14, 16, 19 and 23 (figure B.1) show high values for *PERC*, low values for *LP* and aberrant values for α , compared to calibrated values for the other periods. Low *LP* values lead to lower evapotranspiration and thus more water remaining in the model. The high *PERC* values make this water flow directly into the slow runoff reservoir. The low values for α lead to lower runoff from the fast runoff reservoir. The high value of α in period 19 should lead to a high fast-runoff component, but there is simply not enough water present in the fast runoff reservoir for this to occur. *FC*, K_s and *TT* show no diverging values for these four time periods.

Since this study aims to clarify the relationship between optimal parameter values and climatic variables, proper model functioning is essential. Therefore the periods 14, 16, 19 and 23 were calibrated again with constricted parameter ranges for *LP*, α and *PERC* (table B.1) that are based on the optimal values for the other time periods. *LP* has an increased lower limit, to ensure that evapotranspiration is not artificially lowered in order to keep more water in the model. α is limited on both sides; the increased lower limit should ensure higher effective fast runoff. The upper limit is decreased for more efficient sampling of the parameter space, since the other calibrated values show no tendency for values above 1.5. *PERC* has a lower upper limit in order to keep inflow into the slow runoff reservoir limited.

After recalibration with restricted parameter ranges, model performance for the four periods is markedly better (figure B.2, bottom plot for example period 19). Fast and slow runoff are properly represented by the two different reservoirs and the optimal parameter values are more in line with those of the other periods.

It would be expected that model performance as measured by the objective function would decline, since the SCEM-UA algorithm is supposed to find the global optimum in the total parameter space. The restricted parameter space is located inside the wider range. It therefore stands to reason that the “improper” parameter set by coincidence simulates the discharge really well and that after recalibration the objective function for the four periods would be lower. Strangely, the objective function values are actually better for the periods 14, 16 and 19 after recalibration (figure B.1, blue stars). This points out a flaw in the usage of the SCEM-UA algorithm, since this better performing parameter set was also present in the parameter ranges used in the first calibration round. This might be related to the sensitivity of the algorithm to boundaries set for parameter values (personal communication with experts at IGF).

Table B.1: Restricted parameters ranges for calibration

Parameter	Old range		New range	
	min	max	min	max
LP	0.1	1	0.5	1
α	0	3	0.4	1.5
$PERC$	0	6	0	4

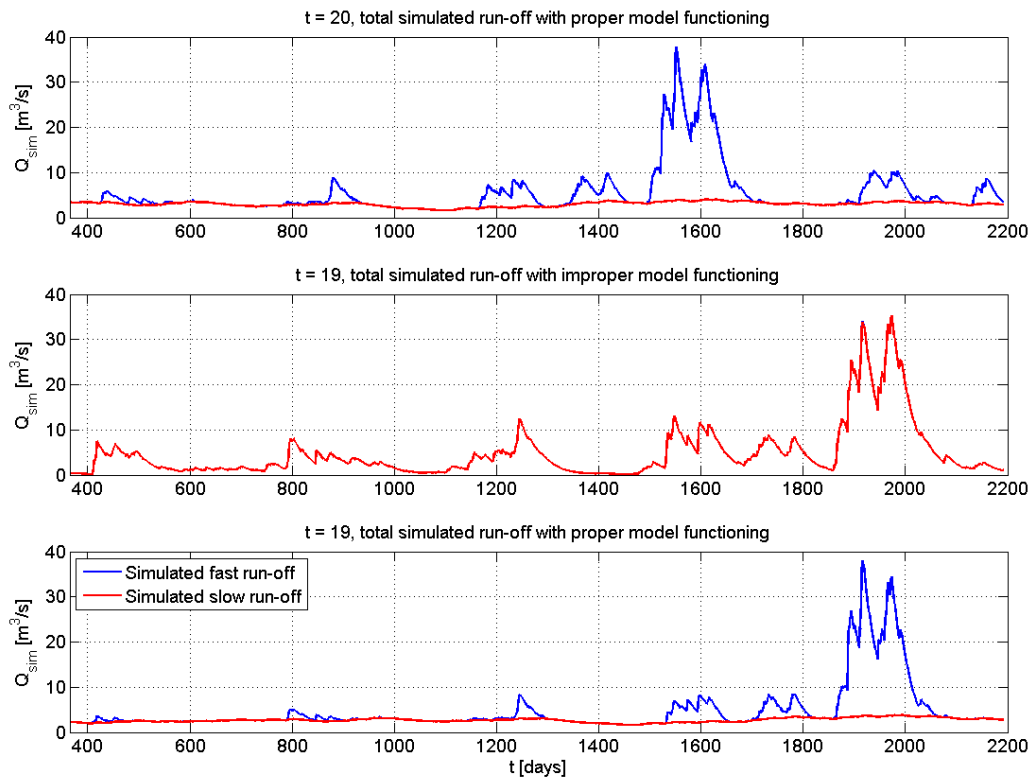


Figure B.2: Top plot: simulated runoff for period 20, which shows a clear distinction between contributions from the fast and slow runoff reservoir. Middle plot: simulated runoff for period 19 ($Y = 0.86$), where the slow runoff reservoir simulates peak flow instead of base flow. Bottom plot: simulated flow for period 19 after recalibration ($Y = 0.90$) where the fast runoff reservoir simulates runoff peaks and the slow runoff reservoir simulates base flow as intended

Appendix C

Regression analysis

This appendix contains regression plots for single (section 5.3.1) and multiple linear regression (section 5.3.2) respectively.

C.1 Single linear regression plots

This section includes single linear regression plots for parameters FC , α , K_s and $PERC$. LP only shows correlations with $P_{wet,\mu,w}$ which is deemed a coincidence, so this plot is not included here. TT shows no significant correlations with any climate characteristic. Linear regression lines are drawn with their corresponding R^2 values, which are a measure of the goodness-of-fit of the regression equation (for an optimal fit, $R^2 = 1$) and F-values that show significance (for $F > 4.28$ the relationship is statistically significant). 95% confidence bands give confirmation of the significance given by F-values.

For FC , the data points are scattered widely around the regression line, explaining the poor fits. All points however are within the 95% confidence interval, so the regressions are significant at this level.

For α , the relationship between α and $P_{wet,\mu,w}$ seems the most linear, while points are more scattered around the other four regression lines. For $P_{wet,\mu,w}$ all points are within the 95% confidence interval, for the other four relationships one point falls outside the interval. Since 1.25 points can reasonably be expected to be outside the interval, all regressions are significant at the 95% level.

For K_s , data points are scattered mainly for high values of P_μ and low values of ar_μ . This might be related to the fact that K_s regulates base flow, which becomes less important for higher precipitation (and thus higher runoff) events. Therefore the value of K_s can fluctuate more during higher precipitation periods, without influencing the objective function much, leading to low identifiability of the optimal K_s value. All points however are within the 95% confidence interval, so the regressions are significant at this level.

For $PERC$, the points are somewhat more scattered for high values for P_μ and $P_{wet,\mu}$ and low ar_μ . This is similar to the scatter of points found for K_s . Since $PERC$ simulates recharge of the slow runoff reservoir, and K_s simulates the discharge from this reservoir, similar reasoning applies for $PERC$ as for K_s . During low precipitation and thus runoff periods, correct modelling of base flow is more important in the overall objective function. This increases the identifiability of $PERC$ during drier periods.

For $PERC$, one data point is outside the 95% confidence interval for $P_{wet,\mu,w}$, and two points are outside the interval for the other three relationships. Since 1.25 points can reasonably be expected to be outside the interval, and 0.25 points has

C.2. Multiple regression results

no practical meaning, it is not unreasonable that two points can be outside the 95% interval while still keeping a significant regression. It is however curious that out of 17 situations, this occurs three times for a regression involving *PERC* and not for any other parameter. The regressions still have a significant F-statistic however, so they are still considered to be significant.

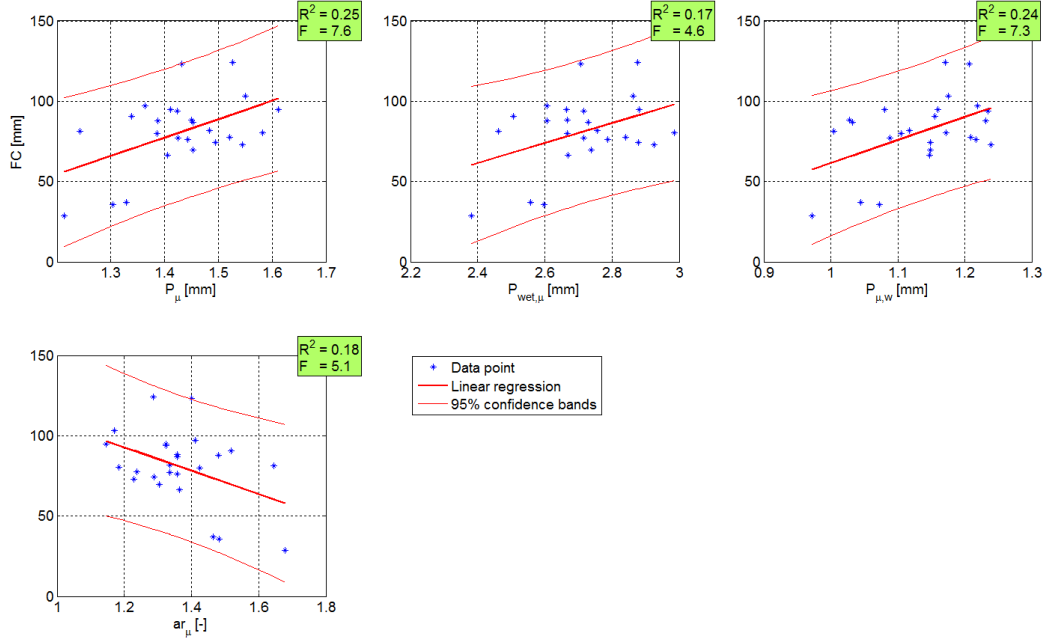


Figure C.1: Single linear regression of the significant correlations between climate characteristics and the optimal values for *FC*. Regressions are significant for $F > 4.28$

C.2 Multiple regression results

Only the climate characteristics that show significant linear correlation with model parameters are included in the multi linear regression analysis (section 5.3.2). This appendix includes the full results of the multiple regression analysis for parameters *FC*, α , K_s and *PERC* (tables C.1, C.3, C.5 and C.7 respectively). The indices refer to the various combinations of climate characteristics and are explained in tables C.2, C.4, C.6 and C.8 for the respective parameters.

C.2.1 Regression equations

This section describes the three regression equations that are established in section 5.3.2. Equations for *FC* and α have a minimum value of 0 (lower boundary for both parameters during calibration), since negative values will disrupt model functioning. The equation for *PERC* has a lower value of 0.05, since a value of 0 will stop groundwater recharge and this is unlikely to occur in reality.

$$FC = \max\{-37.31 + 291.0 * P_\mu - 155.3 * P_{wet,\mu} + 108.2 * P_{\mu,w}, 0\} \quad (C.1)$$

C.2. Multiple regression results

$$\alpha = \max\{-1.4010 + 0.5638 * P_{\mu} + 0.7268 * P_{wet,\mu,w}, 0\} \quad (C.2)$$

$$PERC = \max\{-6.353 + 1.789 * P_{\mu} + 2.286 * P_{wet,\mu,w}, 0.05\} \quad (C.3)$$

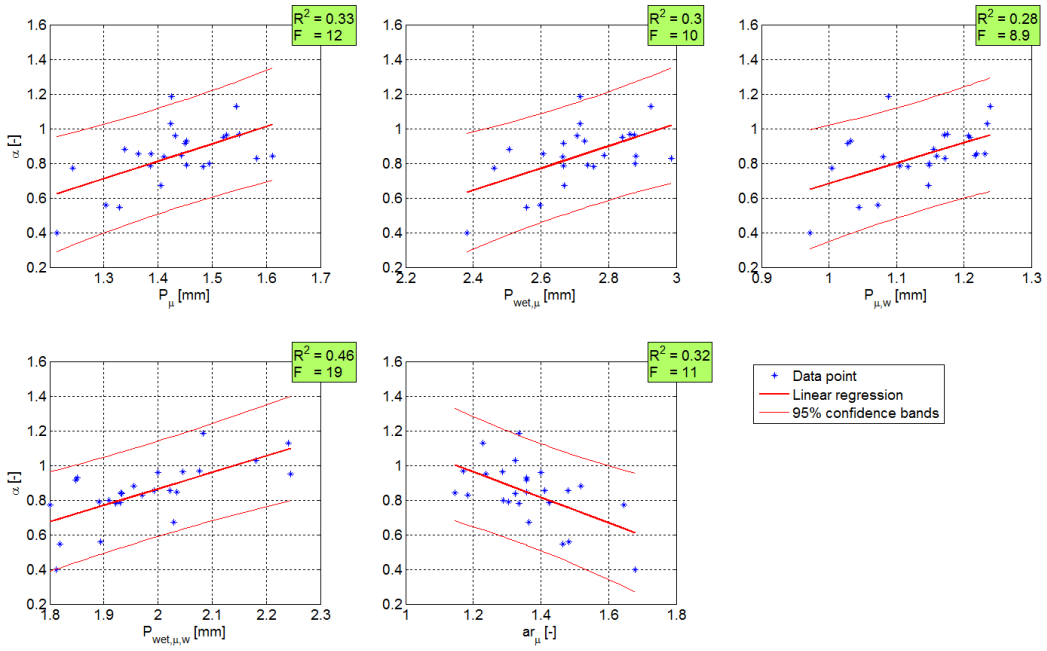


Figure C.2: Single linear regression of the significant correlations between climate characteristics and the optimal values for α . Regressions are significant for $F > 4.28$

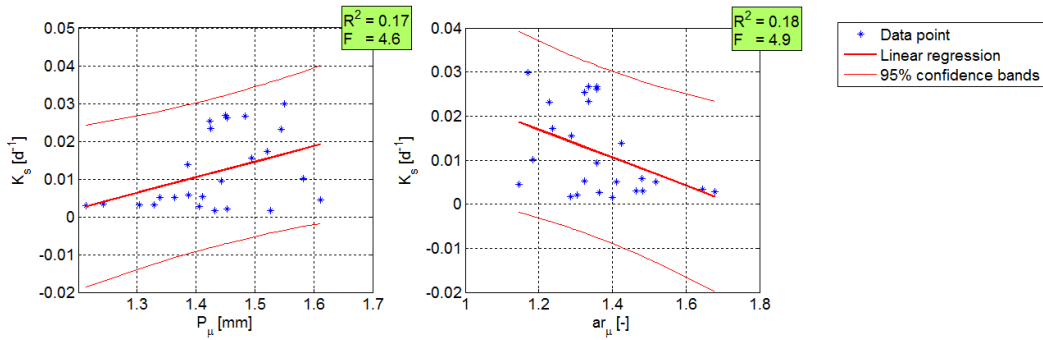


Figure C.3: Single linear regression of the significant correlations between climate characteristics and the optimal values for K_s . Regressions are significant for $F > 4.28$

C.2. Multiple regression results

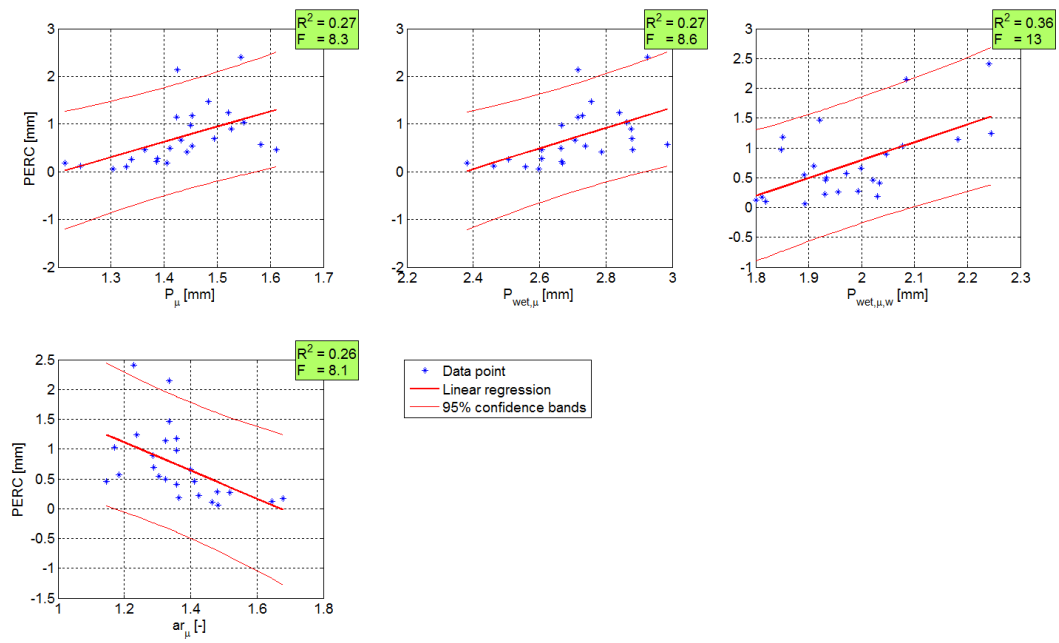


Figure C.4: Single linear regression of the significant correlations between climate characteristics and the optimal values for $PERC$. Regressions are significant for $F > 4.28$

C.2. Multiple regression results

Table C.1: Full multiple linear regression results for parameter FC , indices explained in table C.2

Index	Degrees of freedom	R^2	F	p	Error variance	Required F	Significant?
1	1	0.25	7.63	0.01	405	4.28	yes
2	1	0.17	4.62	0.04	449	4.28	yes
3	1	0.24	7.33	0.01	409	4.28	yes
4	1	0.18	5.07	0.03	442	4.28	yes
5	2	0.31	4.87	0.02	391	3.44	yes
6	2	0.32	5.10	0.02	385	3.44	yes
7	2	0.29	4.54	0.02	399	3.44	yes
8	2	0.27	4.00	0.03	413	3.44	yes
9	2	0.18	2.44	0.11	461	3.44	no
10	2	0.28	4.22	0.03	407	3.44	yes
11	3	0.40	4.66	0.01	354	3.07	yes
12	3	0.33	3.52	0.03	393	3.07	yes
13	3	0.37	4.04	0.02	374	3.07	yes
14	3	0.28	2.70	0.07	426	3.07	no
15	4	0.43	3.76	0.02	354	2.87	yes

Table C.2: Indices of multiple linear regression FC

Index	Climate characteristic(s)			
1	P_μ			
2	$P_{wet,\mu}$			
3	$P_{\mu,w}$			
4	ar_μ			
5	P_μ	$P_{wet,\mu}$		
6	P_μ	$P_{\mu,w}$		
7	P_μ	ar_μ		
8	$P_{wet,\mu}$	$P_{\mu,w}$		
9	$P_{wet,\mu}$	ar_μ		
10	$P_{\mu,w}$	ar_μ		
11	P_μ	$P_{wet,\mu}$	$P_{\mu,w}$	
12	P_μ	$P_{wet,\mu}$	ar_μ	
13	P_μ	$P_{\mu,w}$	ar_μ	
14	$P_{wet,\mu}$	$P_{\mu,w}$	ar_μ	
15	P_μ	$P_{wet,\mu}$	$P_{\mu,w}$	ar_μ

C.2. Multiple regression results

Table C.3: Full multiple linear regression results for parameter α , indices explained in table C.4

Index	Degrees of freedom	R^2	F	p variance	Error	Required F	Significant?
1	1	0.33	11.51	0.00	0.02	4.28	yes
2	1	0.30	9.99	0.00	0.02	4.28	yes
3	1	0.28	8.90	0.01	0.02	4.28	yes
4	1	0.46	19.31	0.00	0.02	4.28	yes
5	1	0.32	10.62	0.00	0.02	4.28	yes
6	2	0.33	5.51	0.01	0.02	3.44	yes
7	2	0.40	7.25	0.00	0.02	3.44	yes
8	2	0.54	12.70	0.00	0.02	3.44	yes
9	2	0.33	5.51	0.01	0.02	3.44	yes
10	2	0.37	6.51	0.01	0.02	3.44	yes
11	2	0.51	11.33	0.00	0.02	3.44	yes
12	2	0.32	5.19	0.01	0.02	3.44	yes
13	2	0.46	9.24	0.00	0.02	3.44	yes
14	2	0.39	6.94	0.00	0.02	3.44	yes
15	2	0.51	11.56	0.00	0.02	3.44	yes
16	3	0.40	4.67	0.01	0.02	3.07	yes
17	3	0.55	8.58	0.00	0.02	3.07	yes
18	3	0.33	3.51	0.03	0.02	3.07	yes
19	3	0.54	8.34	0.00	0.02	3.07	yes
20	3	0.40	4.61	0.01	0.02	3.07	yes
21	3	0.55	8.44	0.00	0.02	3.07	yes
22	3	0.51	7.34	0.00	0.02	3.07	yes
23	3	0.39	4.42	0.01	0.02	3.07	yes
24	3	0.51	7.37	0.00	0.02	3.07	yes
25	3	0.52	7.45	0.00	0.02	3.07	yes
26	4	0.56	6.33	0.00	0.02	2.87	yes
27	4	0.40	3.34	0.03	0.02	2.87	yes
28	4	0.56	6.32	0.00	0.02	2.87	yes
29	4	0.56	6.34	0.00	0.02	2.87	yes
30	4	0.52	5.35	0.00	0.02	2.87	yes
31	5	0.57	5.04	0.00	0.02	2.74	yes

C.2. Multiple regression results

Table C.4: Indices of multiple linear regression α

Index	Climate characteristic(s)				
1	P_μ				
2	$P_{wet,\mu}$				
3	$P_{\mu,w}$				
4	$P_{wet,\mu,w}$				
5	ar_μ				
6	P_μ	$P_{wet,\mu}$			
7	P_μ	$P_{\mu,w}$			
8	P_μ	$P_{wet,\mu,w}$			
9	P_μ	ar_μ			
10	$P_{wet,\mu}$	$P_{\mu,w}$			
11	$P_{wet,\mu}$	$P_{wet,\mu,w}$			
12	$P_{wet,\mu}$	ar_μ			
13	$P_{\mu,w}$	$P_{wet,\mu,w}$			
14	$P_{\mu,w}$	ar_μ			
15	$P_{wet,\mu,w}$	ar_μ			
16	P_μ	$P_{wet,\mu}$	$P_{\mu,w}$		
17	P_μ	$P_{wet,\mu}$	$P_{wet,\mu,w}$		
18	P_μ	$P_{wet,\mu}$	ar_μ		
19	P_μ	$P_{\mu,w}$	$P_{wet,\mu,w}$		
20	P_μ	$P_{\mu,w}$	ar_μ		
21	P_μ	$P_{wet,\mu,w}$	ar_μ		
22	$P_{wet,\mu}$	$P_{\mu,w}$	$P_{wet,\mu,w}$		
23	$P_{wet,\mu}$	$P_{\mu,w}$	ar_μ		
24	$P_{wet,\mu}$	$P_{wet,\mu,w}$	ar_μ		
25	$P_{\mu,w}$	$P_{wet,\mu,w}$	ar_μ		
26	P_μ	$P_{wet,\mu}$	$P_{\mu,w}$	$P_{wet,\mu,w}$	
27	P_μ	$P_{wet,\mu}$	$P_{\mu,w}$	ar_μ	
28	P_μ	$P_{wet,\mu}$	$P_{wet,\mu,w}$	ar_μ	
29	P_μ	$P_{\mu,w}$	$P_{wet,\mu,w}$	ar_μ	
30	$P_{wet,\mu}$	$P_{\mu,w}$	$P_{wet,\mu,w}$	ar_μ	
31	P_μ	$P_{wet,\mu}$	$P_{\mu,w}$	$P_{wet,\mu,w}$	ar_μ

C.2. Multiple regression results

Table C.5: Full multiple linear regression results for parameter K_s , indices explained in table C.6

Index	Degrees of freedom	R^2	F	p	Error variance	Required F	Significant?
1	1	0.17	4.58	0.04	0.00009	4.28	yes
2	1	0.18	4.93	0.04	0.00009	4.28	yes
3	2	0.18	2.36	0.12	0.00009	3.44	no

Table C.6: Indices of multiple linear regression K_s

Index	Climate characteristic(s)
1	P_μ
2	ar_μ
3	P_μ ar_μ

C.2. Multiple regression results

Table C.7: Full multiple linear regression results for parameter $PERC$, indices explained in table C.8

Index	Degrees of freedom	R^2	F	p	Error variance	Required F	Significant?
1	1	0.27	8.30	0.01	0.29	4.28	yes
2	1	0.27	8.60	0.01	0.29	4.28	yes
3	1	0.36	12.98	0.00	0.25	4.28	yes
4	1	0.26	8.11	0.01	0.29	4.28	yes
5	2	0.27	4.17	0.03	0.30	3.44	yes
6	2	0.42	8.11	0.00	0.24	3.44	yes
7	2	0.27	4.03	0.03	0.30	3.44	yes
8	2	0.42	7.90	0.00	0.24	3.44	yes
9	2	0.28	4.19	0.03	0.30	3.44	yes
10	2	0.41	7.66	0.00	0.24	3.44	yes
11	3	0.42	5.16	0.01	0.25	3.07	yes
12	3	0.28	2.67	0.07	0.31	3.07	no
13	3	0.43	5.23	0.01	0.25	3.07	yes
14	3	0.42	5.03	0.01	0.25	3.07	yes
15	4	0.43	3.74	0.02	0.26	2.87	yes

Table C.8: Indices of multiple linear regression $PERC$

Index	Climate characteristic(s)			
1	P_μ			
2	$P_{wet,\mu}$			
3	$P_{wet,\mu,w}$			
4	ar_μ			
5	P_μ	$P_{wet,\mu}$		
6	P_μ	$P_{wet,\mu,w}$		
7	P_μ	ar_μ		
8	$P_{wet,\mu}$	$P_{wet,\mu,w}$		
9	$P_{wet,\mu}$	ar_μ		
10	$P_{wet,\mu,w}$	ar_μ		
11	P_μ	$P_{wet,\mu}$	$P_{wet,\mu,w}$	
12	P_μ	$P_{wet,\mu}$	ar_μ	
13	P_μ	$P_{wet,\mu,w}$	ar_μ	
14	$P_{wet,\mu}$	$P_{wet,\mu,w}$	ar_μ	
15	P_μ	$P_{wet,\mu}$	$P_{wet,\mu,w}$	ar_μ

C.3 Parameter estimates with GCM-RCM input

This section shows estimated values for parameters FC , α and $PERC$, based on GCM-RCM climate projections for periods 1971-2000 and 2071-2100. Parameter estimates are compared to the range of values encountered for each parameter during calibration of all 5-year periods (section 4.1). Parameter values are given for 24 periods, due to missing data for the last year from GCM-RCM combinations. Figures C.8 and C.9 show values for P_μ , $P_{wet,\mu}$, $P_{\mu,w}$ and $P_{wet,\mu,w}$ as projected by GCM-RCM combinations. P_μ , $P_{wet,\mu}$ and $P_{\mu,w}$ are used to estimate FC , P_μ and $P_{wet,\mu,w}$ are used to estimate α and $PERC$.

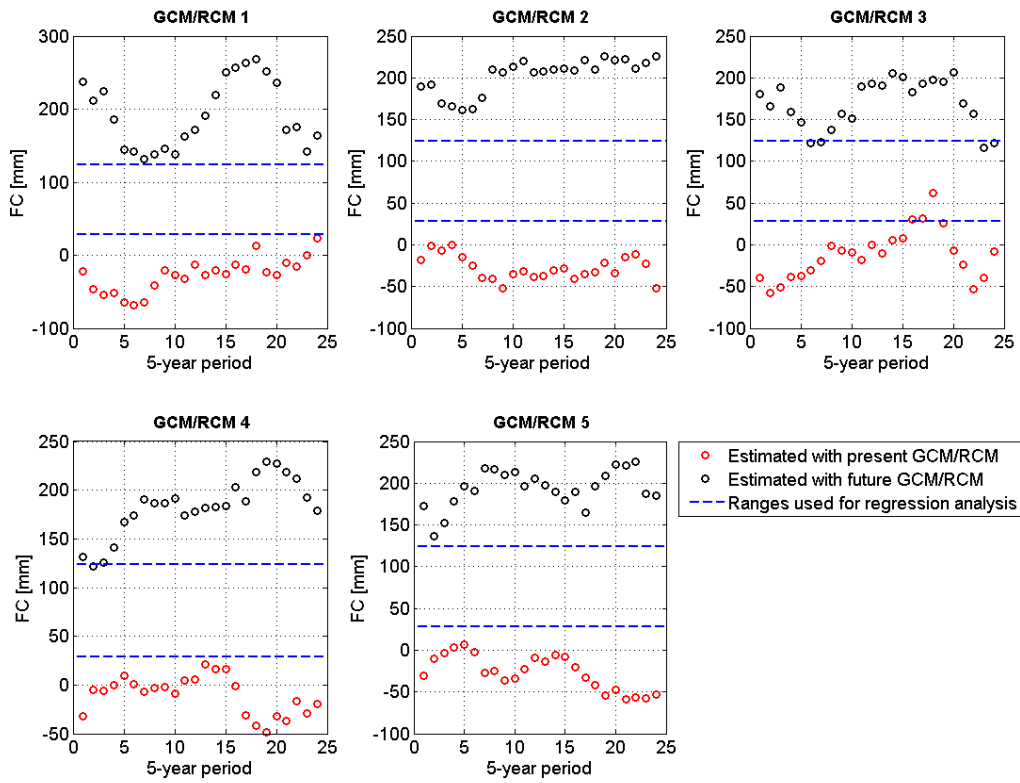


Figure C.5: Estimates of FC values based on GCM-RCM input, compared to the range of values for FC encountered during calibration of all 5-year periods

C.3. Parameter estimates with GCM-RCM input

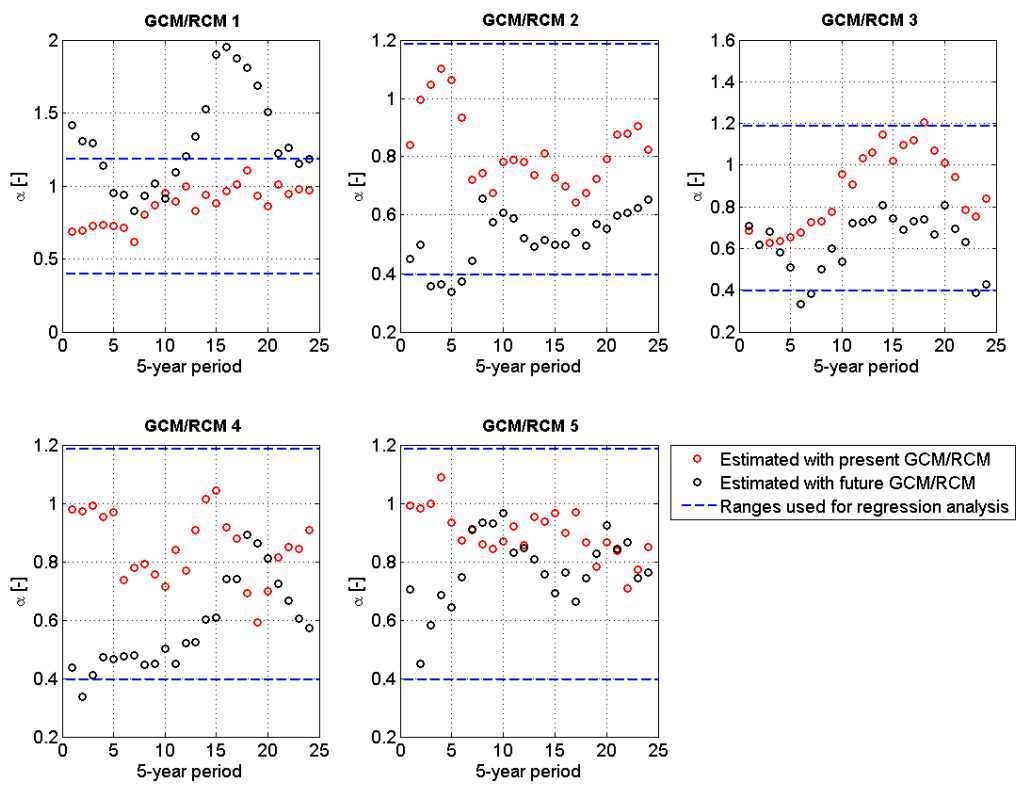


Figure C.6: Estimates of α values based on GCM-RCM input, compared to the range of values for α encountered during calibration of all 5-year periods

C.3. Parameter estimates with GCM-RCM input

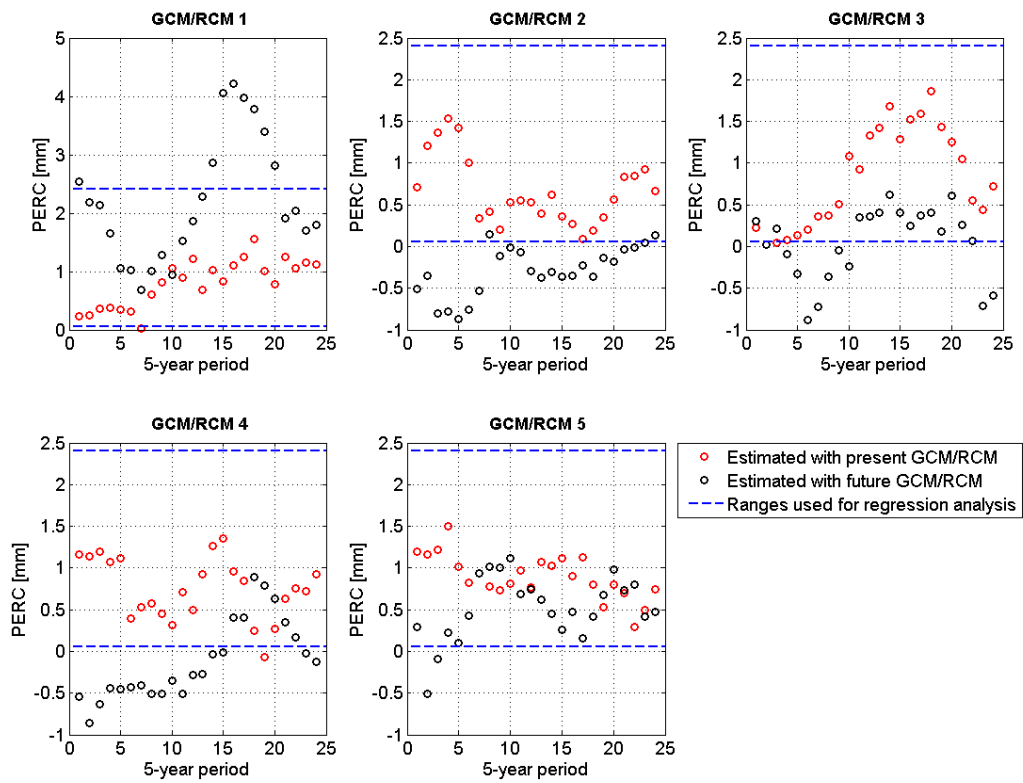


Figure C.7: Estimates of $PERC$ values based on GCM-RCM input, compared to the range of values for $PERC$ encountered during calibration of all 5-year periods

C.3. Parameter estimates with GCM-RCM input

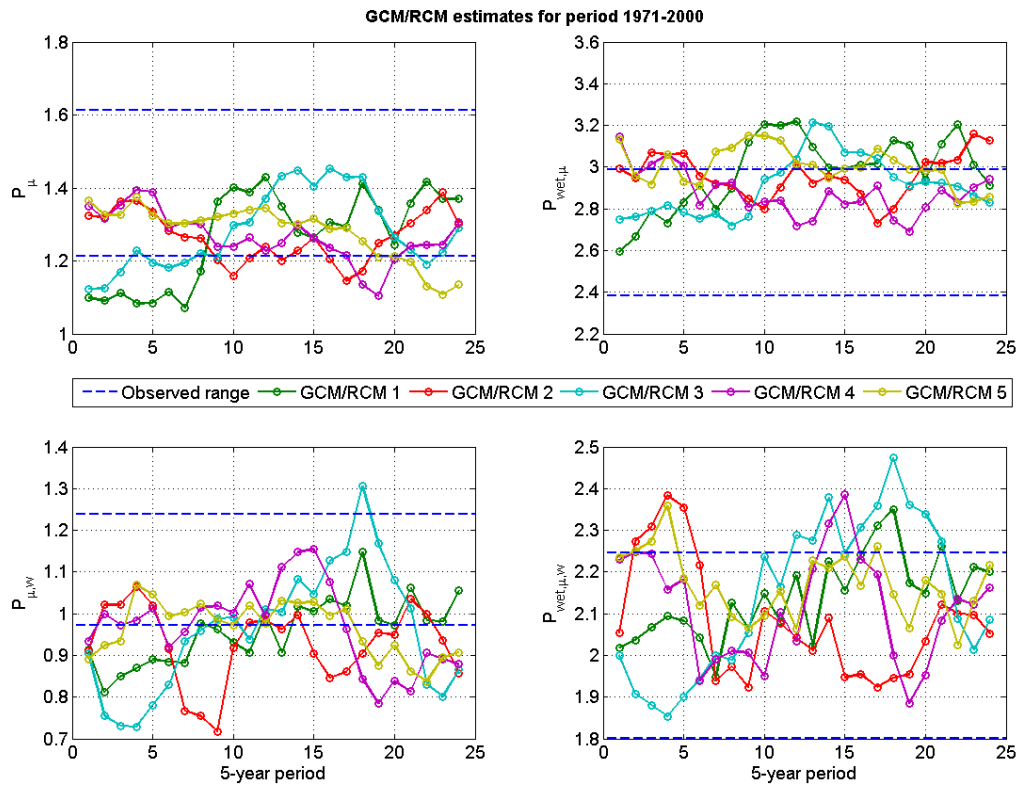


Figure C.8: Climate characteristics based on GCM-RCM estimates of P during period 1971-2000. Dotted horizontal lines represent the range of values found in observed values

C.3. Parameter estimates with GCM-RCM input

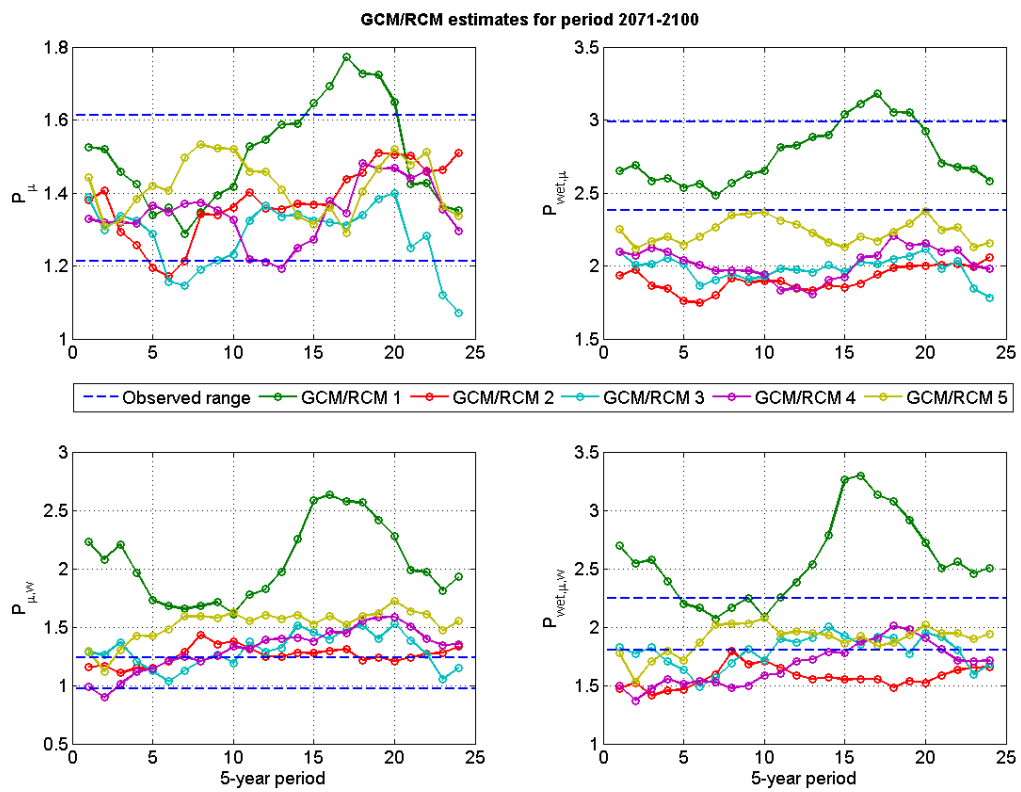


Figure C.9: Climate characteristics based on GCM-RCM estimates of P during period 2071-2100. Dotted horizontal lines represent the range of values found in observed values

Appendix D

Climate change impact assessment

This appendix contains tables related to climate change impact assessment (section 5.5.2). Section D.1 details projected changes in climate for all GCM-RCM combinations. Section D.2 shows simulated runoff based on observed P, T and PET with observed runoff, used to determine hydrological model accuracy. Section D.3 shows simulated runoff based on observed P, T and PET with simulated runoff based on GCM-RCM projections, used to determine GCM-RCM influence. Section D.4 shows simulated runoff based on GCM-RCM projections for 1971-2000 with runoff based on projections for 2074-2098, used to determine expected climate change impact (section 4.5). Seasonal statistics are calculated for winter (December, January, February; DJF), spring (March, April, May; MAM), summer (June, July, August; JJA) and autumn (September, October, November; SON).

D.1 Projected climate change

This section gives the projected changes in precipitation and temperature average values and variability (tables D.1 and D.2 respectively).

Table D.1: Comparison of observed P and projected P by GCM-RCM combinations, mean and standard deviation of both period 1971-2000 and 2071-2100 are given

	1971-2000		2071-2100		Change	
	μ [mm]	σ [mm]	μ [mm]	σ [mm]	μ [%]	σ [%]
Observations	1.43	3.20				
GCM-RCM						
1	1.27	2.72	1.48	3.89	16.5	43.0
2	1.27	2.72	1.35	2.55	6.30	-6.25
3	1.27	2.72	1.27	2.52	0.00	-7.35
4	1.27	2.65	1.33	2.58	4.72	-2.64
5	1.27	2.73	1.39	2.80	9.45	2.56

D.2 Influence of hydrological models

Table D.4 shows seasonal and annual statistics of observed discharge, and simulated discharges by base and regression models with observed P, T and PET as input, for period 1974-1998.

D.2. Influence of hydrological models

Table D.2: Comparison of observed T and projected T by GCM-RCM combinations, mean and standard deviation of both period 1971-2000 and 2071-2100 are given

	1971-2000		2071-2100		Change	
	μ	σ	μ	σ	μ	σ
	[°C]	[°C]	[°C]	[°C]	[°C]	[°C]
Observations	8.29	7.90				
GCM-RCM						
1	8.31	7.94	10.5	7.81	2.19	-0.13
2	8.31	7.94	10.9	7.25	2.59	-0.69
3	8.31	7.94	11.3	8.3	2.99	0.36
4	8.31	7.94	11.4	7.18	3.09	-0.76
5	8.31	7.94	11.3	7.6	2.99	-0.34

Table D.3: Comparison of observed PET and projected PET by GCM-RCM combinations, mean and standard deviation of both period 1971-2000 and 2071-2100 are given

	1971-2000		2071-2100		Change	
	μ	σ	μ	σ	μ	σ
	[mm]	[mm]	[mm]	[mm]	[%]	[%]
Observations	1.95	1.45				
GCM-RCM						
1	1.98	1.72	2.02	1.71	2.0	-0.6
2	1.98	1.74	1.94	1.64	-2.0	-5.7
3	1.97	1.74	2.08	1.76	5.6	1.1
4	1.97	1.64	2.09	1.67	6.1	-4.0
5	1.97	1.75	2.06	1.73	4.6	-1.1

Table D.4: Overview of observed discharge and simulated discharge by base and regression model with observed P, T and PET as input (μ and σ in $[m^3/s]$, for period 1974-1998. I: observed discharge, II.a: simulated discharge by base model with observations as input, III.a: simulated discharge by regression model with observations as input

		DJF		MAM		JJA		SON		Annual	
		μ	σ	μ	σ	μ	σ	μ	σ	μ	σ
I		12.4	3.9	13.6	5.8	5.4	2.3	5.8	2.1	9.3	10.0
II.a		11.4	3.4	11.6	3.7	8.3	3.4	6.8	2.4	9.5	8.0
III.a		11.2	3.8	11.1	4.1	8.0	3.1	6.8	2.4	9.3	8.4

D.3. Influence of GCM-RCM input

D.3 Influence of GCM-RCM input

Table D.5 shows seasonal and annual statistics of simulated discharges by base and regression models with observed P, T and PET as input and simulated discharges by base and regression models with GCM-RCM projections as input, for period 1974-1998.

Table D.5: Overview of simulated discharges by base and regression model with observed P, T and PET and GCM-RCM projections as input (μ and σ in $[m^3/s]$). II.a: simulated discharge by base model with observations as input, II.b: simulated discharge by base model with GCM-RCM input, III.a: simulated discharge by regression model with observations as input, III.b: simulated discharge by regression model with GCM-RCM input

		DJF		MAM		JJA		SON		Annual	
		μ	σ	μ	σ	μ	σ	μ	σ	μ	σ
II.a		11.4	3.4	11.6	3.7	8.3	3.4	6.8	2.4	9.5	8.0
	GCM/RCM										
II.b	1	11.9	4.1	11.5	4.1	5.0	1.6	4.8	1.2	8.3	6.9
	2	9.9	2.9	10.6	4.1	5.0	1.9	4.2	1.0	7.4	5.9
	3	12.0	4.0	11.0	3.9	5.0	2.0	4.8	1.5	8.2	6.8
	4	9.1	3.7	11.3	4.3	3.9	1.0	3.4	0.4	7.0	5.9
	5	9.9	3.7	11.7	4.2	4.1	1.1	3.3	0.5	7.3	5.9
III.a		11.2	3.8	11.1	4.1	8.0	3.1	6.8	2.4	9.3	8.4
	GCM/RCM										
III.b	1	11.5	4.3	10.6	4.1	5.3	1.3	5.4	1.2	8.2	7.0
	2	9.4	2.9	9.9	4.4	5.4	1.4	4.7	0.8	7.3	6.4
	3	12.2	4.7	9.9	3.8	5.4	1.5	5.5	1.5	8.2	7.1
	4	9.1	3.5	11.0	4.6	4.5	0.6	4.2	0.3	7.2	5.8
	5	9.5	3.8	11.6	5.0	4.5	0.6	4.1	0.3	7.4	6.0

D.4 Expected impact of climate change

Table D.6 shows seasonal and annual statistics of simulated discharges by base and regression models with GCM-RCM projections as input, for period 1974-1998 and 2074-2098.

D.4. Expected impact of climate change

Table D.6: Overview of simulated discharge by base and regression model with GCM-RCM projections for period 1974-1998 and 2074-2098 as input (μ and σ in $[m^3/s]$). II.b: simulated discharge by base model with present GCM-RCM input, II.c: simulated discharge by base model with future GCM-RCM input, III.b: simulated discharge by regression model with present GCM-RCM input, III.c: simulated discharge by regression model with future GCM-RCM input

		DJF		MAM		JJA		SON		Annual	
		μ	σ	μ	σ	μ	σ	μ	σ	μ	σ
	GCM/RCM										
II.b	1	11.9	4.1	11.5	4.1	5.0	1.6	4.8	1.2	8.3	6.9
	2	9.9	2.9	10.6	4.1	5.0	1.9	4.2	1.0	7.4	5.9
	3	12.0	4.0	11.0	3.9	5.0	2.0	4.8	1.5	8.2	6.8
	4	9.1	3.7	11.3	4.3	3.9	1.0	3.4	0.4	7.0	5.9
	5	9.9	3.7	11.7	4.2	4.1	1.1	3.3	0.5	7.3	5.9
II.c	1	32.6	13.0	29.4	11.7	7.0	4.0	5.2	3.2	18.6	18.8
	2	17.3	5.7	17.1	5.3	5.9	1.8	5.2	1.0	11.4	8.7
	3	13.4	5.9	17.7	4.6	7.4	3.1	3.9	0.9	10.6	9.3
	4	16.6	5.8	16.4	5.8	5.0	1.3	4.5	1.1	10.6	8.5
	5	23.5	7.8	20.4	7.1	5.2	1.8	4.6	2.0	13.4	11.7
III.b	1	11.5	4.3	10.6	4.1	5.3	1.3	5.4	1.2	8.2	7.0
	2	9.4	2.9	9.9	4.4	5.4	1.4	4.7	0.8	7.3	6.4
	3	12.2	4.7	9.9	3.8	5.4	1.5	5.5	1.5	8.2	7.1
	4	9.1	3.5	11.0	4.6	4.5	0.6	4.2	0.3	7.2	5.8
	5	9.5	3.8	11.6	5.0	4.5	0.6	4.1	0.3	7.4	6.0
III.c	1	43.1	41.9	22.0	18.0	6.1	4.4	7.8	7.7	19.7	38.7
	2	11.5	2.9	14.4	2.1	7.8	1.4	6.3	0.5	10.0	4.9
	3	9.8	3.4	15.1	2.6	8.3	2.4	4.9	0.5	9.5	7.0
	4	12.2	3.5	13.8	3.0	6.7	1.1	5.4	0.5	9.5	6.0
	5	21.3	7.4	19.3	6.3	6.2	1.5	5.4	1.5	13.1	10.9